SEISMIC RETROFITTING OF R/C FRAMES WITH DEFICIENT LAP SPLICES

by

Serap Altın Kaya

B.S. in Civil Engineering, Kocaeli University, 2005

Submitted to the Institute for Graduate Studies in

Science and Engineering in partial fulfillment of

the requirements for the degree of

Master of Science

Graduate Program in Civil Engineering

Boğaziçi University

2009

To my lovely son

and my husband…

ACKNOWLEDGEMENTS

I would like to express my sincere thanks to my thesis supervisor, Assist. Prof. Dr. Kutay Orakçal for his invaluable guidance, continuous support, and helpful suggestions. He has always been supportive for the preparation of this thesis.

My sincere gratitude is also due to the members of my advisory committee Assist. Prof. Dr. Fuad Okay and Assoc. Prof. Dr. Cem Yalçın for their useful suggestions and comments.

I owe special thanks to Assoc. Prof. Dr. Şevket Özden for his endless help and encouragement. I would like to express my special gratitude to the assistants of Structures Laboratory and my friends, Erdal Gökgöz, İbrahim Topçu and Denizhan Uluğtekin for their help, and to the technicians, Hasan Şenel and Hamdi Ayar, for their help in the experimental phase of this research. And special thanks to Selçuk Altay to his suggestions and contributions.

My special gratitude goes to my husband, Osman Kaya, for his patience, suggestions, continuous encouragement and support for every stage of this thesis.

This research has been financially supported by Boğaziçi University Research Fund, under Project No. 08A403. I would also like to acknowledge the BASF-YKS, the Chemical Company, for providing strengthening materials and Akçansa Hazırbeton A. Ş. for providing ready-mixed concrete used in this research. The conclusions and recommendations presented in this report are solely those of the author and do not necessarily represent the views of the sponsor.

Last, but not least, I would like to dedicate this thesis to my family. My special thanks, of course, go to my siblings and their loving support. Finally, and most importantly, I wish to thank my parents. They have always supported and encouraged me to do my best in all matters of life.

ABSTRACT

SEISMIC RETROFITTING OF R/C FRAMES WITH DEFICIENT LAP SPLICES

Many of the existing reinforced concrete frame buildings in use today may not have adequate seismic resistance due to detailing deficiencies including inadequate anchorage of longitudinal reinforcement, inadequate lap splices in the columns, lack of confinement in potential plastic hinge regions, inadequate joint shear strength, and absence of the strong column–weak beam condition. A significant amount of research has been devoted to the study of various strengthening techniques to enhance the seismic performance of such frame systems with detailing deficiencies. An alternative strengthening method consists of using externally applied carbon fiber reinforced polymers (CFRP), the effect of which has been investigated in this study on frames with inadequate lap splices.

Within the scope of this work, 2/3-scale one-bay, one-story frames (portal frames) were constructed and tested under lateral loads for investigating the effect of inadequate lap splices on the frame response, as well as to propose a novel strengthening methodology to mitigate the negative effects. One specimen was constructed with continuous longitudinal reinforcement and according to detailing provisions specified by the latest seismic code, whereas two other specimens were constructed with inadequate lap splices on the column longitudinal reinforcement just above the footing, as well as insufficient transverse reinforcement in the lap splice regions. An original strengthening technique, using a combination of CFRP materials and steel anchorage rods, was developed and applied on one of the lap splice specimens for improving its lateral load behavior. In this technique, the CFRP sheets were installed both in the longitudinal direction of the columns for increasing their flexural capacity, as well as the in transverse direction to induce confinement effects. The test results showed a significant improvement in the lateral load capacity of the strengthened specimen, with no negative influence on its ductility.

ÖZET

YETERSİZ BİNDİRME BOYU BULUNAN BETONARME ÇERÇEVELERİN DEPREME KARŞI GÜÇLENDİRİLMESİ

Günümüzde kullanılmakta olan mevcut betonarme çerçeve binalarının çoğu, boyuna donatısındaki yetersiz ankraj, kolonlarda yetersiz bindirme boyu, olası mafsallaşma bölgesinde etriye eksikliği, birleşim bölgesinde yetersiz kesme kuvveti dayanımı ve güçlü kolon zayıf kiriş durumunun olmaması gibi detaylandırma eksiklikleri sebebiyle, yeterli deprem dayanımına sahip olmayabilir. Bunun gibi eksik detaylandırılmış çerçevelerin sismik performansını arttırmak için, önemli sayıda araştırma yapılmıştır. Bu çalışmada alternatif bir güçlendirme metodu olarak dıştan CFRP uygulamasının, yetersiz bindirme boyuna sahip çerçeve üzerindeki etkisi incelenmiştir.

Bu çalışma kapsamında, olumsuz etkileri ortadan kaldıracak yeni bir güçlendirme yöntemi önerilmesinin yanı sıra yetersiz bindirme boyunun çerçeve davranışı üzerindeki etkisini incelemek amacıyla, 2/3 ölçekli bir katlı bir açıklıklı betonarme çerçeveler üretilmiş ve yatay yükler altında test edilmiştir. Bir numune, sürekli boy donatısı kullanılarak ve en son sismik yönetmeliğin hükümlerine uygun olarak üretilmiş, diğer iki numune ise temelin hemen üzerinde, yetersiz bindirme boyu kullanılarak ve bu bölgede daha az etriye kullanılarak üretilmiştir. Yatay yük davranışlarını iyileştirmek amacı ile bindirme boyu olan numunelerin birinde, CFRP ve çelik ankrajların birlikte kullanılmasıyla orijinal bir güçlendirme tekniği geliştirilmiş ve uygulanmıştır. Bu teknikte, sargılama etkisinin arttırılması için yatay yönün yanı sıra, kolonların eğilme kapasitesini arttırmak amacı ile kolonların her iki tarafında, boyuna yönde de CFRP uygulaması yapılmıştır. Test sonuçları, güçlendirilen numunenin sünekliğinde olumsuz bir etki olmaksızın, yatay yük kapasitesinde önemli bir artış olduğunu göstermiştir.

TABLE OF CONTENTS

ACKNOWLEDGEMENTS iv
ABSTRACT v
ÖZET vi
TABLE OF CONTENTS vii
LIST OF FIGURES ix
LIST OF TABLES xiii
LIST OF SYMBOLS / ABBREVIATIONS xiv
1. INTRODUCTION 1
1.1. General 1
1.2. Literature Review 3
1.2.1. Overview 3
1.2.2. Inadequate Lap Splice Effect 4
1.2.3. Axial Load Effect 8
1.2.4. Strengthening with Fiber Reinforced Polymers 9
1.3. Research Significance, Objectives and Scope 14
1.3.1. Research Significance 15
1.3.2. Objectives 15
1.3.3. Scope 16
1.4. Report Outline 16
2. EXPERIMENTAL SETUP 17
2.1. Introduction 17
2.2. Design of the Test Specimens 17
2.2.1. Turkish Earthquake Code (2007) 18
2.2.2. Design Rules for Columns of High Ductility Level: 18
2.2.3. Design Rules for Beams of High Ductility Level: 23
2.3. Properties of Specimens and Test Parameters 29
2.3.1. Flexural Capacity of Members 30
2.4. Material Properties 32
2.4.1. Concrete 32
2.4.2. Reinforcing Bars 32

2.4.3. Carbon Fiber Reinforced Polymers (CFRP) 34
2.5. Construction of Test Specimens 35
2.5.1. Control Specimen 36
2.5.2. Specimens LS and LS-FRP 37
2.6. CFRP Strengthening Methodology 38
2.6.1. Surface Preparation 39
2.6.2. CFRP Application 40
2.7. Testing Methodology 45
3. EXPERIMENTAL STUDY 49
3.1. Test Observations 49
3.1.1. Control Specimen 49
3.1.2. Specimen LS 52
3.1.3. Specimen LS-FRP 55
3.2. Local Deformation Measurements 58
3.2.1. Load versus Curvature Relationships 58
3.2.2. Load versus Shear Deformations Relationships 71
4. DISCUSSION OF TEST RESULTS 76
4.1. Lateral Load Capacity and Lateral Load vs. Story Drift Response 76
4.2. Stiffness Degradation 77
4.3. Energy Dissipation and Ductility 78
4.4. Failure Modes, Local Deformations, and Distribution of Damage 80
4.4.1. Control Specimen 80
4.4.2. Specimen LS 81
4.4.3. Specimen LS-FRP 82
5. SUMMARY, CONCLUSIONS, AND FUTURE WORK 84
REFERENCES 87

LIST OF FIGURES

Figure 2.1. Provisions of TEC-2007 for Column Reinforcement Layout 24

Figure 2.2. Provisions for the Layout of the Longitudinal Reinforcement in Beams..... 26

Figure 2.3. Beam Longitudinal Reinforcement Hooks used in the Test Specimens 27

Figure 2.4. Transverse Reinforcement Layout Provisions for a Beam..... 28

Figure 2.5. Test Specimen 29

Figure 2.6. Cross-section Properties of Column and a Beam..... 30

Figure 2.7. Flexural Capacity Analysis of a Column and a Beam..... 31

Figure 2.8. Stress-Strain Relationship for ϕ20 Reinforcement..... 33

Figure 2.9. Stress-Strain Relationship for ϕ14 Reinforcement..... 33

Figure 2.10. Stress-Strain Relationship for ϕ12 Reinforcement..... 34

Figure 2.11. Stress-Strain Relationship for ϕ8 Reinforcement..... 34

Figure 2.12. Stress-Strain Relations of CFRP 35

Figure 2.13. Production of Test Specimens..... 36

Figure 2.14. Reinforcement Details for Control Specimen 37

Figure 2.15. Reinforcement Details for Specimen LS and LS-FRP..... 38

Figure 2.16. CFRP Application 39

Figure 2.17. Primer Application 40

Figure 2.18. Epoxy Matrix..... 41

Figure 2.19. Steel Anchorages Holes..... 41

Figure 2.20. CFRP Anchorages Holes..... 42

Figure 2.21. “L Shaped” CFRP 43

Figure 2.22. CFRP Anchorages 43

Figure 2.23. Column Wrapping 44

Figure 2.24. Steel Anchorages 44

Figure 2.25. Loading Protocol 46

Figure 2.26. Test Setup 47

Figure 2.27. 3D Sketch of Test Setup 47

Figure 2.28. Location of Strain Gages for specimen LS and specimen LS-FRP 48

Figure 2.29. Location of LVDTs 48

Figure 3.1. Nomenclature of the Structural Members 49

Figure 3.2. The first Flexural Cracks on Beam in Control Specimen 50

Figure 3.3. Column Flexural Cracks (exterior and interior) 50

Figure 3.4. Joint Shear Cracks and Beam Crushing 51

Figure 3.5. Lateral Load vs. Displacement Relationships of Control Specimen 52

Figure 3.6. Lateral Load vs. Drift Relationships of Control Specimen 52

Figure 3.7. The First Flexural Cracks on the Beam in Specimen LS 53

Figure 3.8. Column Cracks of Specimen LS 54

Figure 3.9. Crackings of Beam and Column at the end of the Test for Specimen LS 54

Figure 3.10. Lateral Load vs. Displacement Relationships of Specimen LS 55

Figure 3.11. Lateral Load vs. Story Drift Relationships of Specimen LS 55

Figure 3.12. Beam Flexure Crack and Joint Crack of Specimen LS-FRP 56

Figure 3.13. Rupture of CFRP in Specimen LS FRP 57

Figure 3.14. Lateral Load vs. Displacement Relationships of Specimen LS FRP 57

Figure 3.15. Lateral Load vs. Drift Relationships of LS FRP Specimen 58

Figure 3.16. Curvature Placement 59

Figure 3.17. Schematic View of Curvature Calculation 59

Figure 3.18. Load vs. Curvature at the Base Location of Left Column for Control Spec. 60

Figure 3.19. Load vs.Curvature at the Base Location of Right Column for Control Spec. 60

Figure 3.20. Load vs. Curvature just above the Base of Left Column for Control Spec... 61

Figure 3.21. Load vs. Curvature just above the Base of Right Column for Control Spec. 61

Figure 3.22. Load vs. Curvature at the Top of Left Column for Control Spec. 62

Figure 3.23. Load vs. Curvature at the Top of Right Column for Control Spec. 62

Figure 3.24. Load vs. Curvature at the Left end of the Beam for Control Spec. 63

Figure 3.25. Load vs. Curvature at the Right end of the Beam for Control Spec..... 63

Figure 3.26. Load vs. Curvature at the Base Location of Left Column for LS 64

Figure 3.27. Load vs. Curvature at the Base Location of Right Column for LS 64

Figure 3.28. Load vs. Curvature just above the Base of Left Column for LS 65

Figure 3.29. Load vs. Curvature just above the Base of Right Column for LS 65

Figure 3.30. Load vs. Curvature at the Top of Left Column for LS..... 66

Figure 3.31. Load vs. Curvature at the Top of Right Column for LS..... 66

Figure 3.32. Load vs. Curvature at the Left end of the Beam for LS 67

Figure 3.33. Load vs. Curvature at the Right end of the Beam for LS 67

Figure 3.34. Load vs. Curvature at the Base Location of Left Column for LS-FRP..... 68

Figure 3.35. Load vs. Curvature at the Base Location of Right Column for LS-FRP..... 68

Figure 3.36. Load vs. Curvature just above the Base of Left Column for LS-FRP..... 69

Figure 3.37. Load vs. Curvature just above the Base of Right Column for LS-FRP 69

Figure 3.38. Load vs. Curvature at the Top of Left Column for LS-FRP 70

Figure 3.39. Load vs. Curvature at the Top of Right Column for LS-FRP 70

Figure 3.40. Load vs. Curvature at the Left end of the Beam for LS-FRP..... 71

Figure 3.41. Load vs. Curvature at the Right end of the Beam for LS-FRP 71

Figure 3.42. Shear Deformation Measurement..... 72

Figure 3.43. Load vs. Shear Deformations at the Left Joint Panel for Control Specimen 73

Figure 3.44. Load vs.Shear Deformations at the Right Joint Panel for Control Specimen 73

Figure 3.45. Load vs. Shear Deformations at the Left Joint Panel for LS Specimen..... 74

Figure 3.46. Load vs. Shear Deformations at the Right Joint Panel for LS Specimen..... 74

Figure 3.47. Load vs. Shear Deformations at the Left Joint Panel for LS-FRP Specimen 75

Figure 3.48. Load vs. Shear Deformations at the Right Joint Panel for LS-FRP Spec. 75

Figure 4.1. Comparison of Backbone Curves (envelopes) 77

Figure 4.2. Calculation of Stiffness of Hysteresis Loops 77

Figure 4.3. Comparison of Stiffness Degradation 78

Figure 4.4. Calculations of Energy 79

Figure 4.5. Comparison of Dissipated Cumulative Energy 79

LIST OF TABLES

Table 2.1. Concrete cover requirements 19

Table 2.2. Concrete Compressive Test Results after 28 Days 32

Table 2.3. Yield Strengths of Reinforcement 33

Table 2.4. Properties of CFRP. 35

LIST OF SYMBOLS / ABBREVIATIONS

A_c	Gross section area of column
A_{ck}	Concrete core area within outer edges of confinement reinforcement
A_g	Gross cross-section area
A_{sh}	Along the height corresponding to transverse reinforcement spacing s, sum of projections of cross section areas of all legs of hoops and crossties of columns or wall end zones in the direction perpendicular to b_k considered
c_c	Concrete cover
b_k	For each of the orthogonal lateral directions, cross section dimension of concrete core of column or wall end zone (distance between the centres or outermost rebars)
b_w	Width of the beam
b	Width of the column
$D_{1,2}$	Gauge lengths of diagonally placed displacement sensors
d	Effective beam height
f'_c	Concrete compressive strength
f_{ctd}	Design tensile strength of concrete
f_{ck}	Characteristic compressive cylinder strength of concrete
f_{yd}	Design yield strength of longitudinal reinforcement
f_{ywk}	Characteristic yield strength of transverse reinforcement
h	Column cross section dimension in the earthquake direction considered
$h_{1,2}$	Gauge lengths of the displacement sensors
h_k	Beam height
$L_{1,2}$	Distance for curvature readings
ℓ_b	Development length of tensile reinforcement as given in TS-500
ℓ_n	Clear height of column between beams, clear span of beam between column or wall faces
l_s	Length of lap splice
N_d	Factored axial force calculated under simultaneous action of vertical loads and seismic loads
N_{dm}	The maximum axial force

s	Spacing of transverse reinforcement
X, Y	Dimensions of undeformed joint panel
$\Delta_{1,2}$	Relative longitudinal displacements readings taken from the displacement sensors
$\varepsilon_{1,2}$	Strain values obtained from LVDTs
ϕ	Curvature values at the beam and column
γ	Shear deformations at the joint (rad)
ρ	Reinforcement ratio of the longitudinal reinforcement

1. INTRODUCTION

1.1. General

Turkey experienced five devastating earthquakes in the last decade, namely the Erzincan (1992), Dinar (1995), Adana-Ceyhan (1998), Kocaeli (1999) and Düzce (1999). These earthquakes have caused thousands of deaths due to collapse of numerous reinforced concrete (RC) buildings, and have illustrated the vulnerability of the existing RC building stock to strong ground motion. Poorly detailed RC frames with poor construction quality, constituting a majority of the existing building stock in Turkey, have been identified as critical structural systems that fail in a non-ductile manner during a severe earthquake. Unfortunately, many of the existing RC buildings in use still possess such deficiencies and are susceptible to collapse during an expected high-intensity earthquake. Since demolishing and reconstruction of all of these buildings is not economically feasible (or possible for that manner), structural rehabilitation of such buildings has been discussed and investigated for some time, for the purpose of ensuring, at the least, the life safety of the occupants.

Structural rehabilitation can be defined as the operation to bring the structural system or some of the structural members to a desired performance level. Depending on the state of (or damage on) the existing structure, structural rehabilitation can be divided into two categories; (a) repair, and (b) strengthening. Structural repair is the rehabilitation of a damaged structure or structural member with the objective of bringing the performance level (e.g., load and / or deformation capacity) back to the pre-damage level or possibly to a higher level. Structural strengthening, on the other hand, is improving the performance of an undamaged, yet deficient structure or structural member to a higher performance level [1]. Reinforced concrete buildings located in seismic zones are strengthened or repaired for three principal reasons: to satisfy the owner's concern for financial protection and occupant safety; to comply with local building codes and regulations; and to repair earthquake damage and obtain improved performance during future events [2].

Strengthening of non-ductile RC frame systems is a challenging task that poses major practical difficulties. A variety of strengthening techniques have been investigated for RC frames, with the most common methodologies being the construction of RC or steel jackets [3]. Reinforced concrete jackets and special forms of steel jackets, namely steel "cages", require intensive labor and artful detailing during application. Moreover, concrete jacketing increases the dimensions and therefore the weight of the structural members. Use of plain or corrugated steel plates has also been investigated [4]; however, in addition to corrosion vulnerability, these elements require special attachment through the use of either epoxy adhesives combined with bolts or special grouting.

A relatively new technique for strengthening of RC structural members involves the use of Carbon Fiber Reinforced Polymer (CFRP) materials as externally-bonded reinforcement in critical regions of the members. CFRP materials, which are available today in the form of strips or in situ resin impregnated sheets, are being used to strengthen a variety of RC elements, including beams, slabs, columns, and shear walls, to enhance the flexural, shear, and axial (through confinement) capacity of such elements. CFRP materials have a number of favorable characteristics including ease of installation, functionality of the building during installation, immunity to corrosion, high stiffness-to-weight and strength-to-weight ratios, availability in convenient "to apply" forms, and the ability to control the material's behavior by selecting the proper orientation of the fibers. All of these features make CFRP a highly engineered material suitable for strengthening applications, in spite of the fact that the cost of carbon fibers is much higher than the cost of conventional construction materials.

Accordingly, this study investigates a novel strengthening methodology, which consists of using externally applied CFRP sheets, to improve the seismic response of RC frames with inadequate lap splice length on column longitudinal reinforcement, which happens to be one of the commonly observed detailing deficiencies in existing RC frame buildings in Turkey. The background, motivation, and scope of this work are presented in the following sections of this chapter.

1.2. Literature Review

1.2.1. Overview

A number of repair and strengthening techniques are currently in use for reinforced concrete structures. However, the majority of these techniques are costly, time-consuming, and cause disruption to the function of the structure during the time which the construction work is conducted. Hence, there is still a need for the development of improved, economical, and less disruptive techniques, which would make seismic rehabilitation of structures economically viable and cause minimal disturbance to the occupants

A widely-used technique for overall strengthening of a structural system is the addition of new structural elements including structural walls, or different types of steel bracing. The addition of new RC structural walls to an existing structure is one of the most common methods of strengthening for improved seismic performance. Braced steel frames can also be added to an existing structure, provided that the existing reinforced concrete system and the added steel bracings are designed to respond in a compatible manner in the event of an earthquake excitation. Compared to structural walls, braced steel frames are lighter, however, they possess relatively low lateral strength and stiffness attributes.

On the other hand, strengthening of individual structural components (including beams, columns and beam-column connections) to improve seismic response of structure was investigated by numerous researchers. Reinforced concrete and steel jacketing were studied as the most common techniques for local (member) strengthening and ductility improvement. Reinforced concrete jacketing techniques involve enlarging the existing cross section of a member, typically a column, with a new layer concrete that is reinforced with both longitudinal and transverse reinforcement [3,5]. Based on available local space conditions, jacketing can be applied on one, two, three or four column sides. Reinforced concrete jacketing was identified as the most reliable and durable technique for member strengthening of frame structures. However, it poses the disadvantages of significant time and labor consumption, as well as costly interruption of the building's use and construction procedures that cause disturbance to occupants [6]. Steel profile jacketing of a column, on the other hand, typically consists of installing four longitudinal angle profiles at column

corners connected to transverse steel straps, forming a skeleton around the column. Gaps between the steel profiles and the column surface must be filled in with cement resign grout, and the straps pre-stressed [6].

Another technique (proposed by Wu et al. [7]) uses composite partial interaction to improve the strength and ductility of rectangular RC columns. The compressive strength of the column concrete is supplemented via bolting a steel plate to the compression face of the column. Test results have shown that this technique delays concrete crushing in the plastic hinge zone. In addition, the strength and ductility properties of columns can be increased by providing active confinement with the use of pre-stressing cables wrapped around the column [8].

In addition to using concrete or steel jacketing techniques for member rehabilitation of RC frames, relatively new Carbon Fiber Reinforced Concrete (CFRP) materials possess great potential of usage for retrofitting and strengthening of RC columns – circular columns in particular – since the circumferential pressures are equally exerted on a circular column by the CFRP material, which is very strong in tension, although it has negligible compressive or flexural stiffness. CFRP is therefore preferred for its high tensile strength, light weight, high resistance to corrosion and versatility [9]. However, it is important to mention that its use is often limited to improving confinement effect and shear strength only, and ultimate care is needed during installation of CFRP for strengthening purposes.

1.2.2. Inadequate Lap Splice Effect

Presently, many of the existing RC frame buildings in Turkey have inadequate seismic resistance due to inadequate lap splice length on the longitudinal reinforcement of columns. For ease of construction, in old buildings, longitudinal column bars are typically spliced just above the floor level (in the potential plastic hinge region), with the lap splice length being only 20 times the column bar diameter or even less, and the lap splice region not adequately confined with transverse reinforcement. Columns with such lap splice deficiencies are expected to experience splice failure (splitting type bond slip failure) before the column bars develop yield strength or even before yielding (plastic hinge formation) in the beams, which results in a very a non-ductile failure of the frame system.

To investigate the effectiveness of various types of steel jacketing for improving the seismic performance (lateral load behavior) of damaged RC columns with lap splice failure, six large scale columns were tested by Aboutaha et al. [10]. The efficiency of different steel jacketing techniques, including rectangular jackets with and without adhesive anchor bolts and with unbonded through rods was investigated in the study. One of the column specimens tested was repaired by welding of the column longitudinal reinforcement in the lap splice region. It was concluded from the results of these tests that rectangular steel jackets used together with unbonded through-rods were highly effective in the repair of damaged columns with lap splice failure.

Paulay et al. carried out an experimental research program to see the influence of confinement on the performance of columns with deficient lap splices [11]. Twelve specimens with rectangular (16 in. x 12 in.) and square (16 in.) cross sections and with inadequate lap splice length ($l_{s,provided} / l_{s,required}$ = 0.82 to 0.95) were tested in this program. The test results revealed that although the lap splice lengths were inadequate, well-confined splices were able to develop the tensile yield stress of the column reinforcement and such columns maintained their lateral load capacity up to a displacement ductility level of four. It was concluded that increasing the splice length did not have a significant effect on the lateral load capacity of a column; however, closely-spaced transverse reinforcement substantially improved the ductility and cyclic response of a column by preventing splitting of concrete in the lap splice region and maintaining the bond stress transfer along the splice.

The observed beneficial effect of confinement on the behavior of members with inadequate lap splices directed researchers to investigate increasing confinement effect as a rehabilitation measure to improve the performance. Several different methods of providing improved confinement to deficient lap splice regions were evaluated [12].

Valluvan et al. conducted a study on strengthening of the lap splice region of RC columns. They constructed and tested twelve, approximately two-thirds scale columns under cyclic lateral loads. In order to examine the behavior of the strengthened lap splice region, several different strengthening methodologies were considered. These

methodologies included welding of the spliced rebars, confinement of the region with steel angles and straps, and providing external and internal transverse ties in the splice region. The specimens were subjected to reversed, cyclic loads. According to the tests results, the unstrengthened specimen exhibited poor behavior under cyclic loading, with a sudden loss in the lateral load capacity at approximately two-thirds the nominal moment capacity of the critical section. External confinement (with steel elements or ties) improved the strength in the splice region, and adding internal ties alone to the splice region was found to be not an effective technique for strengthening, because spalling of the cover concrete surrounding the ties resulted in concrete cracking reducing the bond strength [13].

Lynn et al. tested 3 pairs of identical column specimens with pre-1970s construction details to evaluate the influence of lap splices on their lateral load response. Eight, 18 in. square columns with eight longitudinal reinforcing bars and #3 hoops/ties at either 12 in. or 18 in. spacing on center were constructed. Longitudinal reinforcement consisted of either #8 or #10 diameter bars. In each specimen pair, one specimen was reinforced with continuous bars and the other specimen was detailed with a 20 and 25-bar diameter long lap splice at the end region of the column. The specimens were subjected to reversed cyclic lateral displacements while the axial load was held constant resulting in axial stress levels either $0.12\,f'_c$ or $0.35\,f'_c$ throughout the duration of the tests. The test results indicated that all specimens exhibited lateral strength degradation due to shear failure. Specimens with low axial load and longitudinal steel ratio exhibited fairly ductile response compared with other specimens. The lap splice did not have an adverse effect on the performance of shear-critical columns with high longitudinal reinforcement ratios (3.0 %). However, the capacity of columns with lower reinforcement (not shear critical) deteriorated due to the presence of the lap splice [14].

Chai and Priestley conducted tests on circular columns, retrofitted with steel jackets installed on plastic hinge regions. Six large scale columns with 610 mm diameter were prepared, and tested under constant axial load and reversed cyclic lateral load. In this study, lap splice effects and the influence of the steel jackets effects on column behavior were investigated as the main parameters. The test results showed that the steel jacketing increased column stiffness by 10 % to 15 %, and the strength deterioration due to bond-slip

failure was rapid in columns with lap spliced bars compared with the columns with continuous longitudinal bars [15].

Aboutaha et al. investigated the use of steel jackets on RC columns with square and rectangular cross sections [4]. The experiments revealed that reference specimens, with 20 bar diameter lap splice lengths, experienced bond deterioration prior to reaching the nominal moment capacity at the critical column section. The reference specimens exhibited bond deterioration around 1.0 % and 1.5 % lateral drift ratio, and lap spliced specimens experienced substantial lateral strength degradation after the bond failure. These test results clearly indicated that the columns with 20 bar diameter lap-splice length showed non-ductile responses and required rehabilitation. Different variations of steel jacketing and bonding techniques were used on other test specimens. An evaluation of these test results presented by Aboutaha discussed that use of a steel jacket is an effective method for improving the cyclic response of the columns with inadequate lap splice lengths. The confining of the lap splice region allowed a more ductile response of the column under monotonic loading, as test specimens with added confinement successfully developed yield stress in the reinforcement, reached the nominal moment capacity, and were able to maintain their lateral load carrying capacity up to relatively large displacements for subsequent larger drift levels. Upon evaluation of the test parameters, it was concluded that rehabilitation of lap splices in columns with rectangular cross sections requires steel jacketing along a distance longer than the lap splice length as well as use of adhesive anchor bolts on all faces of the column.

Coffman et al. also investigated the effectiveness of using external ties as a rehabilitation measure on bridge columns with 35 bar diameter lap splice lengths. Four, one-half scale, circular reinforced concrete columns with construction details representative of those used in the 1950s through the mid-1970s were tested. The splice regions of the specimens were confined with pre-stressed external hoops along the lower 1220 mm (4 ft) of the column. The size and spacing of the external hoops were varied to evaluate the effectiveness of adding pre-stressed hoops. Columns were subjected to cyclic lateral loads and constant axial load ($0.10\,A_g f'_c$). The control specimen, with a 35 bar diameter lap splice length, was able to maintain the lateral load capacity up to a displacement ductility of four and longitudinal reinforcing strains of five times the yield

strain. The response of specimens strengthened with pre-stressed hoops indicated that the external hoops did not increase the lateral strength of specimens appreciably; however, the energy dissipation capacity for each cycle was improved and the displacement ductility increased (the lateral load capacity was maintained for an increased number of cycles to higher drift ratios) [16].

Panahshahi et al. tested seven full-scale RC specimens with compression lap splices. The specimens consisted of three columns and four beams. The scope of the research was to determine the response of compression lap splices under cyclic loading. Column specimens were loaded axially with an eccentricity of 1.5 inches to apply a combination of axial and flexural effects on the lap splice provided at the specimen mid-span. Grade 60 #8 and #11 reinforcement bars were used as longitudinal reinforcement and lap splice lengths were varied between 30 and 32 bar diameters. Test results revealed that the provided compression lap splices were able to develop yield stress along the splice length and sustain a minimum of 12 cycles of loading in the nonlinear deformation range. It was suggested to use closely spaced ties to prevent premature compression-induced failure due to buckling of longitudinal bars or concrete crushing [17].

1.2.3. Axial Load Effect

Axial load on RC columns may vary depending on location of the column in the structure. The axial load is higher in the lower stories, and decreases gradually towards upper floors. A representative axial load level is generally around 30 % of the axial load capacity of a column. The stresses at any section of the column must be calculated under the combined effects of axial compression and flexure; therefore, axial load level influences the response of RC columns subjected to lateral loading.

Sheikh et al. tested 12 circular columns to investigate the effects of axial load level, spacing of spirals, thickness and type of Fiber Reinforced Plastics (FRP) used to strengthen the columns. Column specimens were subjected to constant axial load and cyclic lateral load. The test results indicated that, Carbon FRP and Glass FRP can be used effectively to strengthen deficient columns to improve the strength, ductility and energy absorption capacity attributes. To characterize the influence of axial load on column response, one of

the columns was tested under an axial load of 0.54 $A_g f'_c$ and another identical other one subjected to an axial load of 0.27 $A_g f'_c$. Increase in axial load resulted in reduced ductility (deformation capacity) of the column, as expected. The energy dissipation capacity of the column under lower axial load was found to be more than 10 times that of the column subjected to higher axial load [18].

Bayrak conducted tests on high strength concrete columns. Two of the specimens tested were identical, yet subjected to different levels of axial load. Both of the specimens contained the same amount of longitudinal and transverse reinforcement; however, one was tested under a constant axial load level of 36 % of its axial load capacity, whereas the other 50 %. The increase in the axial load resulted in substantial reduction in the measured curvature ductility. Moreover, as a result of increased axial load level, the cumulative energy dissipation showed significant reduction. Higher axial load also resulted in an increase in the rate of stiffness degradation with every load cycle [19].

1.2.4. Strengthening with Fiber Reinforced Polymers

Fiber reinforced polymer (FRP) composites are increasingly used in the construction industry. One of the areas of their application is repair and strengthening of reinforced concrete columns. This is achieved by encasing of columns with FRP composite jackets which provides lateral confinement on the concrete and, as a result, enhances the strength as well as ductility of RC columns. A number of techniques have been developed to fabricate FRP composite jackets, the most commonly used ones being wrapping of fabric, bonding of prefabricated shells [20-21].

Experimental and analytical studies on the compressive behavior of reinforced concrete blocks with square cross-sections and externally wrapped with CFRP sheets were carried out by Campione. The effects of local reinforcement at the corners, use of horizontal and vertical discontinuous CFRP strips, and number of CFRP layers, and the length of specimens were investigated as test parameters. An analytical model was proposed to estimate the compressive capacity of concrete members with square cross-section externally wrapped with FRP. Results of the proposed analytical model showed good agreement with the experimental data [22].

Antoniades et al. conducted cyclic tests on eleven wall specimens for investigating the cyclic lateral load responses of RC structural walls. Specimens were first tested under lateral loads until the failure, and then repaired by removing the heavily cracked and crushed concrete, lap splicing of the fractured steel bars by welding of new short bars, and placing of new transverse web reinforcement. The specimens were then strengthened using FRP sheets, strips, and bonded metal anchors in order to increase flexural strength as well as the shear strength and the ductility. The test results indicated that FRP-strengthening of RC walls was effective in preventing development of unfavorable failure mechanisms [23].

Yalcin et al. carried out five tests to investigate the CFRP strengthening techniques on columns with deficiencies including use of plain reinforcing bars, inadequate lap splicing of longitudinal reinforcement, and use of low-quality concrete. One of the columns was repaired by welding of the lap splice prior to strengthening with CFRPs. The test results showed that strengthening of columns with CFRP sheets in the transverse direction was effective for columns with continuous reinforcing bar (without lap splices). However, only a slight improvement was obtained in the performance of the strengthened lap spliced column, since the confinement effect of the CFRP in the transverse direction did not significantly improve the anchorage of the plain bars in the lap splice region. However, for a column specimen that was retrofitted by welding of dowel rebars with longitudinal reinforcement in the splice region and then wrapped with CFRP sheets, strength, ductility and energy dissipation capacity properties improved significantly [24-26].

In the study of Val, the behavior of FRP-confined short columns with circular cross sections was investigated experimentally. Based on the test results, a relationship between the strength reduction factor and the confinement ratio was proposed for FRP-confined columns in axial compression and axial compression combined with flexure. The influence of longitudinal reinforcement ratio, live-to-dead load ratio, and eccentricity on the response of FRP-confined columns was also investigated [27].

In the study of Sheikh, circular columns with 356 mm-diameter were subjected to a constant axial load and reversed cyclic lateral load. The main variables investigated were

axial load level, spacing of spirals, and the thickness and type of the FRP material. The test specimens were divided into three groups. The first group of specimens, which had four columns, had conventional longitudinal and spiral reinforcement. The second group, including six columns, was strengthened with carbon fiber reinforced polymers (CFRP), or glass fiber reinforced polymers (GFRP) prior to testing. In the third group, which includes two specimens, the columns were damaged to a certain extent, repaired with FRPs while the axial load was maintained, and then tested under lateral loads. It was observed from the test results that the strength, ductility, energy dissipation capacity of the FRP-strengthened columns was improved. It was concluded that the FRP composites were very effective for the rehabilitation of damaged RC columns [18].

Saadatmanesh conducted a series of tests on four columns in order to observe the effects of type of column geometry and FRP wrapping methodologies on the behavior. Two circular and two rectangular columns were prepared and tested until failure under reversed cyclic loading. The columns were repaired and strengthened with prefabricated FRP wraps, and re-tested. The tests results showed that all of the repaired columns performed extremely well under lateral loading. The repaired columns were observed to exhibit relatively larger lateral displacement at low load levels compared to the control specimens. For all of the repaired specimens, the rate of stiffness degradation under large levels of reversed cyclic load was lower than that of the corresponding original columns [9].

Fiber orientation of FRP sheets has been observed to influence the load-carrying capacity of a structural member, as well as of its mode of failure. It was suggested by numerous researchers that fiber orientation should be determined in order to increase the effect of FRP-strengthening for a desired response improvement. The study by Chaallal, and Shahawy investigated the effects of the orientation of the confining fibers on the performance of RC columns, and showed that the optimum angle of fiber orientation for axially loaded columns would range between 0 and 15 degrees. A parametric study was conducted on fiber orientation involving five different winding angles (0, 15, 30, 45 and 60 degrees). As a result of this study, it was concluded that the axial compressive strength of a RC columns decreases as the winding angle increases, its flexural capacity increases with the winding angle up to 45 degrees, and further increase in the winding angle reduces

the flexural capacity of the column in the tension-controlled portion of the interaction diagram [28].

The bond between the concrete surface and the FRP sheets is critical for FRP-strengthening applications as in every retrofitting procedure involving externally attached materials to existing members. Researchers have investigated the effects of mainly two different surface preparation techniques, namely wire brushing and water jetting, on the effectiveness of FRP applications. Superior performance has been achieved by water jetting of the concrete surface and using a high strength adhesive which results in improved bonding between the FRP composite and the concrete surface. In order to achieve the desired bond between the FRP and the concrete surface, Engindeniz et al. have pointed that the concrete surface should be thoroughly cleaned, a penetrating epoxy primer should be applied, and each ply should be placed between two coats of resin [29].

In tests conducted by Ghobarah and El-Amoury, the influence of using FRP sheets for improving the behavior of anchorage - deficient RC beams were investigated. “L-shaped” FRP sheets were installed with one leg of the “L” attached on the beam bottom surface and the other on the column to overcome the anchorage deficiency of beam bottom reinforcement. In addition, the shear deficient joint region was wrapped with FRP sheets. In order to prevent debonding of the FRP sheets, steel plates were installed in critical locations. This rehabilitation technique was found to be effective in eliminating the brittle joint shear and beam bond-slip failure modes. Importantly, Ghobarah and El-Amoury underlined the importance of an adequate anchorage system for the FRP application in order to maintain the efficiency of this strengthening technique [30].

Sheikh and Yau performed column tests on circular columns having 356 mm diameter, for evaluating the effectiveness of FRP as external reinforcement to strengthen deficient columns and repair damaged columns. 12 column specimens were tested under constant axial load and reversed cyclic lateral loads for investigating the effects of axial load level, spacing of spiral reinforcement, and the thickness and type of the FRP material. Four of the columns had conventional longitudinal and spiral transverse reinforcement and were tested without FRP wrapping. Six columns were strengthened with carbon FRP or glass FRP before testing, and the remaining two were tested to a certain damage level,

repaired with FRP and tested again to failure. FRP was used only in the transverse direction of the columns for confining the concrete. Test results showed that use of FRP resulted in remarkable improvement in the performance of the columns, resulting in significant increase in strength, ductility, energy dissipation capacity [31].

A theoretical study on the behavior of reinforced concrete columns externally confined with high-strength fiber composites straps was conducted by Saadatmanesh et al. Both GFRP and CFRP confining straps were wrapped around the column to improve the strength and ductility of existing RC columns. The results of this study showed that that the concrete compressive strength and strain ductility increased substantially when the columns were wrapped with GFRP or CFRP. In addition, the behavior of concrete columns, their strength and ductility in particular, were found to be significantly improved when wrapped with FRP straps [32].

Harajli and Rteil performed tests for evaluate the lateral load behavior of RC columns confined using FRP or containing steel fiber reinforcement. A total of 12 column specimens were tested in this study. The specimens were grouped into two series. In each series, six specimens were tested: one control specimen, two specimens confined with FRP, two specimens containing steel fiber reinforcement, and one confined with the minimum amount specified for conventional transverse reinforcement. The test results showed that CFRP confinement increased the strength of the columns and reduced the level of concrete spalling (crushing) and bond deterioration in the lap splice region. Similarly, internal confinement of concrete using steel fiber reinforcement was observed to reduce bond deterioration and improve the column behavior [33].

Iacobucci et al. investigated the prospect of strengthening deficient columns and repairing damaged columns with CFRP jackets. 8 specimens were constructed and tested under constant axial load and reversed cyclic lateral load. The test results showed that confinement with CFRP at critical locations enhances the ductility, energy dissipation capacity and strength of RC columns. It was observed that repaired columns behaved better as more layers of CFRP were used. Also, the level of damage before repair influenced the behavior of the repaired column specimens [34].

In the study of Mirmiran and Shahawy, columns of hybrid construction with FRP and concrete were tested to investigate their performance. The column specimens were produced by casting of concrete into an FRP tube. The tube acted as a formwork, a protective jacket, as well as confinement, shear and flexural reinforcement, all at the same time. For the study, 30 cylindrical specimens of 152.5 x 305 mm were tested under uni-axial compression. The results indicated that the FRP tubes, when used in this manner, significantly increase both the compressive strength and ductility of concrete subjected to axial loading [35].

Berthet et al. investigated the compressive behavior of short RC columns externally confined by carbon and E-glass FRP jackets. The influence of different parameters such as the confinement level, the mechanical properties of the jackets, and the compressive strength of the concrete core were studied. The results showed that external confinement can significantly improve the ultimate strength and ductility of the column specimens. The stress-strain response of confined concrete in compression was found to be almost bilinear: in the linear region, the behaviors of plain and confined concrete specimens were similar, whereas in the plastic region, the behavior of the confined concrete was found to depend mainly on the mechanicals properties of the FRP material. The test results demonstrated that the plastic region of the stress-strain response of concrete in compression depends on the stiffness of the jacket, and that the ultimate strength of the FRP jacket and the unconfined concrete strength are the most influential factors affecting the compressive strength and strain at compressive strength of the confined concrete. Also, the study indicated that the effectiveness of the confinement effect of the FRP jacket is reduced when the compressive strength of the concrete core increases [36].

1.3. Research Significance, Objectives and Scope

As outlined in the previous section, numerous experimental programs have been conducted by prior researchers for investigating the behavior of reinforced concrete members strengthened using various methodologies, some of which involve the use of Fiber Reinforced Polymers (FRPs) in different configurations. The effects of inadequate lap splices on reinforced concrete column behavior and retrofitting of lap splice-deficient

columns using FRP materials (oriented in the transverse direction) for confinement has also been previously investigated to some extent.

1.3.1. Research Significance

The significance of this study in particular is that it focuses on the effect of lap splice deficiency on the behavior of a reinforced concrete system, as opposed to the behavior of an individual member (column), as is mostly the case in the literature. The experimental study is conducted on a simple one-story one-bay frame system (portal frame) with inadequate lap splice length in the columns, in order to investigate how bond-slip deformations in the lap splice regions of the columns can influence the failure mechanism of such a simple frame system. As well, a new strengthening methodology is proposed, which involves the use of CFRP materials oriented both in longitudinal and transverse directions of the column, in order to improve not only the confinement properties, but also the flexural capacity of the column in the deficient lap splice region, for the intention of changing the failure mode of splice-deficient frames from bond-slip in the lap splice region to plastic hinge formations in beams. The experimental work was conducted on relatively large scale specimens, for a more reliable assessment of the efficiency of the strengthening methodology proposed.

1.3.2. Objectives

The primary objective of the study is to determine the effectiveness of a novel strengthening technique using Carbon Fiber Reinforced Polymers (CFRP) on RC frames with inadequate lap splices. The effects of lap splice deficiency on the behavior of one-bay one-story frames (portal frames) under reversed cyclic lateral loading will be investigated. The strength, ductility, energy dissipation capacity, and failure types / locations will be investigated in detail for the frame specimens tested. The improvements on the response, provided by the strengthening technique will also be discussed.

1.3.3. Scope

In order to reach the objectives mentioned above, an experimental program was conducted at the Boğaziçi University Structural Engineering Laboratory. Due to limitations on the experimental set up, this study includes only 2 / 3 scale two dimensional (plane) one-story one-bay frame specimens. The effects of infill walls on the response were not considered in this study. Two main deficiencies, including inadequate lap splice length on column longitudinal reinforcement and inadequate transverse reinforcement the in lap splice region, were selected as the key parameters to be investigated throughout the experimental study.

1.4. Report Outline

The scope and findings of an experimental study on the lateral load behavior and CFRP-strengthening of lap splice-deficient RC frames is presented in this thesis. In the first chapter, an introduction and a literature review, as well as the objectives and scope of this study were provided. The experimental setup, including design of the test specimens based on provisions of the latest Turkish Earthquake Code (TEC2007), specimen properties and parameters, the strengthening methodology used, instrumentation, and the testing methodology are described in Chapter 2. Experimental results and test observations are presented in Chapter 3. Details on test measurements (local deformation data) are also presented in Chapter 3. A discussion of the experimental results is provided in Chapter 4. Chapter 5 presents a summary of findings and recommendations for further research in this area.

2. EXPERIMENTAL SETUP

2.1. Introduction

Strengthening of RC frames with CFRP is a noteworthy issue because of ease of application and time-savings. Furthermore, the buildings can remain functional during the strengthening process. In order to find the effective strengthening technique, the deficiencies in the existing reinforced concrete frame elements must be identified correctly and improvements should be implemented to mitigate the negative effects of such deficiencies. In this study, the effect of inadequate lap splices on column longitudinal reinforcement at the bottom of the column was investigated, and a methodology was proposed to strengthen deficient lap splice regions.

Three large scale (2 / 3) reinforced concrete frames were constructed for the study. The first specimen, which is the control specimen, was designed and detailed according to the provisions of the Turkish Earthquake Code 2007. For the second specimen, the column longitudinal reinforcement was spliced over a length of 280 mm (20 bar diameter) at the bottom, and the spacing of transverse reinforcement was increased. The last specimen was identical with the second one, and was strengthened with CFRP application prior to testing. The strengthening methodology was determined to mitigate bond-slip failure in the deficient lap splice region and to migrate the location of nonlinear behavior (damage) to the beams, in the form of plastic hinge formation.

2.2. Design of the Test Specimens

In this section, the rules applied for the design and detailing of the test specimens are presented, in connection with provisions of the 2007 Turkish Earthquake Code. The frame specimens were detailed following the provisions for “high-ductility level” frame systems specified by the code. It should be noted that the size of the frame specimens, member dimensions, and longitudinal reinforcement ratios (influencing capacity) were selected also considering the limitations of the testing facility.

2.2.1. Turkish Earthquake Code (2007)

The general principle of earthquake resistant design provisions specified in TEC-2007 [37] is to prevent structural and non-structural elements of the buildings from any damage in low-intensity earthquakes, to limit the damage in structural and non-structural elements to repairable levels in medium-intensity earthquakes, and to prevent the overall or partial collapse of buildings in high-intensity earthquakes in order to avoid the loss of life.

2.2.2. Design Rules for Columns of High Ductility Level:

- For rectangular columns, the minimum dimension is 250 mm and minimum cross-sectional area is 75000 mm^2. For the frame specimens, column dimensions were selected as 250 mm, resulting in a cross-sectional area of $250x250 = 62500$ mm^2. This does not satisfy the minimum cross-sectional area requirements specified in the code; however, it must be noted that the specimens were not intended to be full-scale, but 2 / 3 scale.

- The gross sectional area of columns, should satisfy the following equation:

$$A_c \geq N_{dm} / (0.50\, f_{ck}) \tag{2.1}$$

where A_c is the gross section area of column, N_{dm} is the maximum axial force calculated by using load factors, and f_{ck} is the characteristic compressive strength of concrete.

- Table 2.1 indicates the required concrete cover from external surface of outermost reinforcing bar in TS 500 [38].

Table 2.1. Concrete cover requirements

In members which are in direct contact with the soil	$c_c \geq 50$ mm
Exterior columns and beams open to the atmosphere	$c_c \geq 25$ mm
Interior columns and beams not open to external effects	$c_c \geq 20$ mm
In shear walls and slabs	$c_c \geq 15$ mm
In shells and folded plates	$c_c \geq 15$ mm

The concrete cover was selected as $c_c = 20$ mm for all members of the frame specimens.

- The longitudinal reinforcement ratio should not be less than 1.0 % and more than 4.0 % of the gross area of the column. Accordingly, column longitudinal reinforcement ratio was selected to be larger than $\rho = 0.01$ for the test specimens, which results in a reinforcement area larger than $A_c\rho = (250x250)x0.01 = 625$ mm^2

- The minimum longitudinal reinforcements are 4ϕ16 or 6ϕ14 for rectangular columns. Accordingly, the longitudinal reinforcement of the columns of the test specimens was selected as 8ϕ14 (1232 mm^2).

- At the upper and lower ends of the columns, the code defines column confinement zones. Each of the confinement zones should be greater than 1 / 6 of the clear height of the column, and greater than 500 mm. Column mid-span zone is the zone between the two confinement zones.

- Lap splices of column longitudinal reinforcement should be made, as much as possible, within the column central zone. In this case the splice length shall be equal to the development length ℓ_b given in TS 500 for tension bars. The development length ℓ_b is calculated from;

$$\ell_b = 0.12(f_{yd}/f_{ctd})\phi \geq 20\phi \qquad (2.2)$$

where; f_{yd} is design yield strength of longitudinal reinforcement and f_{ctd} is design tensile strength of concrete.

Based on the equation above, for the test specimens, the development length is calculated as; $\ell_b = 41\phi \geq 20\phi$

- In the case where more than 50 % of longitudinal reinforcement is spliced at the bottom end of column, lap splice length shall be at least 1.5 times ℓ_b.

$$1.5\ell_b = 61.5\phi \geq 20\phi \tag{2.3}$$

Therefore, for the test specimens, a lap splice length of $1.5\ell_b = 61.5\phi = 61.5 \times 14 = 861$ mm $\approx$ 87 cm lap splice length should be used. In order to make the columns of the test specimens lap splice deficient, an inadequate lap splice length of $20\phi = 280$ mm was used.

- Longitudinal reinforcement ratio should not exceed 6.0 % at spliced regions. For the test specimens, $\rho = 0.0197$ is longitudinal reinforcement ratio, and therefore the total reinforcement ratio for the columns at the lap spliced region is $\rho = 2$ x 1.97% = 3.94 % < 6 %, which satisfies the code requirement.

- Special detailing (confinement) zones shall be arranged at the bottom and top ends of each column. Length of each of the confinement zones shall not be less than smaller of column cross section dimensions (diameter in circular columns), 1 / 6 the clear height of column (measured upward from floor level or downward from the bottom face of the deepest beam framing into the column), and 500 mm. Requirements for transverse reinforcement to be used in confinement zones are given below. Such reinforcement shall be extended into the foundation for a length equal to at least twice the smaller of column cross section dimensions.

For the test specimens, the clear height of the column is 1750 mm. Therefore, the length of the special confinement zones in the columns was calculated as:

$$\text{Greater of} \left.\begin{matrix} 1750/6 = 291\,\text{mm} \\ 500\,\text{mm} \end{matrix}\right\} \text{Length of confinement zone} = 500\ \text{mm}$$

- The minimum diameter of transverse reinforcement is ϕ8 in the confinement zones. The spacing of transverse reinforcement should not be greater than 1 / 3 of the smallest dimension and 100 mm, and not less than 50 mm. Less than ϕ8 bars shall not be used in confinement zones as transverse reinforcement. Lateral distance between legs of hoops and crossties, *a*, shall not be more than 20 times the hoop diameter.

  For the test specimens, the smallest column dimension is 250 mm. Therefore, the spacing of transverse reinforcement should not:

  be greater than 250/3 = 83 mm
  be greater than 100 mm
  less than 50 mm

  } Accordingly, the spacing between transverse reinforcement in confinement zones was selected as 80 mm for the columns.

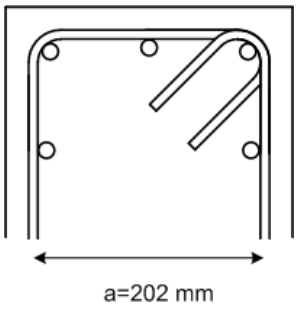

The unsupported tie length ***a*** should be smaller than 20 x 8 = 160 mm. For this reason either cross-ties must be used on the side bars, or the rectangular ties must be supplemented by diamond-shaped ties. The latter was used for the test specimens, as shown below.

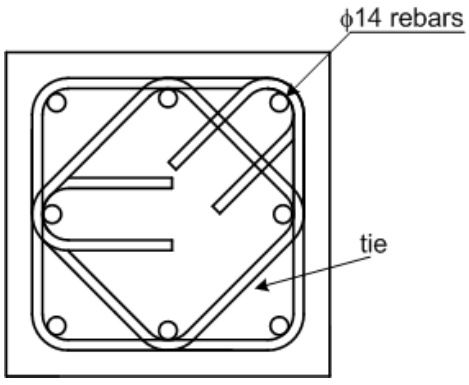

- In the case where $N_d > 0.20\, A_c f_{ck}$ for columns with hoops, minimum total area of transverse reinforcement to be used in confinement zones shall be calculated to satisfy the more unfavorable of the requirements given in Eq.(2.4). In this calculation, core diameter of column, b_k, shall be considered separately for each direction. Where; A_{sh} can be defined as along the height corresponding to transverse reinforcement spacing s, sum of projections of cross section areas of all legs of hoops and crossties of columns or wall end zones in the direction perpendicular to b_k considered, A_{ck} is concrete core area within outer edges of confinement reinforcement and f_{ywk} is characteristic yield strength of transverse reinforcement.

$$A_{sh} \geq 0.30 s\, b_k \left[\left(A_c / A_{ck}\right) - 1\right]\left(f_{ck} / f_{ywk}\right) \tag{2.4}$$

Thus, for the test specimens, $A_{sh} / s \geq 0.30 \times 202 \left[\left(250^2 / 210^2\right) - 1\right]\left(20 / 420\right) = 1.2040$

$$A_{sh} \geq 0.75\, s\, b_k \left(f_{ck} / f_{ywk}\right) \tag{2.5}$$

$$A_{sh} / s \geq 0.75 \times 202 (20 / 420) = 0.725$$

For a selected spacing of s = 80 mm;

$A_{sh} = 8 \times 1.2040 = 9.632$ mm^2 (unfavorable)

$A_{sh} = 3\pi 8^2 / 4 = 150.8$ mm^2 (existing)

The existing amount of transverse reinforcement on the columns is therefore adequate. To check:

$150.8 / s \geq 1.2040 \rightarrow s$ should not be bigger than 125 mm.

Column central zone is the region between the confinement zones defined at the bottom and top ends of the column (Figure 2.1). Transverse reinforcement with a diameter less than ϕ8 shall not be used along the column central zone. Along this zone, spacing of

hoops and crossties shall not be more than half the smaller cross section dimension and 200 mm. Lateral distance between the legs of hoops and crossties, a, shall not be more than 25 times the hoop diameter. Therefore, for the test specimens, the spacing of the ties in column central zone:

Shall not be more than;
$s = 250 / 2 = 125$ mm
$s = 200$ mm

Accordingly, $s = 120$ mm is selected for transverse reinforcement in the central zone

2.2.3. Design Rules for Beams of High Ductility Level:

- Dimensional requirements of cross-section of beams forming frames together with columns, or of beams connected to structural walls in their own planes are given below:

  (a) Width of the beam web shall be at least 250 mm. Web width shall not exceed the sum of the beam height and the width of the supporting column in the perpendicular direction to the beam axis.

  (b) Beam height shall not be less than 3 times the thickness of floor slab and 300 mm, nor shall it more than 3.5 times the beam web width.

  (c) Beam height should not be more than 1 / 4 the clear span.

  Therefore, for the test specimens, beam dimensions were selected as $b_w = 250$ mm (width of the beam) and $h = 350$ mm (beam height)

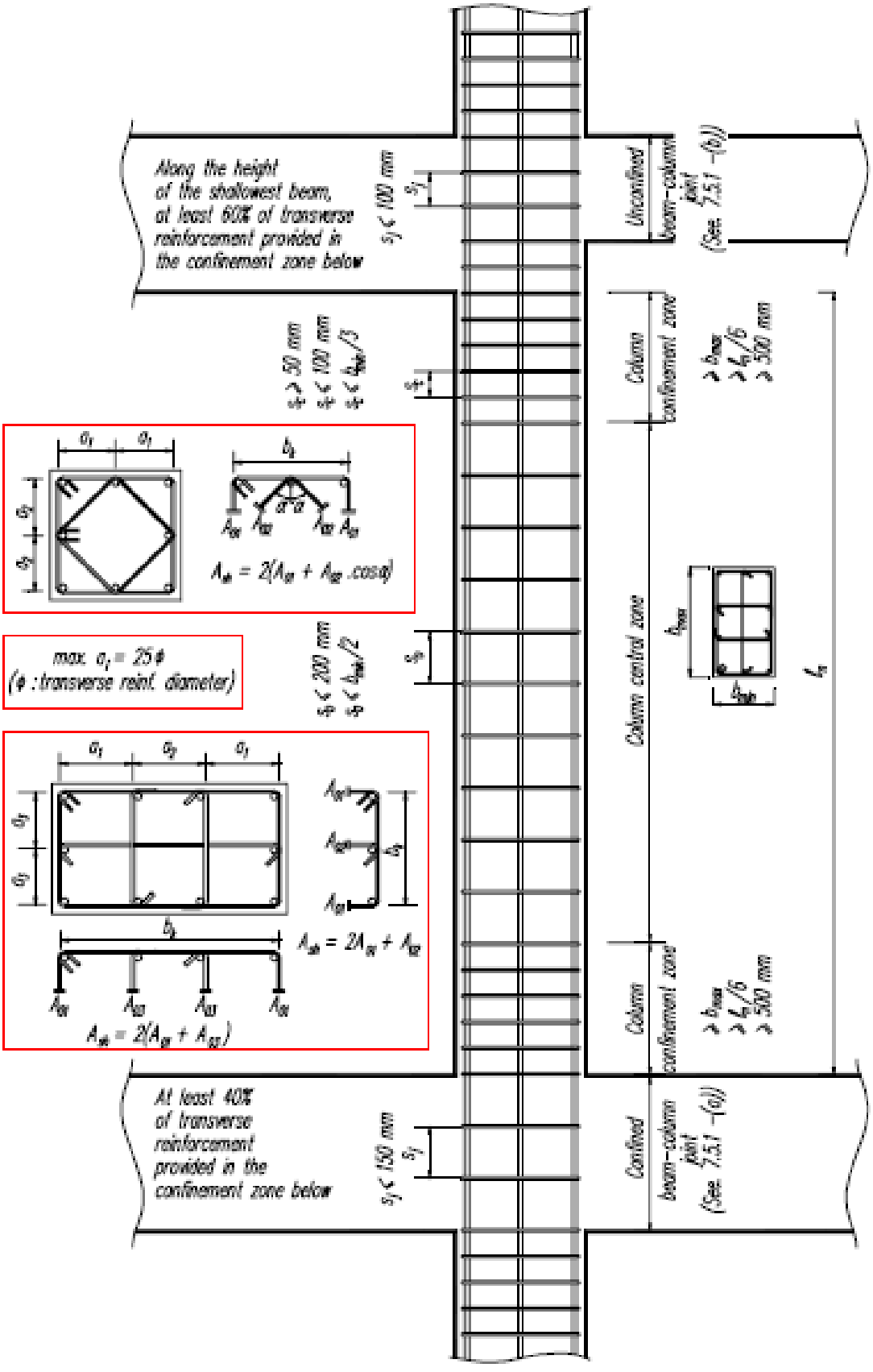

Figure 2.1. Provisions of TEC-2007 for Column Reinforcement Layout

- The requirement given by Eq.(2.6) shall be applied as the minimum ratio of top tension reinforcement at beams supports.

$$\rho \geq 0.8 f_{ctd} / f_{yd} \tag{2.6}$$

Therefore, for the specimens, $\rho \geq 0.8 f_{ctd} / f_{yd} = 0.002$ is the minimum reinforcement ratio for the beams.

- Diameter of longitudinal rebars shall not be less than 12 mm. At least two rebars each at the bottom and top of the beam shall be continuously provided along the full span length of the beam. For the specimens, two ϕ12 rebars at the bottom and two ϕ12 rebars at the top of the beam are used, as shown below.

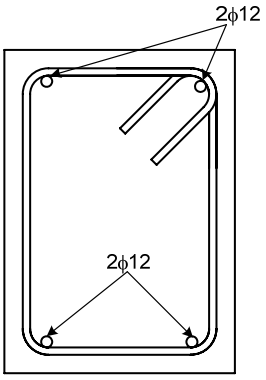

- At least 1 / 4 of the maximum of the top reinforcement at the supports of a beam shall be extended continuously along the full span length. The remaining part of the top support reinforcement shall be arranged in accordance with TS 500. The specimens satisfy this requirement since beam reinforcement is continuous across entire beam span.

- In cases where beams framing into columns are not extended to the other side of columns, bottom and top beam reinforcement shall be extended up to the face of the other side of the confined core of the column and then shall be bent 90 degrees from inside the hoops. In this case, total length of the horizontal part of the longitudinal rebar inside the column and the 90 degree bent vertical part shall not be less than the

straight development length specified in TS 500. Horizontal part of the 90 degree bent shall not be less than 0.4 ℓ_b and vertical part shall not be less than 12 ℓ_b (Figure 2.2). For the test specimens, the beams were anchored into the confined beam-column joint with adequate hooks satisfying this provision, as illustrated in Figure 2.3.

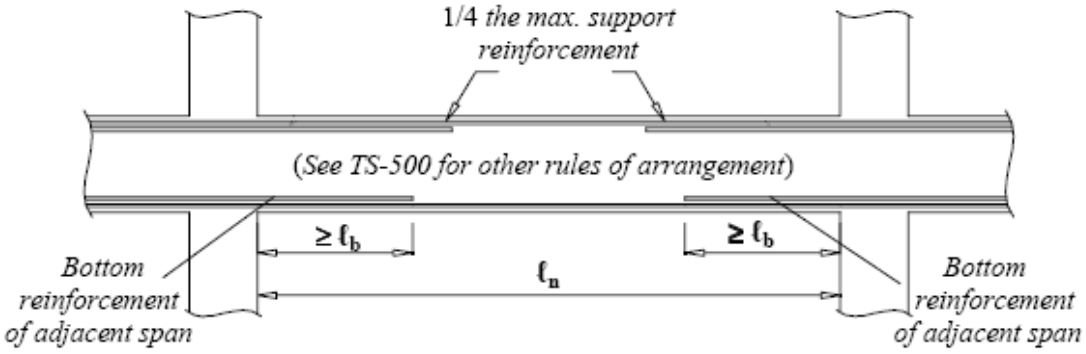

(a)

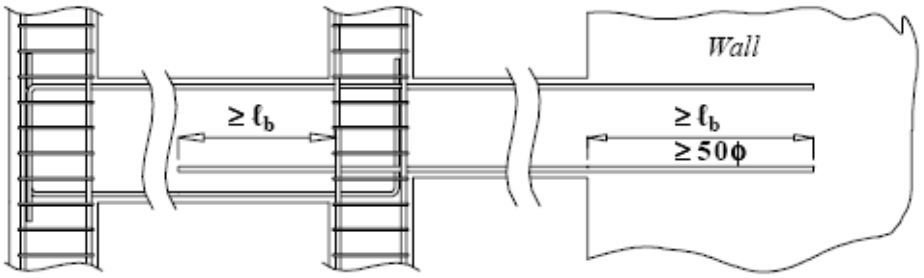

(b)

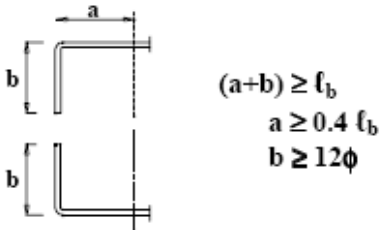

(c)

Figure 2.2. Provisions for the Layout of the Longitudinal Reinforcement in Beams

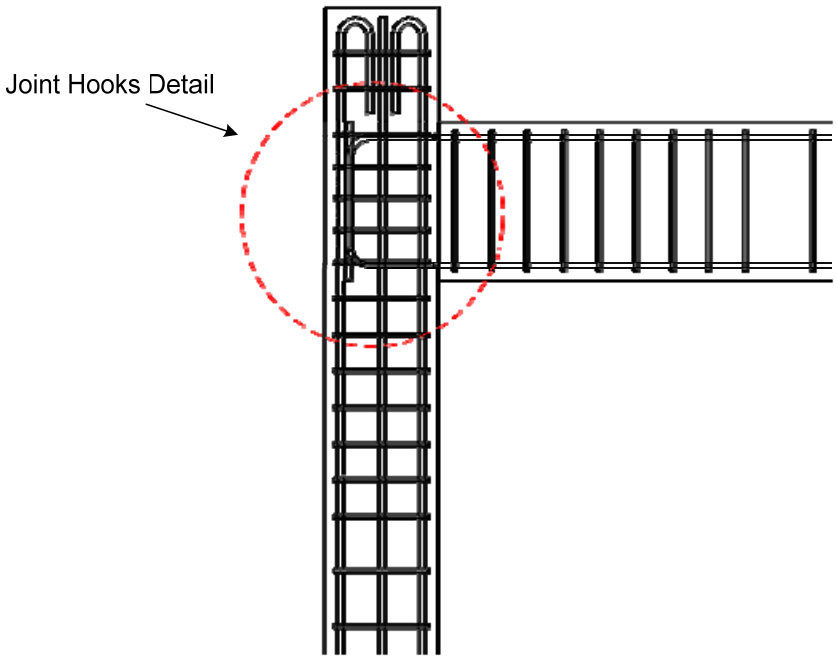

Figure 2.3. Beam Longitudinal Reinforcement Hooks used in the Test Specimens

- In the case where beams frame into columns from both sides, beam bottom rebars shall be extended to the adjacent span from the column face by at least the development length, ℓ_b, given in TS 500. In cases where this is not possible because of reasons such as the depth difference in beams, development shall be achieved in a way similar to parameter above, i.e., to the case where beam is not extended to the other side of the column. This provision does not apply to the test specimens since the beam frames into the column only on one side.

- A region with a length twice the beam depth measured from the column face of a beam support shall be defined as confinement zone and special seismic hoops shall be used along this region. In the confinement zone, distance of the first hoop to the column face shall be maximum 50 mm. Unless a more unfavorable value is obtained, hoop spacing shall not exceed 1 / 4 the beam depth, 8 times the minimum diameter of the longitudinal reinforcement and 150 mm (Figure 2.4.). Outside the confinement zone, minimum transverse reinforcement requirements specified in TS 500 shall be applied.

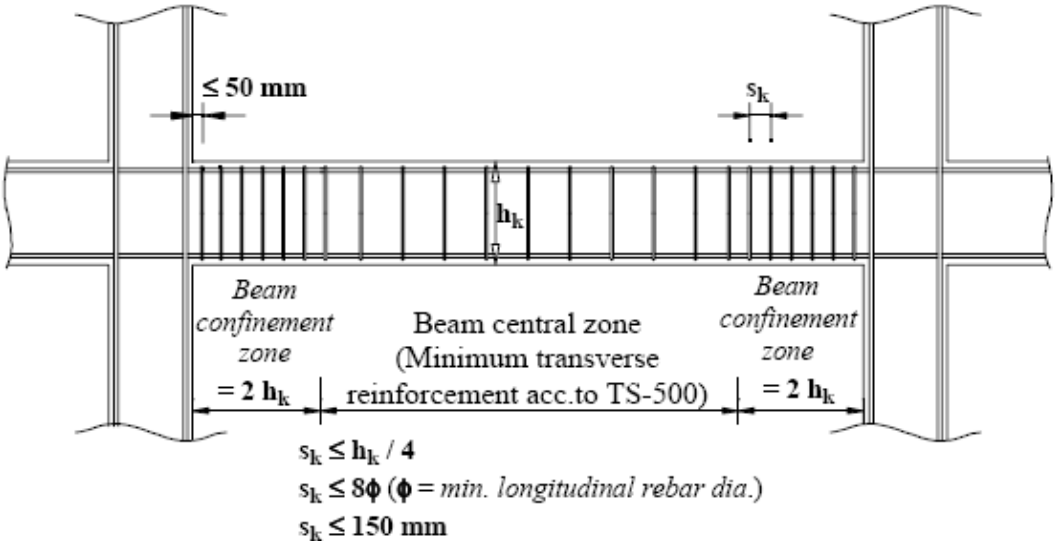

Figure 2.4. Transverse Reinforcement Layout Provisions for a Beam

Therefore, for the beam of the test specimen a length of $= 350 \times 2 = 700$ mm should be confined. Within this confinement zone, the spacing of the stirrups should not exceed:

$$\left.\begin{array}{c} h/4 = 350/4 = 87.5 \text{ mm} \\ 8 \times 14 = 112 \text{ mm} \\ 150 \text{ mm} \end{array}\right\} \text{within confinement zone}$$

Accordingly, a stirrup spacing of $s = 80$ mm for the confinement zone of the beam for the test specimens.

On the other hand, outside the beam confinement zone, which corresponds to a span of 2400 - (700 + 700) = 1000 mm, the spacing of the stirrups cannot exceed:

$$s \le \frac{d}{2} \quad \text{from TS} - 500$$

$$s \le \frac{315}{2} = 157.5 \text{ mm} \approx 150 \text{ mm}$$

Accordingly, a stirrup spacing of 150 mm was selected for the beams of the test specimens outside of the confinement zones.

2.3. Properties of Specimens and Test Parameters

Test specimens were designed as one-bay one-story frames (portal frames). The column lengths were selected as 2500 mm and the cross-section of the columns were 250 mm x 250 mm. The length of the beam from the column face was 2400 mm, and it had 250 mm x 350 mm cross-section. The beam reinforcement was selected based on the flexural capacity ratio of the column to the beam. In order to satisfy strong column-weak beam requirements, the flexural capacity ratio was selected to be larger than 1.2. The dimensional details of the specimen are illustrated in Figure 2.5.

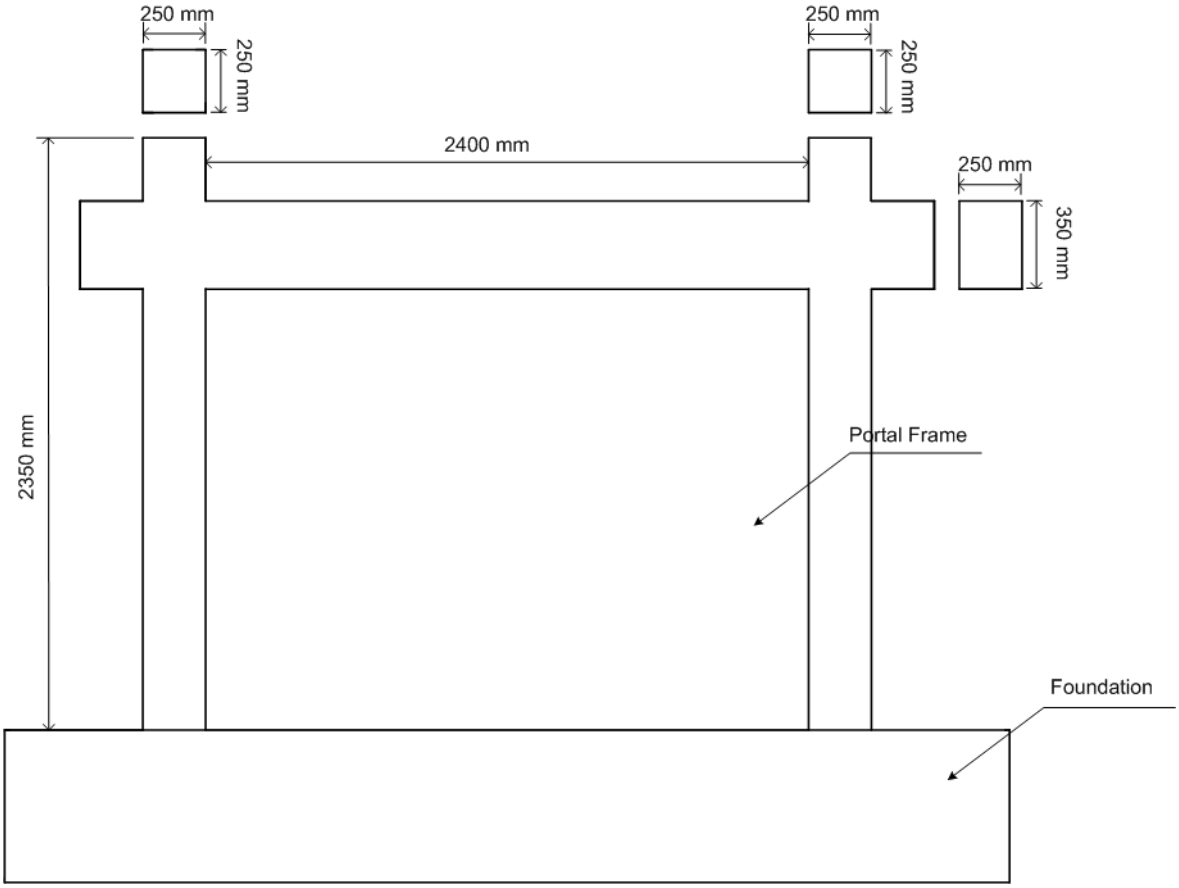

Figure 2.5. Test Specimen

In the study, 3 RC frame specimens were constructed. The first specimen was detailed to satisfy the requirements of the TEC-2007, and was called the “Control Specimen”. The other two specimens were also designed according to the TEC-2007. However, in order to understand the effects of the inadequate lap splice length on the behavior, the lap splice length was held shorter than that proposed by the TEC-2007. The

second specimen was called specimen “LS”. The third specimen, which was named specimen “LS-FRP” was strengthened with CFRP sheets, as well as CFRP and steel anchorages to improve the behavior.

2.3.1. Flexural Capacity of Members

During the design process of the test specimens, sectional (moment vs. curvature) analyses were conducted for the beam and the column (under 30 % $A_g f'_c$ axial load) sections of the test frames, using the software “Response-2000: Reinforced Concrete Sectional Analysis” [39]. The properties of column and beam cross-sections are given in Figure 2.6 and the results of the sectional analyses are shown in Figure 2.6. As can be deducted from the analysis results, the column-to-beam flexural moment capacity ratio for the test frames exceeds the minimum required ratio of 1.2 specified in the earthquake code. A relatively larger ratio was used to ensure flexural yielding (plastic hinge formation) in the beam of the test specimen, prior to yielding at the bottom of the columns, since larger bending moments were expected to develop at the bottom of the columns, compared to the top.

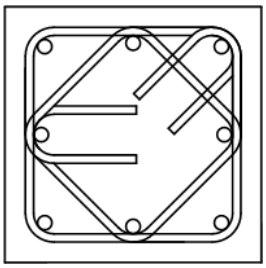

8ϕ14 Longitudinal Reinforcement
ϕ8 ties

(a) Column cross-section

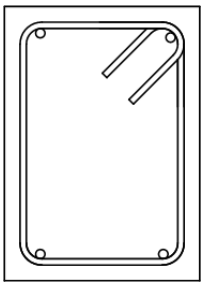

4ϕ12 Longitudinal Reinforcement
ϕ8 ties

(b) Beam cross-section

Figure 2.6. Cross-section Properties of Column and a Beam

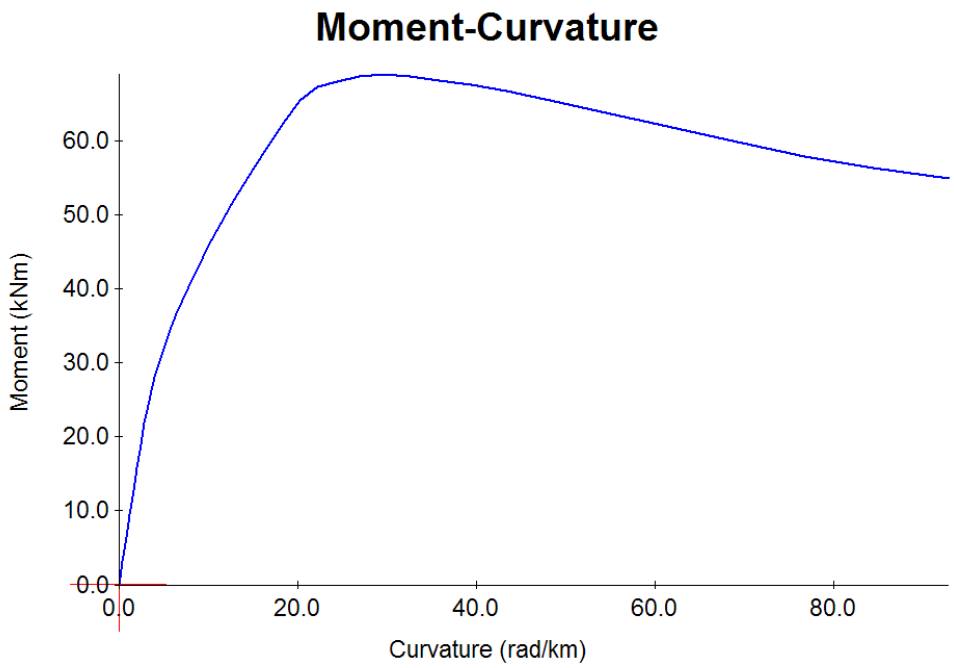

(a) Moment Curvature relationships of column (M_{max}= 69.1 kNm)

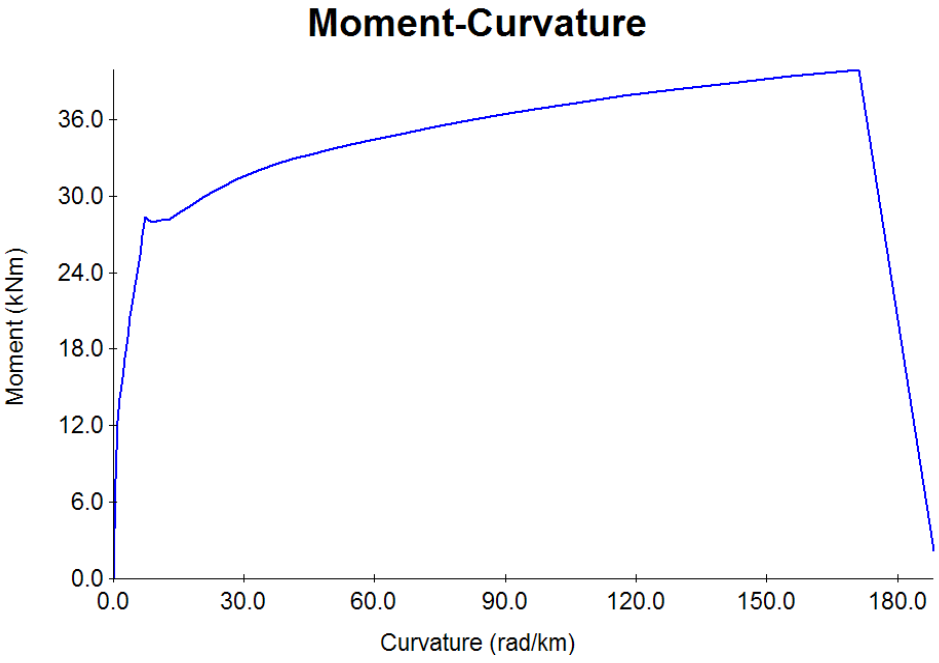

(a) Moment Curvature relationships of beam (M_{max}= 39.9 kNm)

Figure 2.7. Flexural Capacity Analysis of a Column and a Beam

2.4. Material Properties

2.4.1. Concrete

According to TEC-2007, the design compressive strength of concrete should not be less than 20 MPa. Therefore, the design compressive strength of the concrete used in the construction of the specimens was 20 MPa. Ready mixed concrete was used in the construction. 9 samples of concrete cylinders were taken from each specimen. These samples were tested on 7^{th} day, 28^{th} day and the day that the experiments were conducted. Out of 2 cylinder specimens that were tested on the testing day, an average compressive strength of 30 MPa was obtained.

While concrete is poured, cylindrical test specimens with 150 x 300 mm dimensions were taken. After a 28 day period, compressive strength tests were conducted on three specimens. The modulus of elasticity of the concrete was computed according to uni-axial stress-strain test data. The initial slope of the stress-strain curves was taken as the modulus of elasticity. The uni-axial compressive test results are given in Table 2.2.

Table 2.2. Concrete Compressive Test Results after 28 Days

Test Specimen	Compressive Strength	Modulus of Elasticity
Test 1	28 MPa	26.5 GPa
Test 2	30 MPa	27.4 GPa
Test 3	31 MPa	27.9GPa
Average	**30 MPa**	**27.3 GPa**

2.4.2. Reinforcing Bars

Designed yield strength of the reinforcing steel used in the construction of the test specimens was 420 MPa. Deformed bars were used for both transverse and longitudinal reinforcement of the columns and the beam. Uni-axial tension tests conducted on these reinforcing bars revealed an average yield strength of 520 MPa. Table 2.3 indicates the measured yield strengths of the reinforcement used. In addition, stress vs. strain relationships for all types of reinforcements are given in Figures 2.8. to 2.11.

Table 2.3. Yield Strengths of Reinforcement

Diameter	f_y (MPa)	Location
ϕ 20	500	Pedestal longitudinal reinforcement
ϕ 14	510	Column longitudinal reinforcement
ϕ 12	540	Beam longitudinal reinforcement
ϕ 8	500	All transverse reinforcement

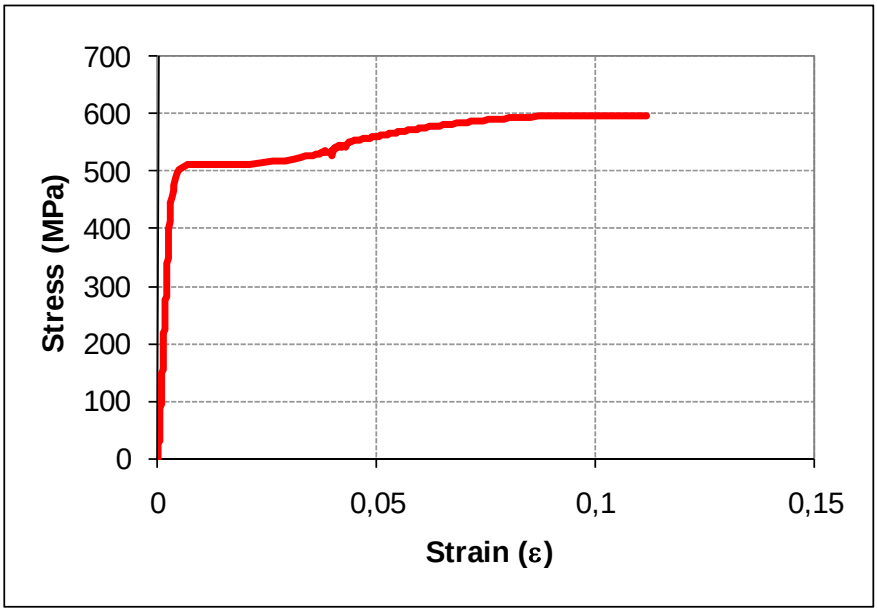

Figure 2.8. Stress-Strain Relationship for ϕ20 Reinforcement

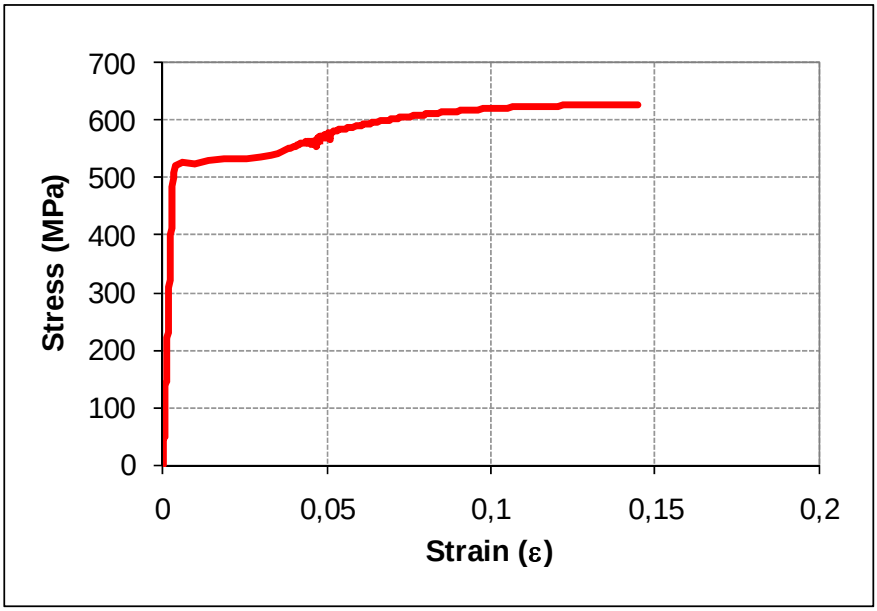

Figure 2.9. Stress-Strain Relationship for ϕ14 Reinforcement

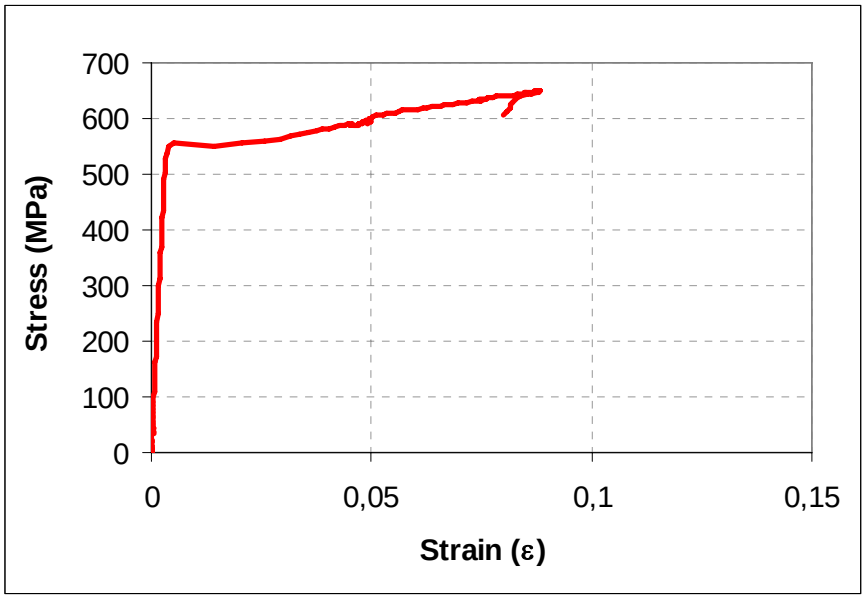

Figure 2.10. Stress-Strain Relationship for ϕ12 Reinforcement

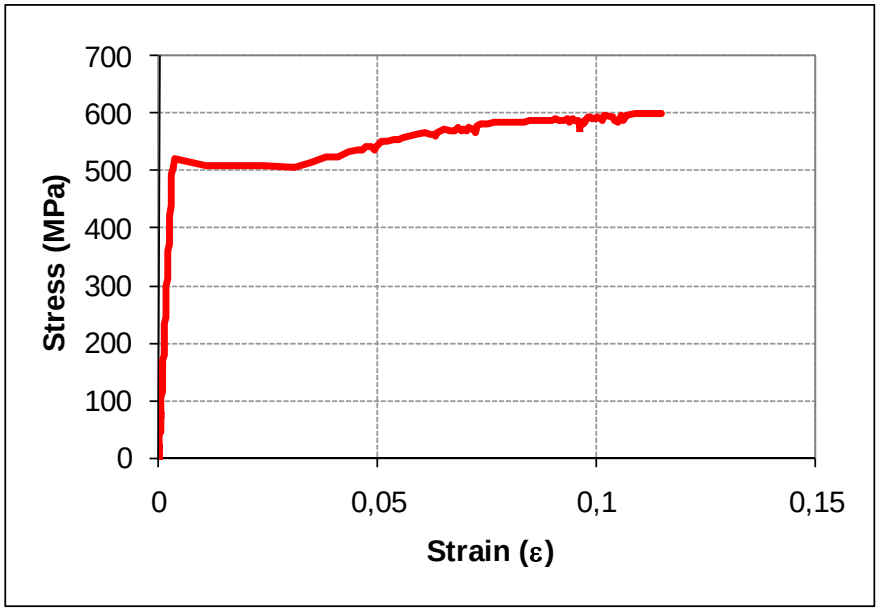

Figure 2.11. Stress-Strain Relationship for ϕ8 Reinforcement

2.4.3. Carbon Fiber Reinforced Polymers (CFRP)

In this research, CFRP materials were used in order to strengthen the deficient lap splice regions of the frame specimens tested. For the strengthened specimen, CFRP wrapping orientation was applied considering the damage and crack pattern that occurred

in the control specimens. Properties of the CFRP used are given in Table 2.4 and its stress-strain relationship is given in Figure 2.12. Properties of the CFRP sheets were taken from the manufacturer data sheet.

Table 2.4. Properties of CFRP.

Nominal Thickness	0.117 mm/ply
Ultimate Tensile Strength (0°)	3800 MPa
Tensile Modulus (0°)	240 GPa
Ultimate Rupture Strain (0°)	1.55 %
Weight	230 g/m^2

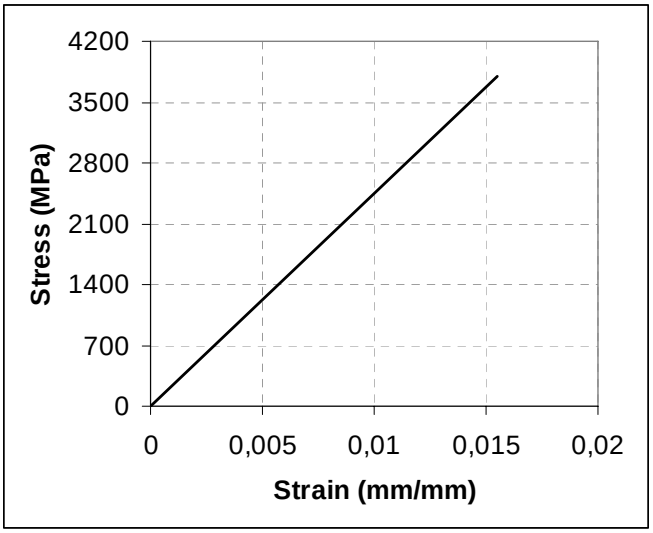

Figure 2.12. Stress-Strain Relations of CFRP

2.5. Construction of Test Specimens

Three reinforced concrete frame specimens were constructed at the Structures Laboratory of Boğaziçi University. The pedestals of the specimens were first constructed, followed by construction of the columns and the beams. Figure 2.13 shows various stages of construction of the test specimens.

Figure 2.13. Production of Test Specimens

2.5.1. Control Specimen

The control specimen was designed according to detailing provisions of the 2007 Turkish Earthquake Code (TEC-2007). The reinforcement detail of the control specimen is illustrated in Figure 2.14. 8ϕ14 deformed bars were used for column longitudinal reinforcement and 4ϕ12 deformed bars were used for beam longitudinal reinforcement. The spacing of stirrups was selected as 80 mm in the special detailing regions of the column and the beam. Outside the special detailing regions, 120 mm and 150 mm spacings were used for transverse reinforcement of the column and the beam, respectively. Column longitudinal reinforcement ratio was selected as 1.0 %, which satisfies the minimum column reinforcement requirements in TEC-2007. The beam longitudinal reinforcement

was selected to satisfy a strong column-weak beam condition, as also specified by the code.

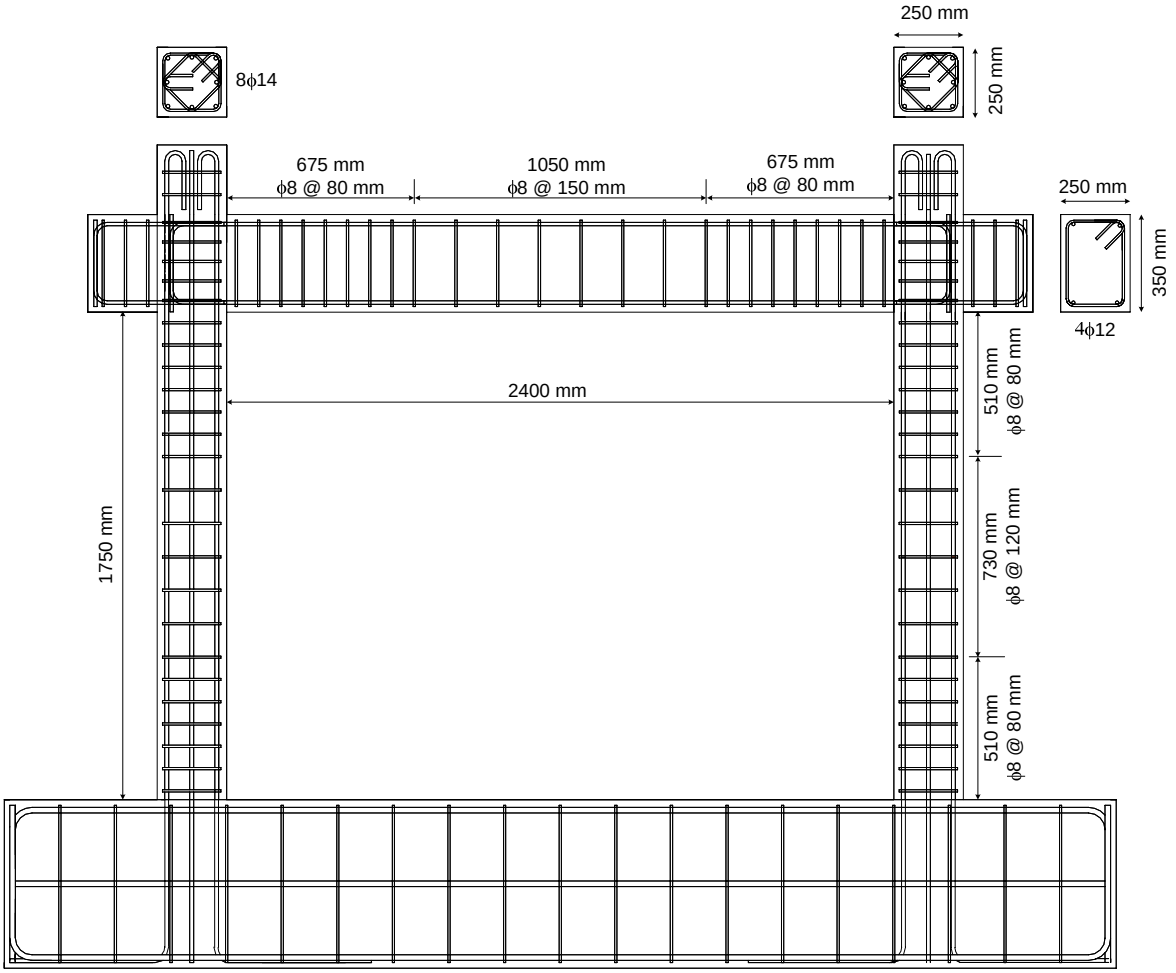

Figure 2.14. Reinforcement Details for Control Specimen

2.5.2. Specimens LS and LS-FRP

The deficient lap splice specimens (specimen LS and specimen LS-FRP) were also designed according to the requirements of TEC-2007, except for lap splice length. Dimensions and reinforcing details were identical with the control specimen, with the exception of lap splice length of 280 mm (20 bar diameter) at the base of the columns, and inadequate transverse reinforcement (1 stirrup only) in the lap splice region. Figure 2.15 shows the reinforcement details of specimens LS and LS-FRP. Specimen LS was tested as it is, and specimen LS-FRP was strengthened with the methodology described in next section.

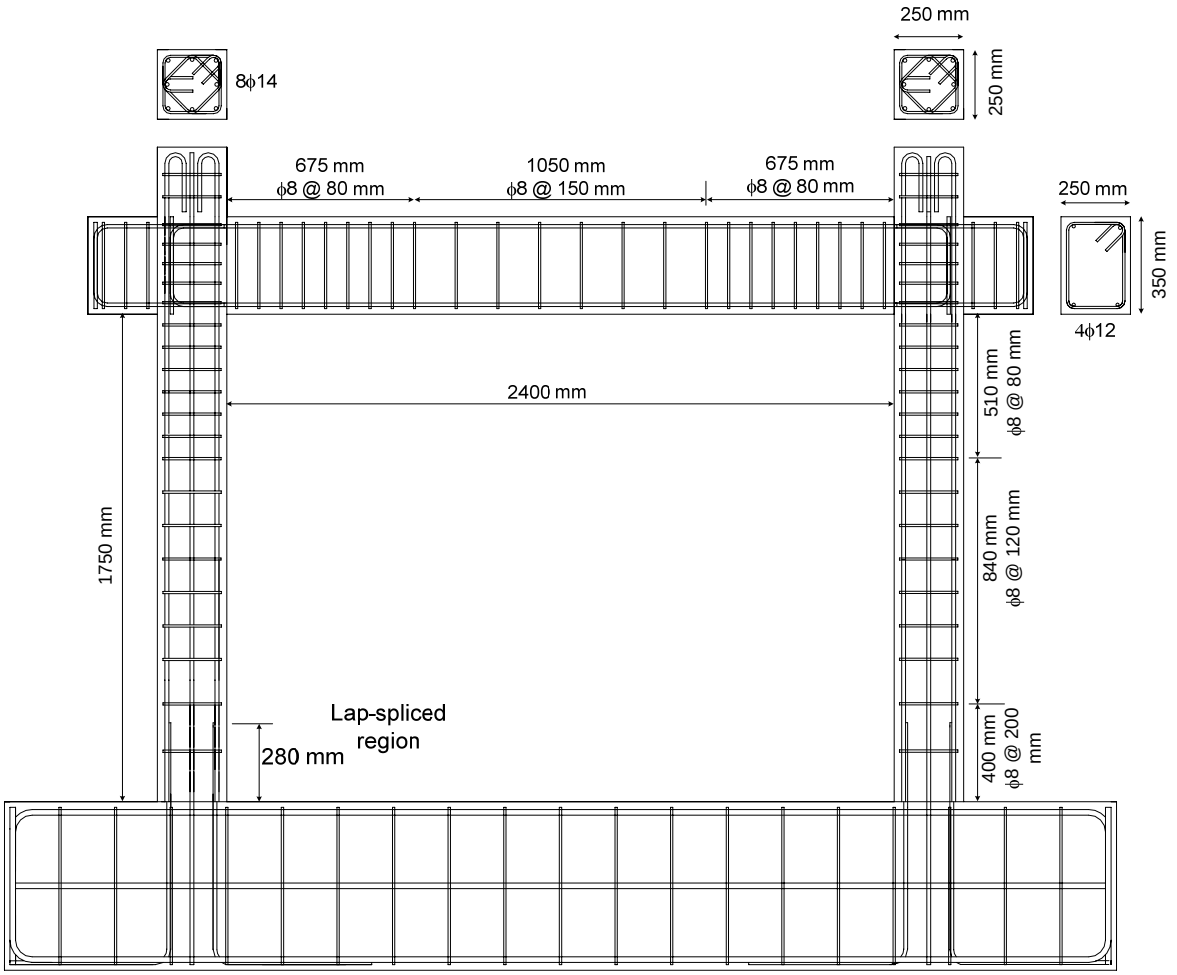

Figure 2.15. Reinforcement Details for Specimen LS and LS-FRP

2.6. CFRP Strengthening Methodology

Installation of CFRP sheets need special care and only can only be carried out by trained technicians. When combined with epoxy, CFRP sheets become very strong in tension. CFRP wrapping provides excellent passive type of confinement effect to the reinforced concrete members. Stages of the CFRP application technique used in this study to strengthen the deficient lap splice regions of the columns is illustrated in Figure 2.16. The procedure for installing the CFRP sheets is described in detail in the following subsections.

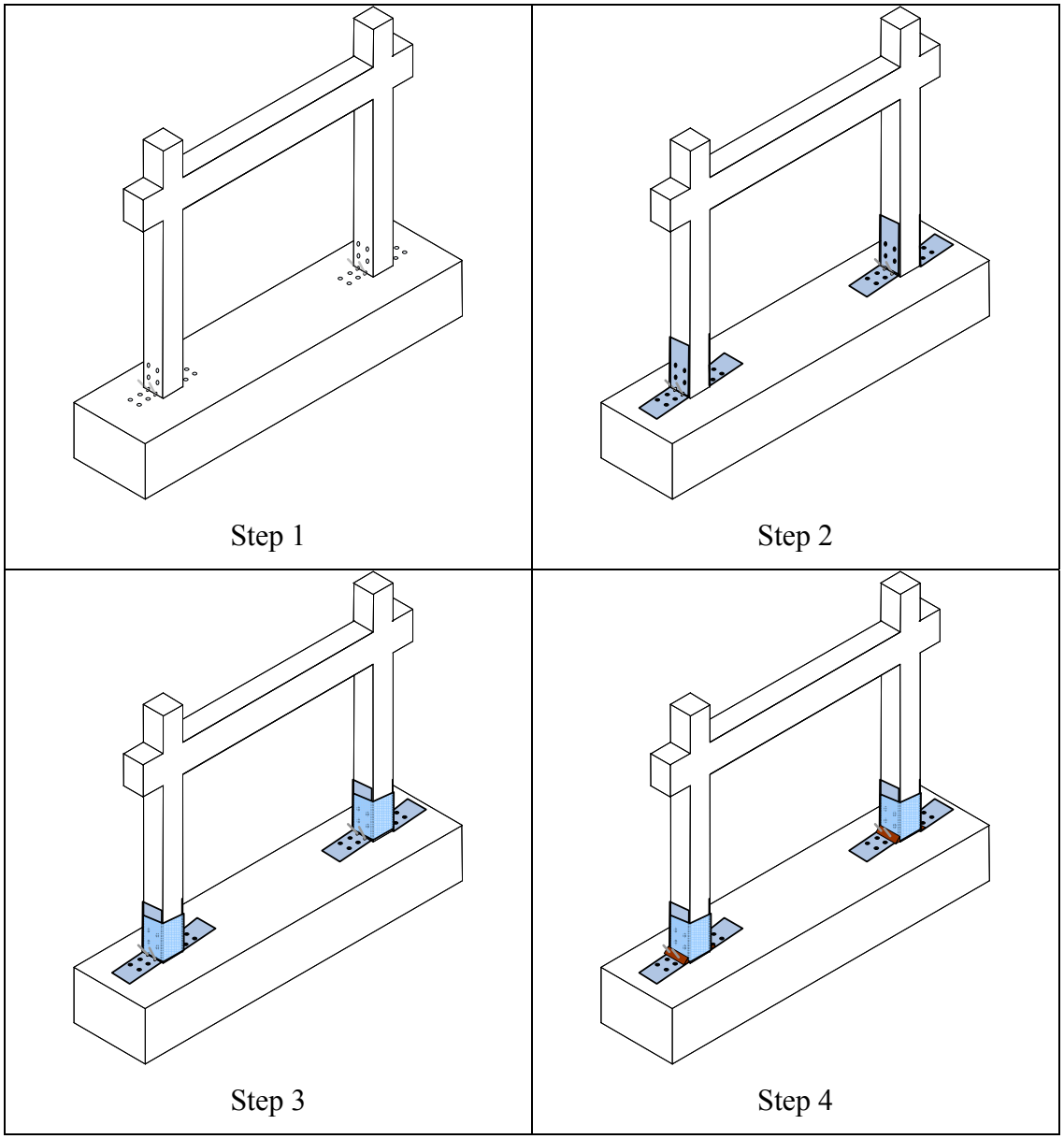

Figure 2.16. CFRP Application

2.6.1. Surface Preparation

As a first step, all the faces of the column and pedestal (footing) regions were smoothened and column corners were rounded. The corners were smoothened at about 20 mm radius, since increasing the radius of corner, increases the confinement effects of CFRP [40]. All large gaps in concrete were filled with putty (*Concressive 1406*), large particles were removed, and the area which is going to be wrapped was cleaned with a wire brush. The surface was vacuumed to obtain a clean surface.

A primer (*MBrace Primer*), which helps the adhesion of the CFRP to the concrete, was applied to the surfaces with roll brush. A 24-hour curing time was passed prior to application of the CFRP (Figure 2.17).

Figure 2.17. Primer Application

2.6.2. CFRP Application

After the primer was cured, the two components- epoxy adhesive of CFRP, *MBrace Adesivo* (*Saturant*), was prepared and CFRP fabrics were installed on the lap spliced region. It was made sure that, no air pockets remained under the CFRP sheets. It should be noted that the epoxy mix has approximately 30 minute working time before it gets hot and dense (Figure 2.18)

Figure 2.18. Epoxy Matrix

The CFRP strengthening methodology used is explained step by step in the following.

Step 1: Diagonal Steel Anchorages in Column – Footing Interface

In order to prevent debonding of CFRP from the corner of the column-footing intersection, two 20 mm diameter and 200 mm long holes were drilled diagonally at each corner (Figure 2.19). Next, 18 mm diameter rods were installed in the holes using high strength chemical epoxy (*Concresive 1495*).

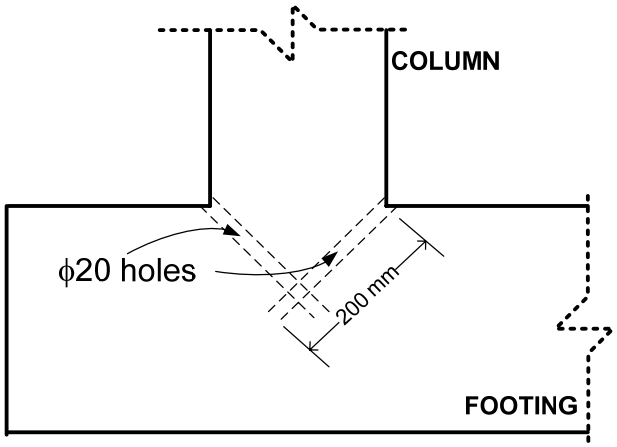

Figure 2.19. Steel Anchorages Holes

Step 2: Drilling of CFRP Anchorage Holes

In order to prevent debonding of the CFRP from the column surface and the footing surface, 4 holes with 12 mm diameter were drilled in each column and a total of 16 holes with 150 mm depth were drilled in the footing. The holes were drilled for the purpose of installing CFRP anchorages in the columns and footing. Locations of the anchorage holes are illustrated in Figure 2.20.

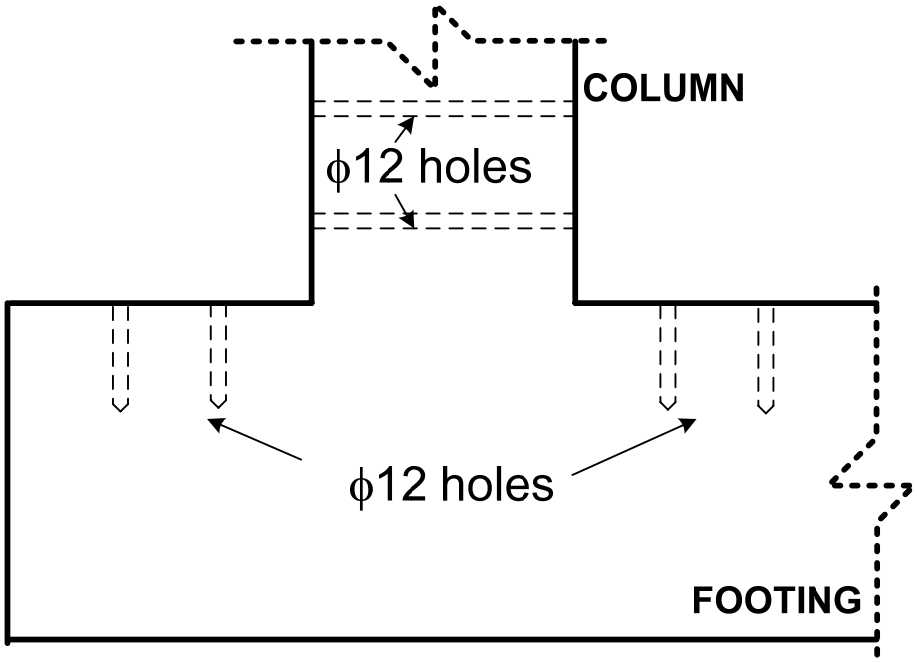

Figure 2.20. CFRP Anchorages Holes

Step 3: “L shaped” CFRP sheets

For increasing the flexural capacity of the columns, in the deficient lap splice region, three layers of “L shaped” CFRP sheets were applied on the exterior and the interior surfaces of the column - footing intersections. These “L shaped” CFRP sheets were intended to act as supplemental longitudinal reinforcement for the columns in the splice region. Application of the “L shaped” CFRP sheets are shown in Figure 2.21.

Figure 2.21. “L Shaped” CFRP

Step 4: CFRP Anchorages

In order to avoid premature debonding, the “L shaped” CFRP sheets were anchored in the concrete using CFRP anchors installed into the holes drilled in the footing and the columns. To produce the CFRP anchors, 150 mm-wide CFRP sheets were rolled into tubes and were sliced open at one end into four strips, which were spread out (Figure 2.22).

Figure 2.22. CFRP Anchorages

Step 5: Column Wrapping

In order to induce confinement effect using the CFRP material the lap splice region of the columns were wrapped with 3 layers of 500 mm wide CFRP sheets (Figure 2.23).

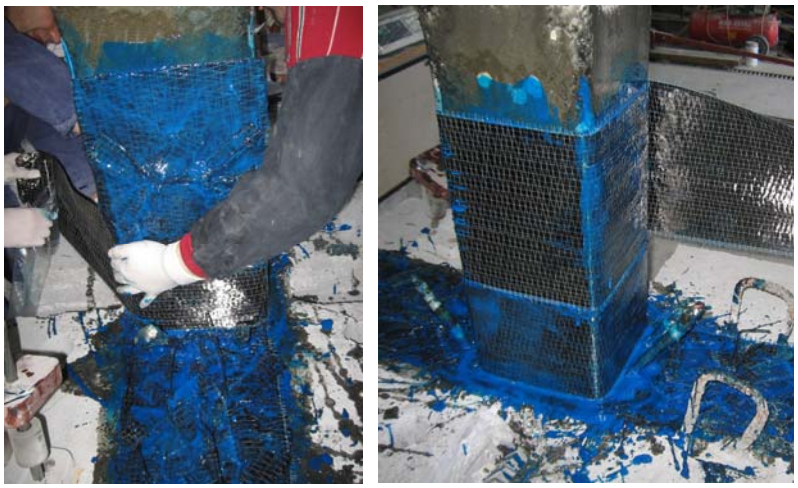

Figure 2.23. Column Wrapping

Step 6: Diagonal Steel Anchorages

Finally, as shown in Figure 2.24, the “L shaped” CFRP sheets were anchored to the column - footing intersection with special steel assemblies that include L-shape steel plates, semi-circular connectors with slots, and 18 mm diameter high strength steel rods epoxied into the holes described in Step 1. By this method, the corners of the “L shaped” CFRP sheets, which are the most critical regions for debonding, were strongly anchored.

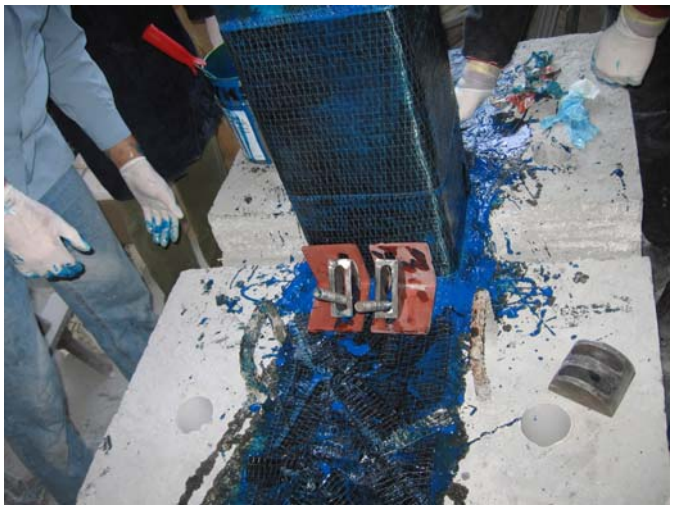

Figure 2.24. Steel Anchorages

2.7. Testing Methodology

The tests were performed according to ACI T1 [41] document. The requirements of the test procedure can be summarized as follows:

- Test modules shall be subjected to a sequence of displacement-controlled cycles representative of the drifts expected under earthquake motions for that portion of the frame represented by the test module. Cycles shall be to predetermined drift ratios.

- Three fully reversed cycles shall be applied at each drift ratio. (Figure 2.25)

- The initial drift ratio shall be within the essentially linear elastic response range for the module. Subsequent drift ratios shall be to values not less than one and one-quarter times, and not more than one and one-half times, the previous drift ratio.

- Testing shall continue with gradually increasing drift ratios until the drift ratio equals or exceeds 0.035.

- Data shall be recorded from the test such that a quantitative, as opposed to qualitative, interpretation can be made of the performance of the module. A continuous record shall be made of test module drift ratio versus column shear force, and photographs shall be taken that show the condition of the test module at the completion of testing for each sequence of three cycles.

The lateral load was applied based on the displacement control criteria. The loading cycles are shown in Figure 2.25. Approximately 35-40 reversed cycles, depending on the behavior of the specimen, were applied throughout the test. All data was collected with a TML 602, 50 Hz. and 50 channel data acquisition system. Observations on cracks on concrete surface, CFRP fractures and debonding, and failure modes were recorded in each of 3-cycle loading set.

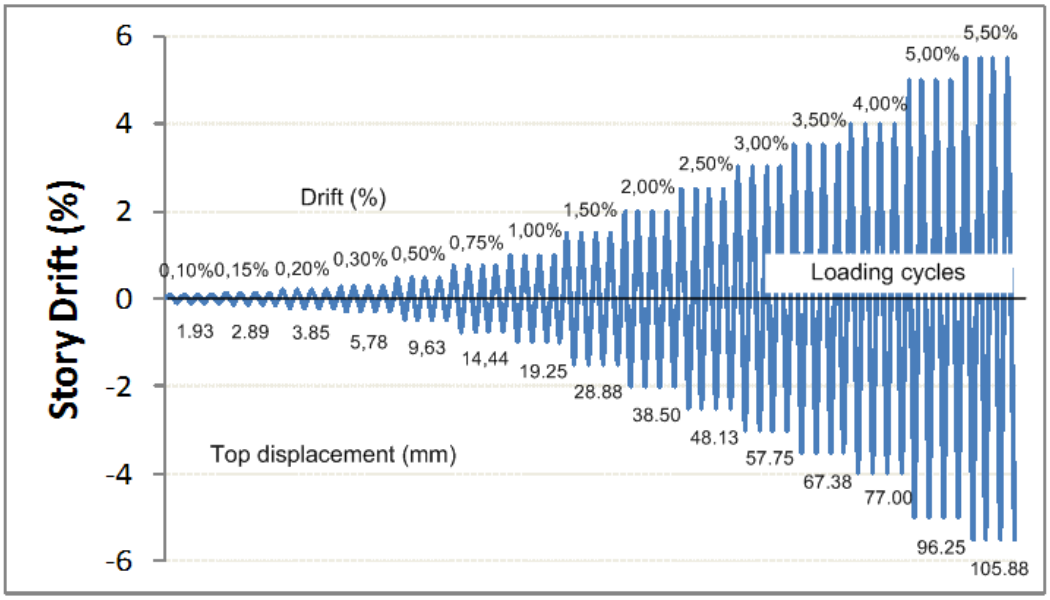

Figure 2.25. Loading Protocol

The loading set up is shown in Figure 2.26 and 3-dimenesional view of test setup is shown in Figure 2.27. Constant axial load was applied vertically by a load-control loading system with a 600 kN-capacity hydraulic jack at the top of both columns, connected to the pedestal of the specimens with steel cables. Horizontal loads were applied by a displacement-control loading system through a 250 kN-capacity dynamic actuator. Three cycles of the same amplitude in every story drift level were repeated before displacement amplitudes were increased. The amount of the axial force applied on each column is 30 % $f'_c A_g$ (30 % of column axial load capacity) where f'_c is the compressive strength of concrete and A_g is the gross cross-sectional area of each column.

A total of 16 strain gauges, which are shown in Figure 2.28, were mounted on the column longitudinal bars in the lap-splice region to gather the strain values during the tests. All of these strain gauges were connected to the data acquisition system. In addition to the strain gauges, lateral displacement of the beam, shear deformation in the beam column joint, and curvature readings on the beam and columns at or close to the maximum moment regions were monitored and measured by Linear Variable Differential Transducers (LVDTs), and their data was also transferred to the same data acquisition system. Overall, each data was recorded with 4-second intervals. The locations LVDTs are shown in Figure 2.29.

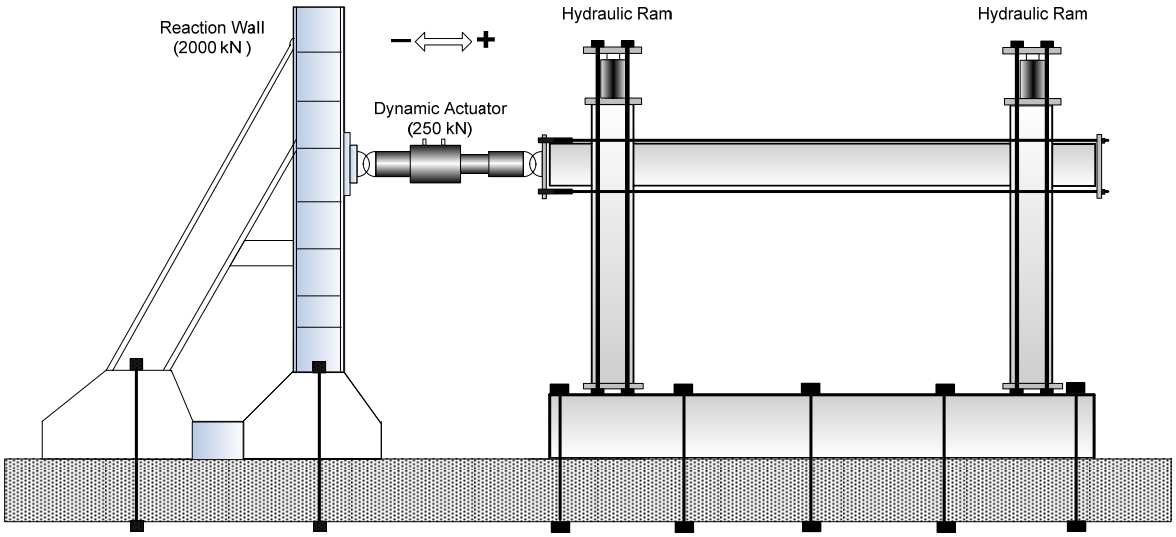

Figure 2.26. Test Setup

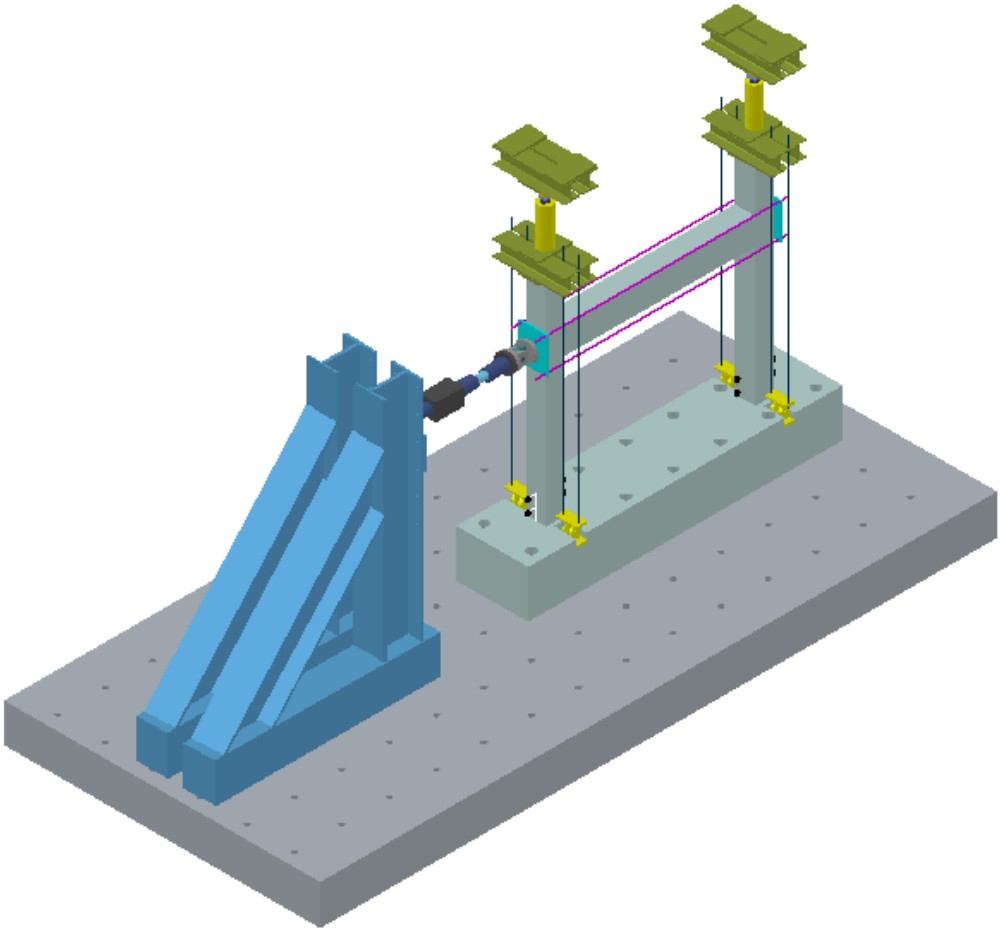

Figure 2.27. 3D Sketch of Test Setup

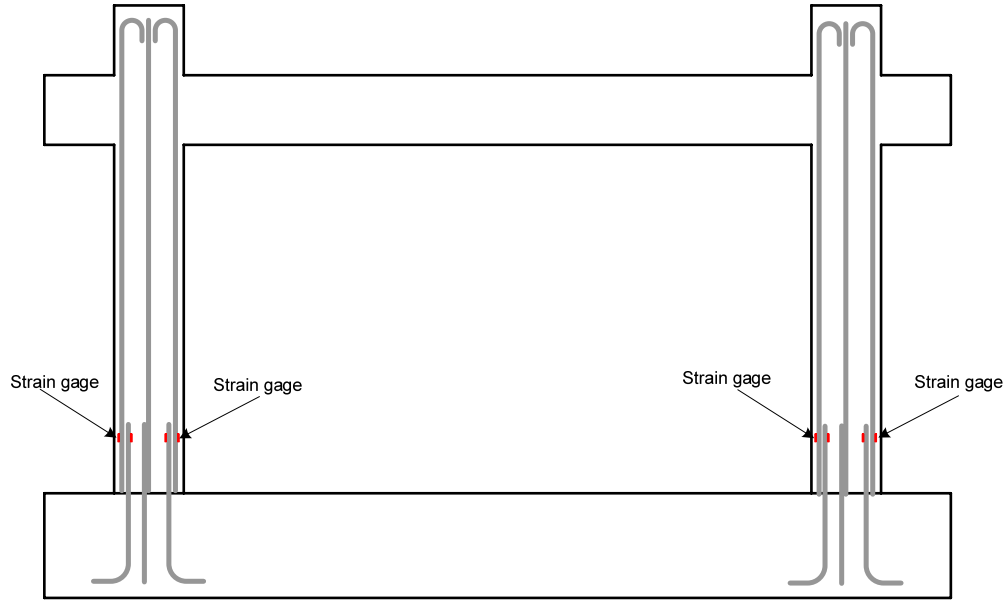

Figure 2.28. Location of Strain Gages for specimen LS and specimen LS-FRP

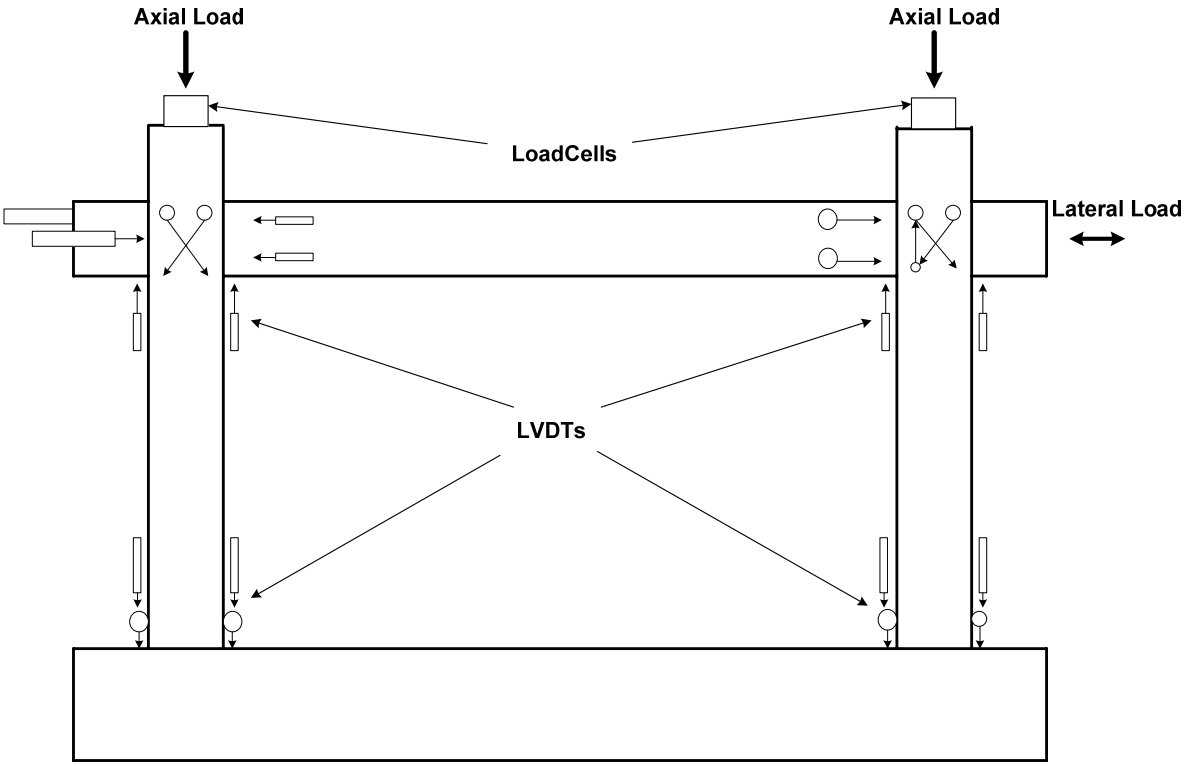

Figure 2.29. Location of LVDTs

3. EXPERIMENTAL STUDY

3.1. Test Observations

This chapter describes the observed behavior of the specimens tested and presents the data obtained from the experiments. In the explanation of the behavior of the specimens, the location of the cracks and observations are referenced according to the nomenclature depicted in Figure 3.1.

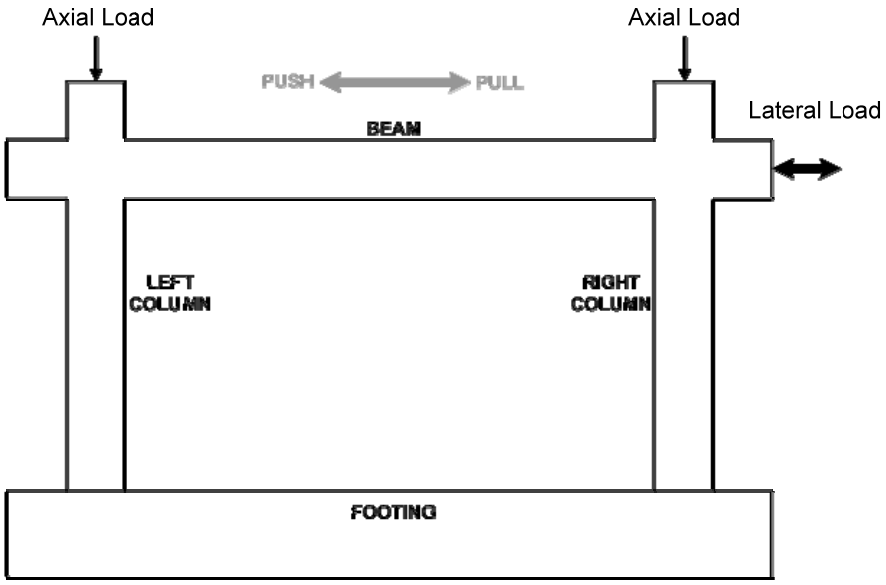

Figure 3.1. Nomenclature of the Structural Members

3.1.1. Control Specimen

At the first drift level, which is 0.10 %, when the specimen was forced in the pull direction with a peak force of 35.5 kN, a 200 mm long- flexural crack formed at the top of the beam, at 90 mm distance from the right column (Figure 3.2). The second flexural crack developed symmetrically at the top of the beam, at a distance of 180 mm from the left column. The length of the crack was measured at about 90 mm. During subsequent drift levels, up to 0.30 %, existing flexural cracks were extended and new cracks were formed on the beam.

Figure 3.2. The first Flexural Cracks on Beam in Control Specimen

The first column flexural cracks were observed during the cycles of 0.30 % drift levels when the applied load was 66 kN in the push direction. The locations of the cracks were 150 and 240 mm from the footing on the exterior face of the right column. Similar cracks were observed on the interior face of the same column in the pull direction of loading (Figure 3.3). A vertical crack on the column was observed at the right joint region at this drift level. Vertical cracks were observed on both left and right beam joint interfaces.

Figure 3.3. Column Flexural Cracks (exterior and interior)

The maximum lateral load, measured as 163 kN, was obtained during loading to 3.00 % drift cycles in the pull direction of loading. Up to the 3.50 % drift level, existing cracks elongated and the widened and new flexural cracks were formed at the maximum moment regions of the columns and the beam. During 3.50 % drift cycles, the cover concrete at the bottom of the columns crushed and spalled off. The cover concrete at the beam ends also crushed at a drift level of 4.00 %. At this drift level, the maximum lateral load, which was 176 kN, was reached in the push direction of loading

The first joint shear cracks were formed at a drift level of 5.00 % at the right beam-column joint region (Figure 3.4). Also, beam longitudinal reinforcement buckled at the maximum moment region. During the final cycles to 5.00 % drift level, the top longitudinal reinforcement of the beam fractured.

Figure 3.4. Joint Shear Cracks and Beam Crushing

The Figure 3.5 and 3.6 present the measured lateral load vs. displacement and lateral load vs. story drift relationships of the specimen, respectively.

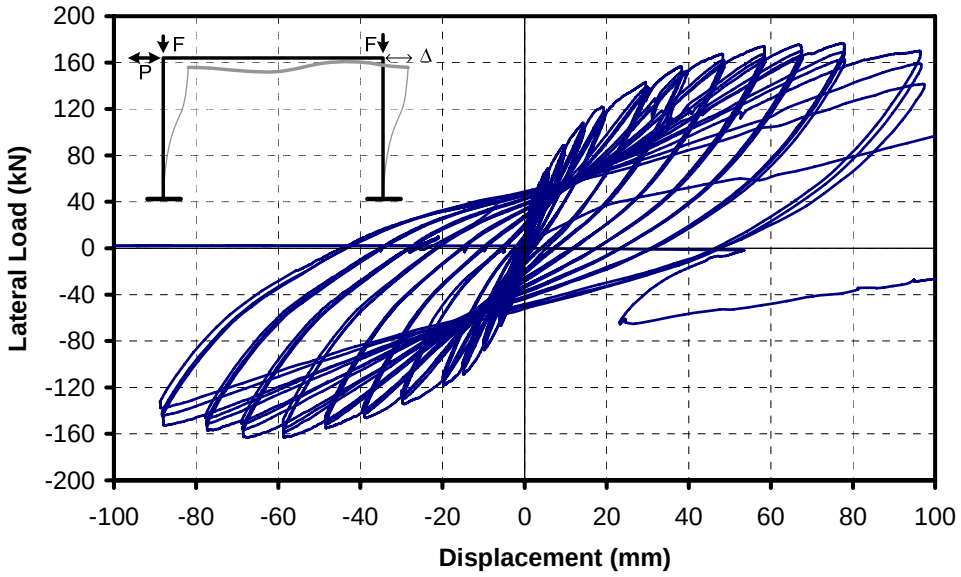

Figure 3.5. Lateral Load vs. Displacement Relationships of Control Specimen

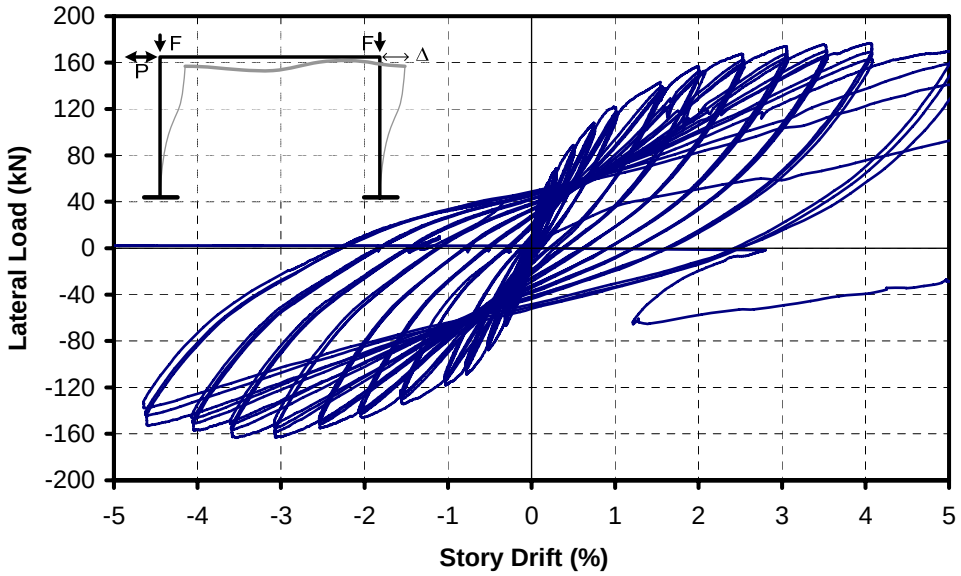

Figure 3.6. Lateral Load vs. Drift Relationships of Control Specimen

3.1.2. Specimen LS

Specimen LS had a 280 mm (20 bar diameter) lap splice at the bottom of the column longitudinal reinforcement. During loading, the first flexural crack formed at the bottom of the beam and 30 mm distant from the left column at a drift level of 0.15 %. A second crack also developed at a close location, 320 mm distant from the left column (Figure 3.7). The

length of both cracks was almost 200 mm. During loading to cycles to 0.20 % drift, symmetrical flexural cracks observed on the right column side of the beam.

Figure 3.7. The First Flexural Cracks on the Beam in Specimen LS

Up to a drift level of 1.50 %, existing flexural cracks elongated and widened, and new flexural cracks were formed on beam and columns. During the 1.50 % drift cycles, vertical cracks were observed in the lap splice region of columns, indicating bond-slip behavior along the lap splice. Bond-slip behavior was also evident due to significant widening of flexural cracks at the column - footing intersections. Also, as seen in Figure 3.8, the bottom of the column started to crush at a drift level of 2.00 %.

A vertical crack was formed at the beam column joints during the 3.00 % drift cycles. The crack initiated from the bottom interior corner of the right joint. A flexural crack also formed at the bottom region of the right column, at a distance of 260 mm from the footing.

Figure 3.8. Column Cracks of Specimen LS

During loading to 3.00 %, 3.50 % and 4.00 % drift levels, the new vertical cracks developed in the columns lap splice regions. The horizontal cracks at the column - footing interfaces widened up to 8 mm, which also indicated significant bond-slip deformation. The width of the cracks on the beam reached 3.0 mm (Figure 3.9). The lateral load capacity, which was 140 kN for both the push and pull directions of loading was reached at a drift level of 3.00 %. The lateral load vs. top displacement and lateral load vs. story drift relationships for the specimen are shown in Figures 3.10 and 3.11 respectively.

Figure 3.9. Crackings of Beam and Column at the end of the Test for Specimen LS

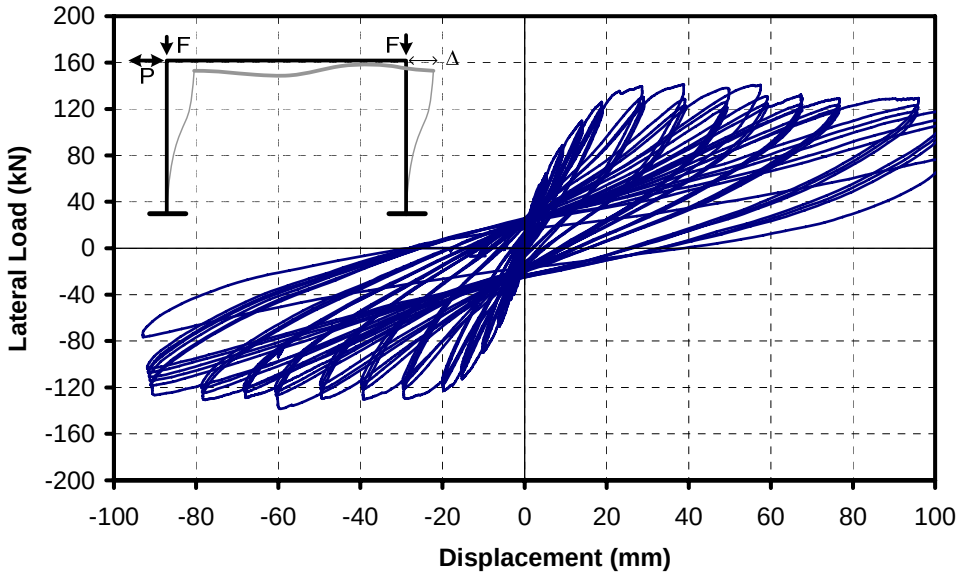

Figure 3.10. Lateral Load vs. Displacement Relationships of Specimen LS

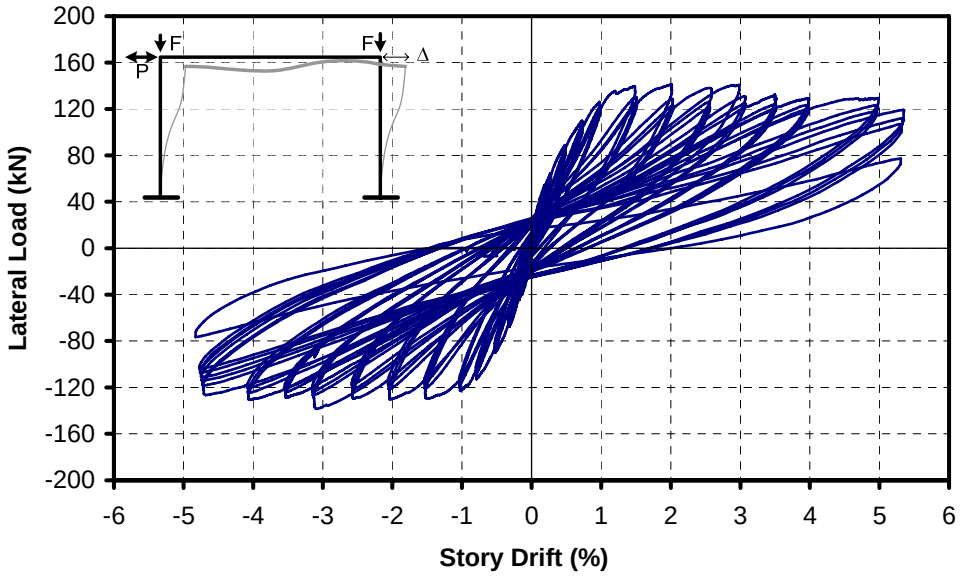

Figure 3.11. Lateral Load vs. Story Drift Relationships of Specimen LS

3.1.3. Specimen LS-FRP

On the specimen strengthen with CFRP in the lap splice region, the first crack observed was flexural and it formed at the interface of the beam and left beam column joint during loading to 0.10 % drift level. The first joint shear crack was observed in the left joint region at a load of 40 kN (Figure 3.12).

The first flexural crack on a column formed at a drift level of 0.75% on the right column and at a distance of 100 mm from the beam bottom surface. A symmetrical crack developed on the left column at the same drift level in opposite direction.

No damage was observed on CFRP in the lap splice region up to a drift level of 2.50 %. During the 2.50 % drift cycles, the CFRP material started to make cracking sounds. During subsequent cycles to 3.00 % drift, the CFRP was started to rupture when the lateral load reached a maximum level of 180 kN in the pull direction. 180 kN was the lateral load capacity of the specimen in both push and pull directions of loading. After 3.00 % drift level, the lateral load capacity of the specimen started to degrade due to progressive rupture of the CFRP (Figure 3.13). At the same time, the flexural cracks in the beam column joint interfaces continued to widen; however, no fracture of the beam reinforcement was observed.

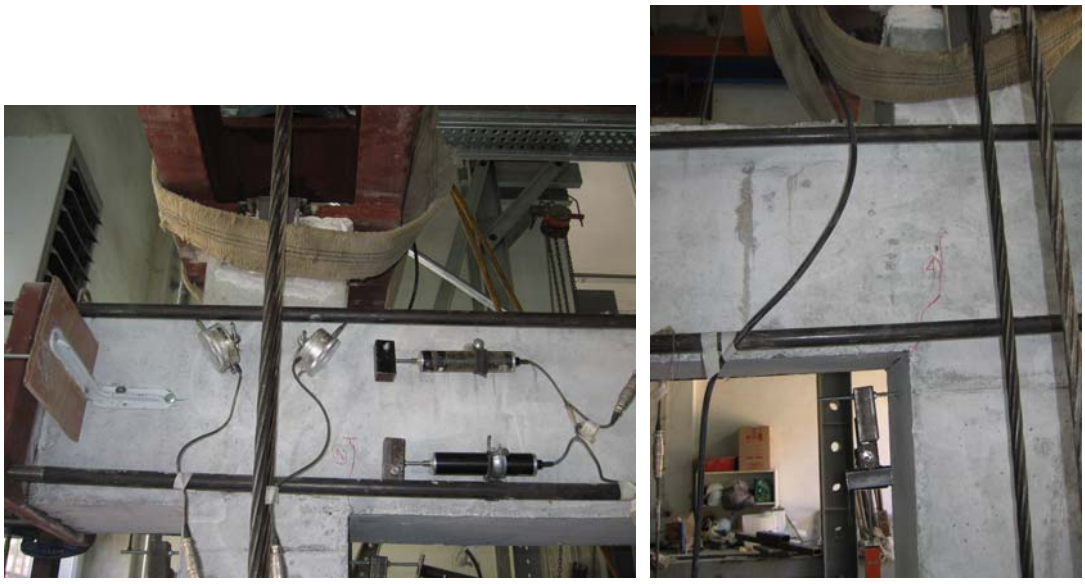

Figure 3.12. Beam Flexure Crack and Joint Crack of Specimen LS-FRP

Figure 3.13. Rupture of CFRP in Specimen LS FRP

The lateral load vs. displacement and lateral load vs. story drift relationships for the specimen LS-FRP are shown in Figure 3.14 and 3.15 respectively.

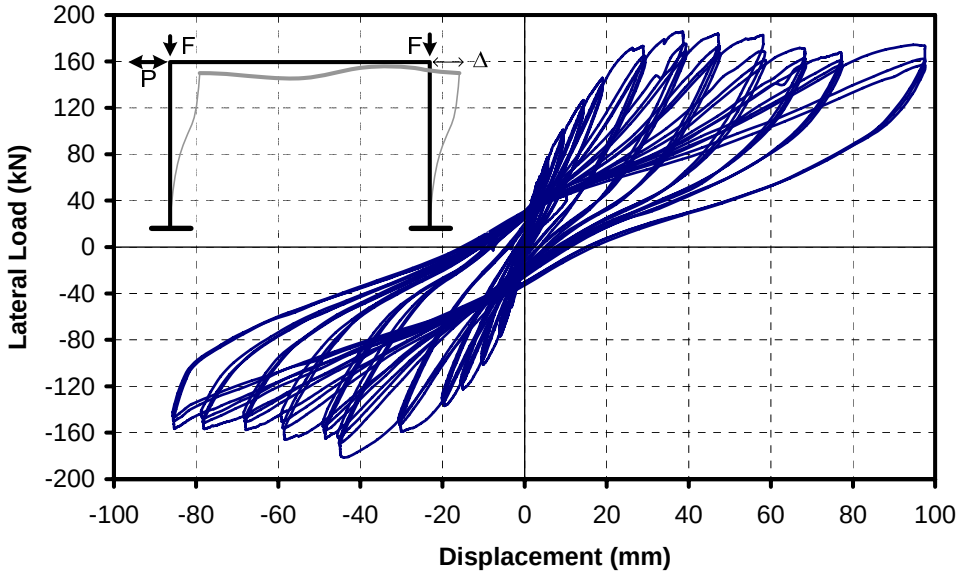

Figure 3.14. Lateral Load vs. Displacement Relationships of Specimen LS FRP

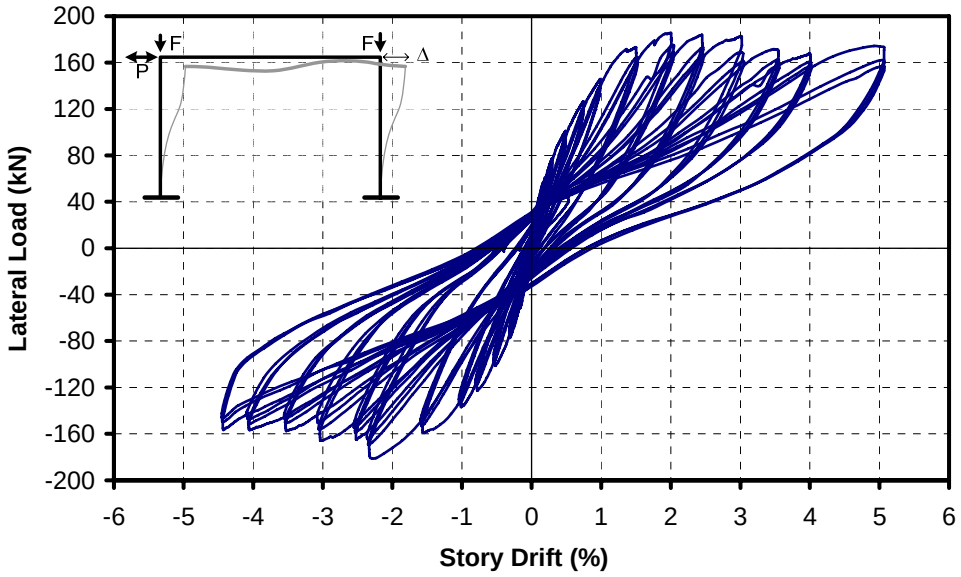

Figure 3.15. Lateral Load vs. Drift Relationships of LS FRP Specimen

3.2. Local Deformation Measurements

3.2.1. Load versus Curvature Relationships

As defined in section (2.7) on instrumentation, average curvature readings were taken at three different locations on each column and two locations on the beam.

The placement of displacement sensors close to the maximum tensile and compressive strain regions of the column allows an average curvature measurement along the gauge length of the sensors. Placement of the LVDTs for curvature measurement is shown in Figure 3.16. . The curvature is described schematically in Figure 3.17 and can be calculated by using Eq (3.1).

$$\phi = \frac{\Delta_1 / h1 + \Delta_2 / h2}{b + L1 + L2} = \frac{\varepsilon 1 + \varepsilon 2}{\sum L} \tag{3.1}$$

where; Δ_1, Δ_2 are relative longitudinal displacements readings taken from the displacement sensors, h_1 and h_2 are the gauge lengths of the displacement sensors, b is the width of the member (column or beam), and L_1 and L_2 are the distances shown in Figure 3.17.

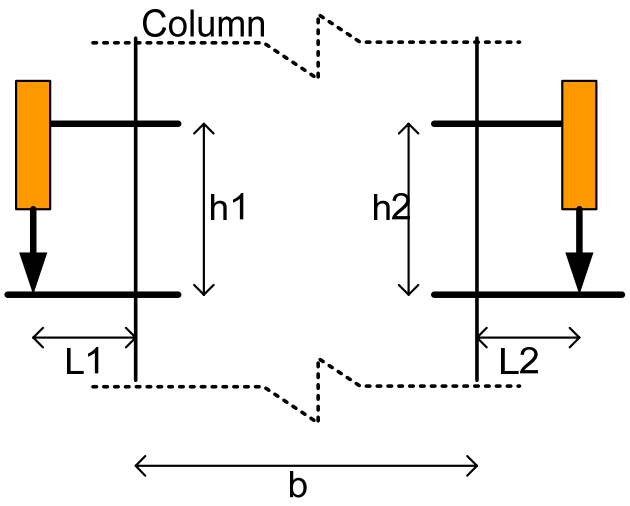

Figure 3.16. Curvature Placement

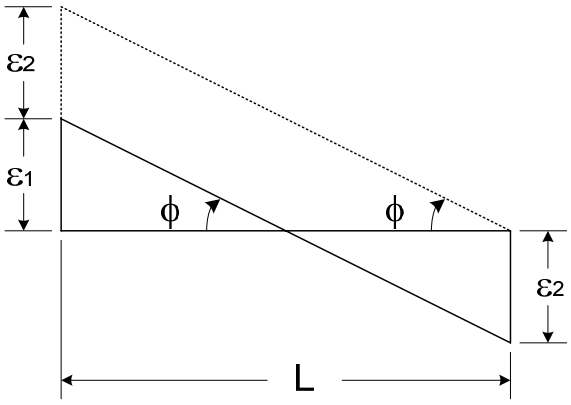

Figure 3.17. Schematic View of Curvature Calculation

By using the equation above, experimental load vs. curvature relationships were obtained. These relationships can be obtained at the base of each column, just above of the each column, at the top of each column and at each end of the beam. The relationships are presented in Figures 3.18 to 3.25 for the control specimen, Figures 3.26 to 3.33 for specimen LS, and Figures 3.34 to 3.41 for specimen LS-FRP. The reason that moment vs. curvature relationships cannot be presented is because each specimen is a statically indeterminate and therefore, bending moments on the sections cannot be measured experimentally.

3.2.1.1. Control Specimen

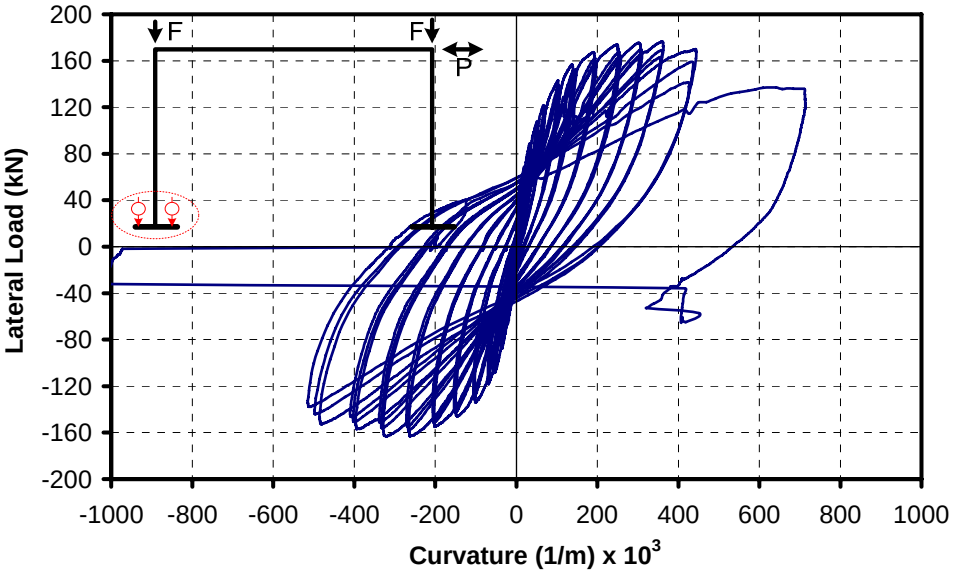

Figure 3.18. Load vs. Curvature at the Base Location of Left Column for Control Spec.

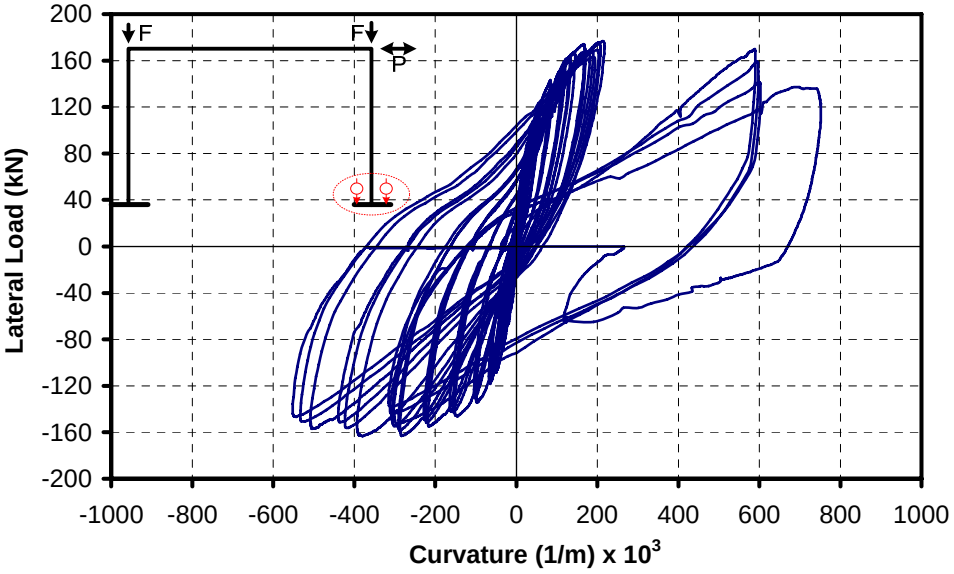

Figure 3.19. Load vs. Curvature at the Base Location of Right Column for Control Spec.

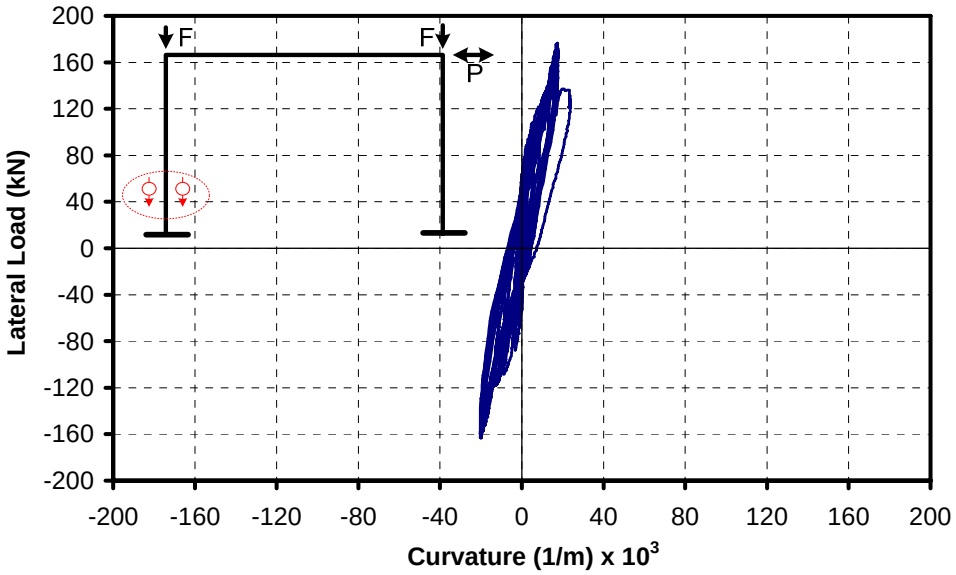

Figure 3.20. Load vs. Curvature just above the Base of Left Column for Control Spec.

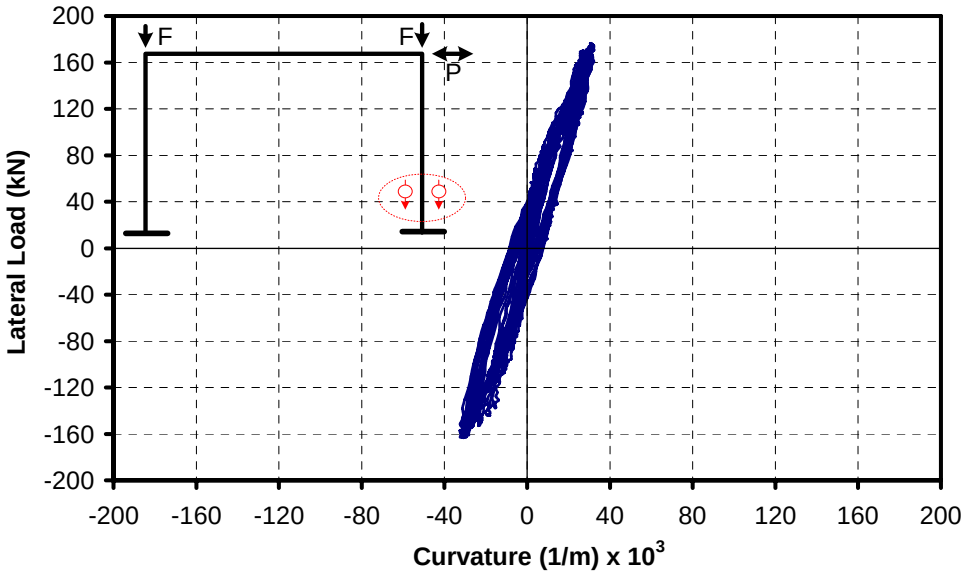

Figure 3.21. Load vs. Curvature just above the Base of Right Column for Control Spec.

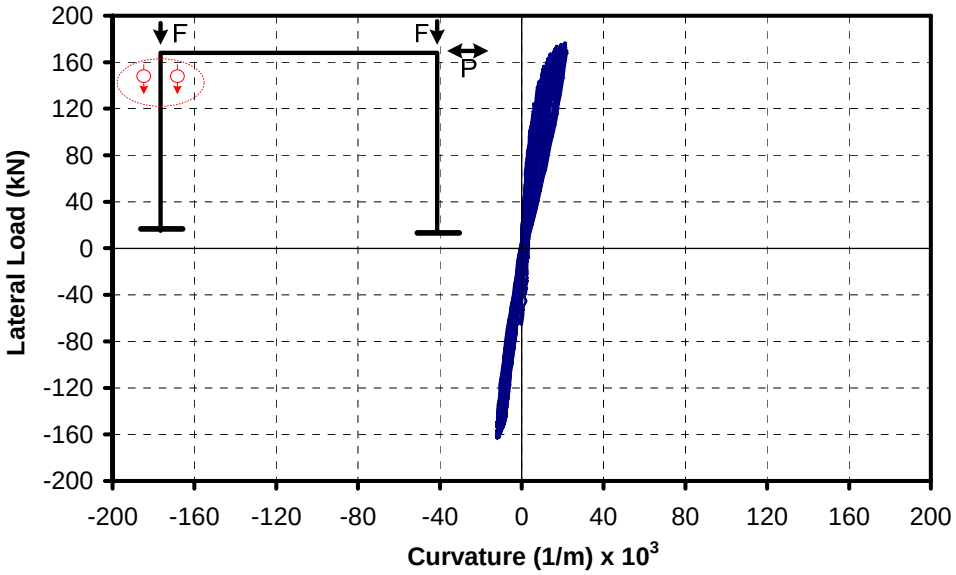

Figure 3.22. Load vs. Curvature at the Top of Left Column for Control Spec.

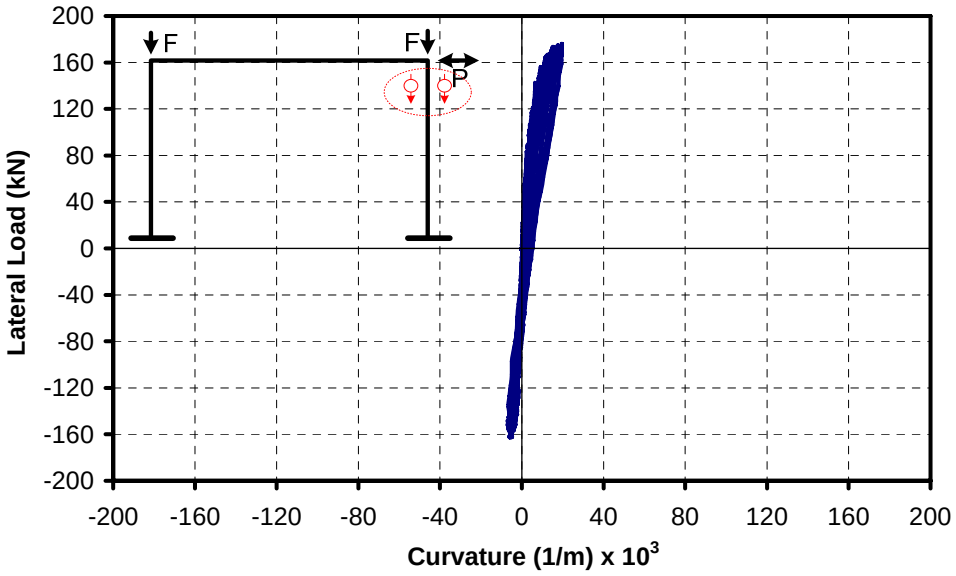

Figure 3.23. Load vs. Curvature at the Top of Right Column for Control Spec.

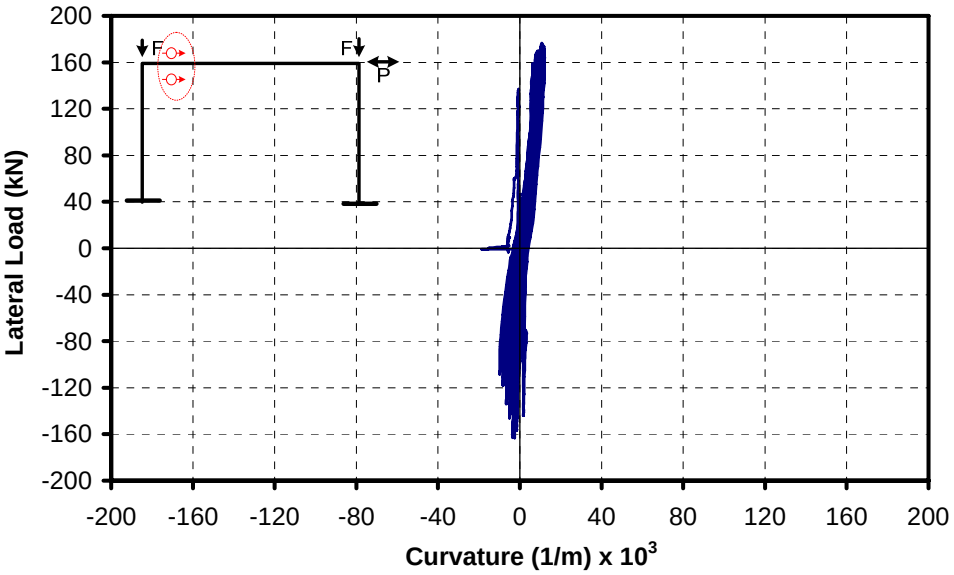

Figure 3.24. Load vs. Curvature at the Left end of the Beam for Control Spec.

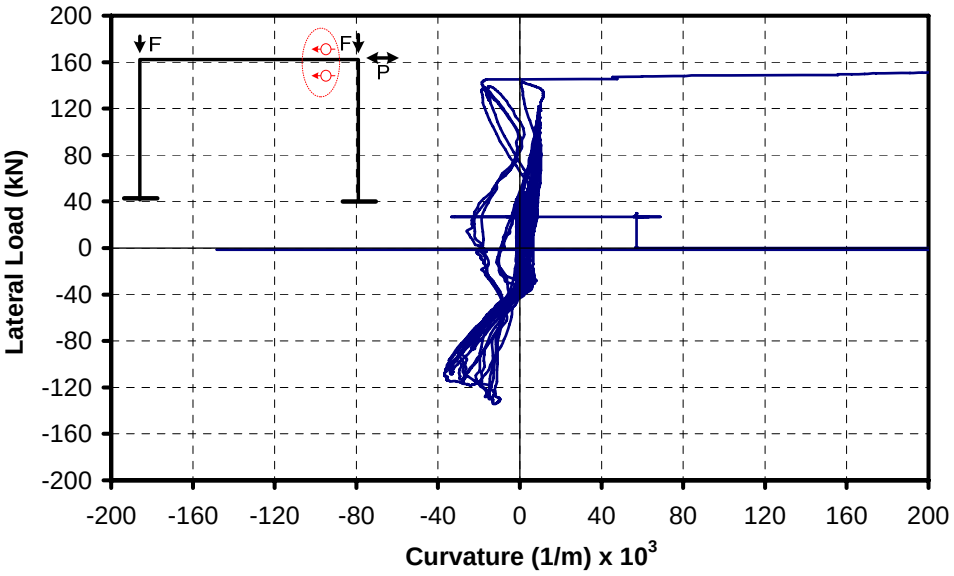

Figure 3.25. Load vs. Curvature at the Right end of the Beam for Control Spec.

3.2.1.2. Specimen LS

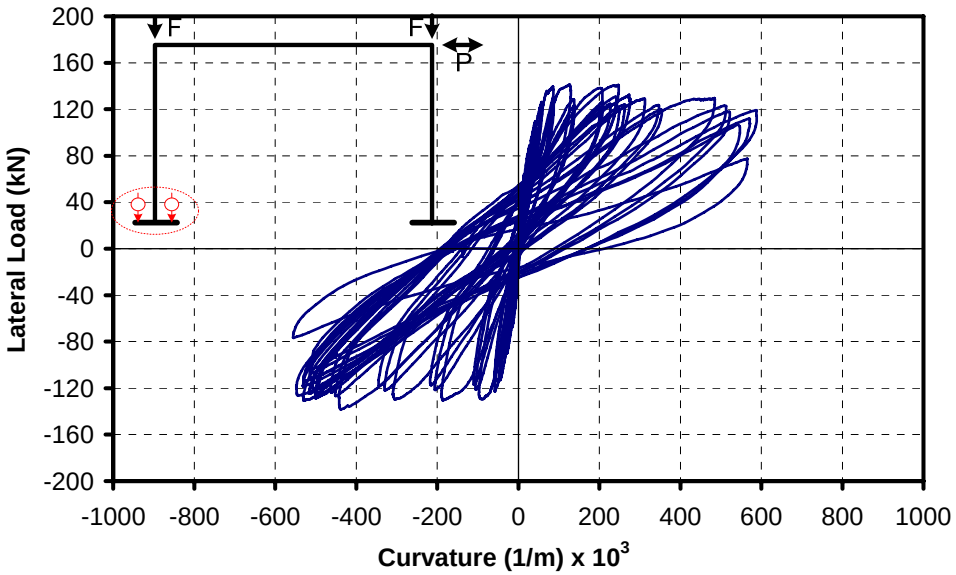

Figure 3.26. Load vs. Curvature at the Base Location of Left Column for LS

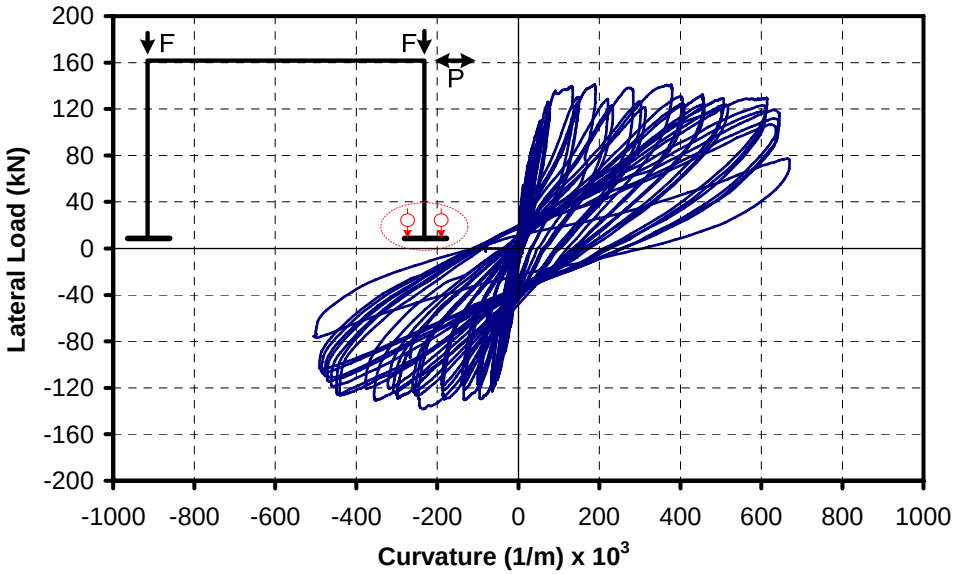

Figure 3.27. Load vs. Curvature at the Base Location of Right Column for LS

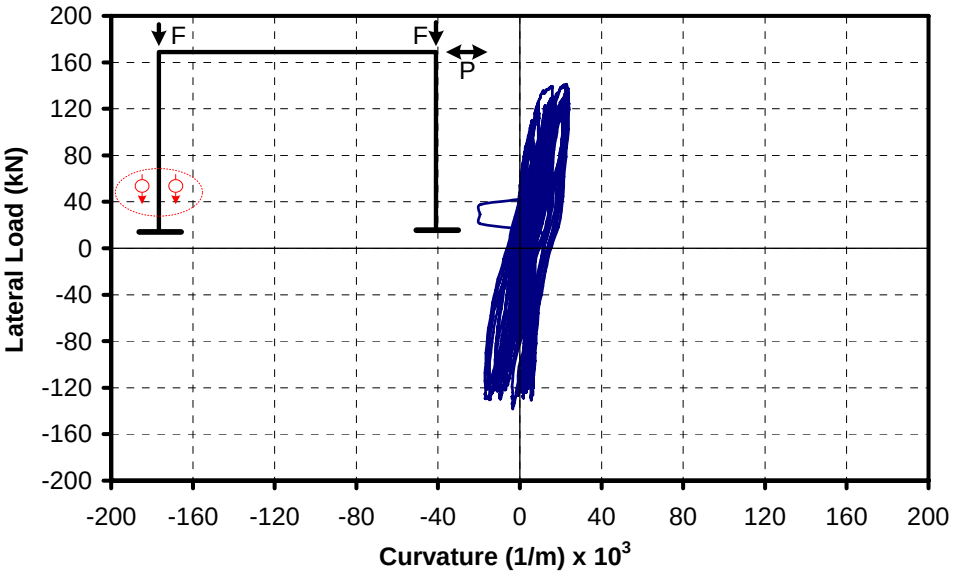

Figure 3.28. Load vs. Curvature just above the Base of Left Column for LS

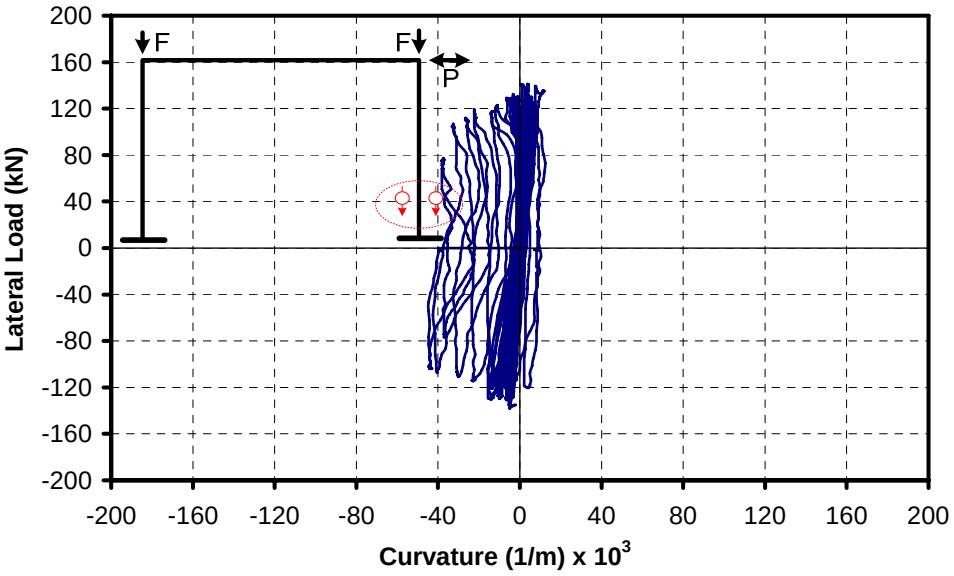

Figure 3.29. Load vs. Curvature just above the Base of Right Column for LS

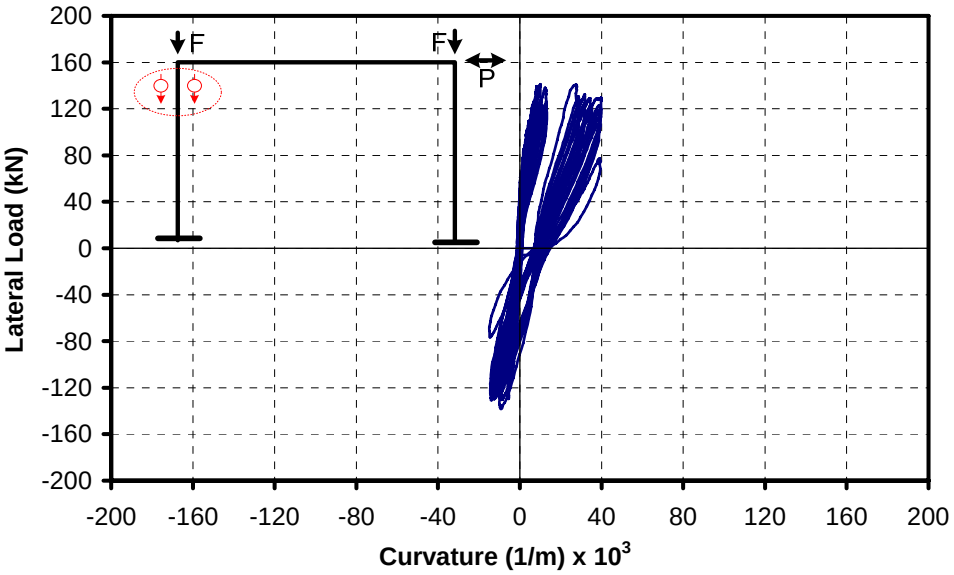

Figure 3.30. Load vs. Curvature at the Top of Left Column for LS

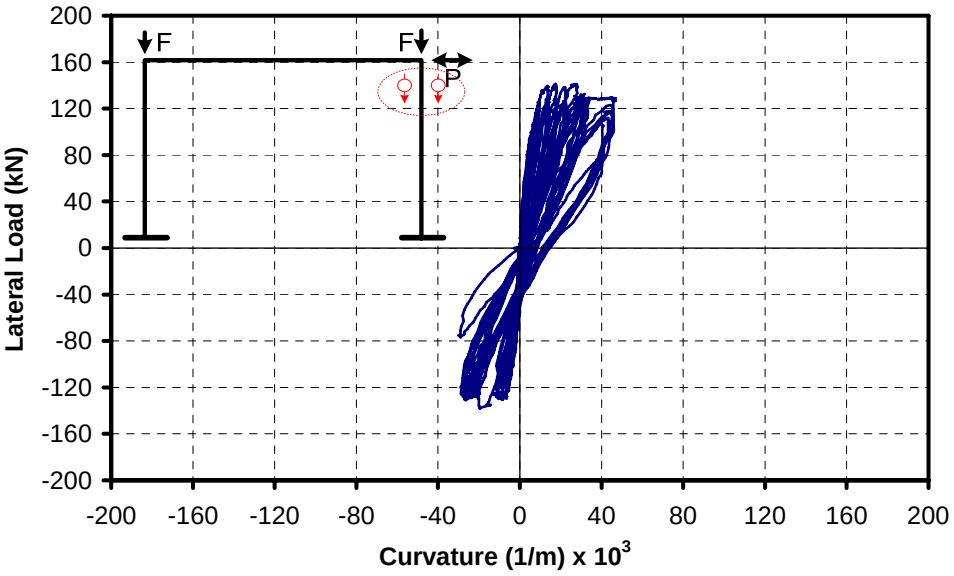

Figure 3.31. Load vs. Curvature at the Top of Right Column for LS

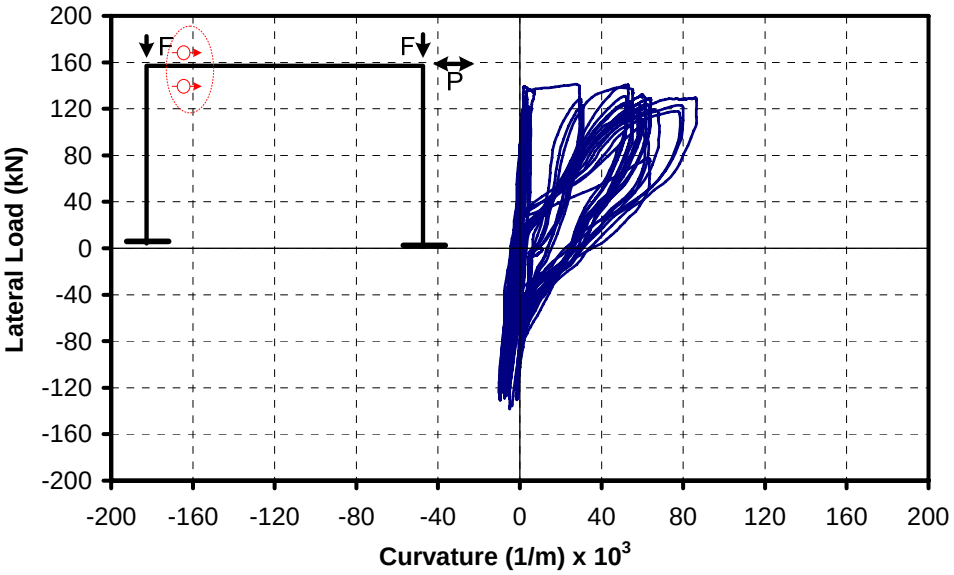

Figure 3.32. Load vs. Curvature at the Left end of the Beam for LS

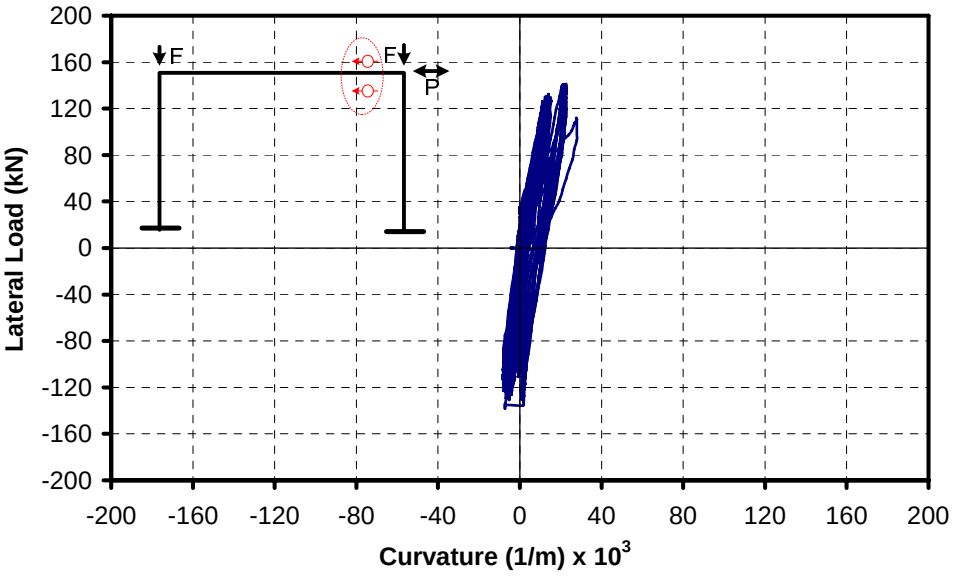

Figure 3.33. Load vs. Curvature at the Right end of the Beam for LS

3.2.1.3. Specimen LS-FRP

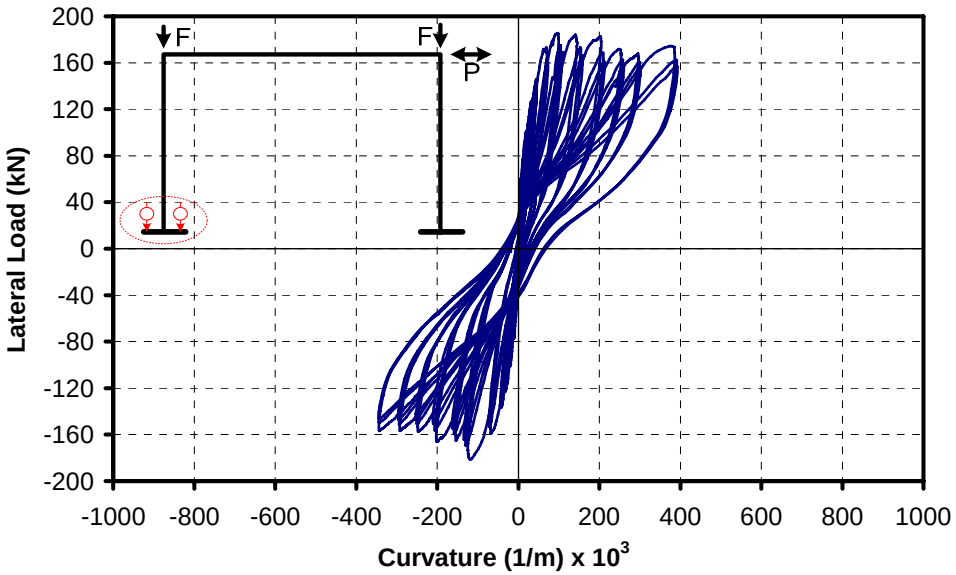

Figure 3.34. Load vs. Curvature at the Base Location of Left Column for LS-FRP

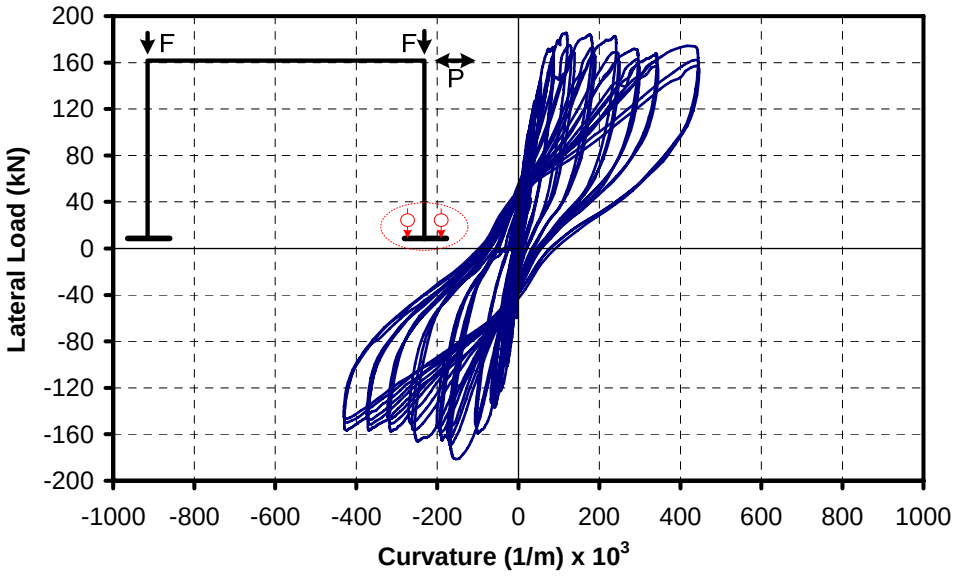

Figure 3.35. Load vs. Curvature at the Base Location of Right Column for LS-FRP

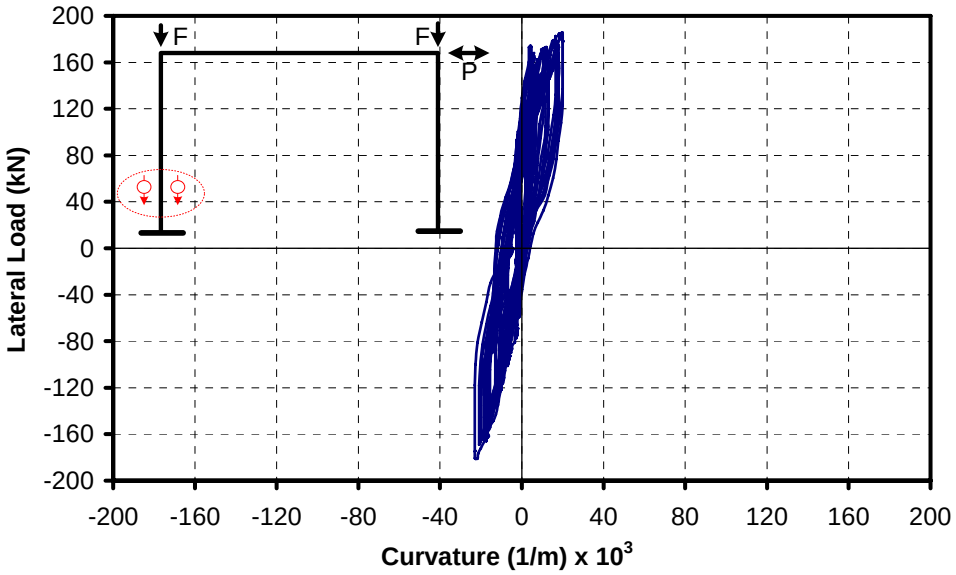

Figure 3.36. Load vs. Curvature just above the Base of Left Column for LS-FRP

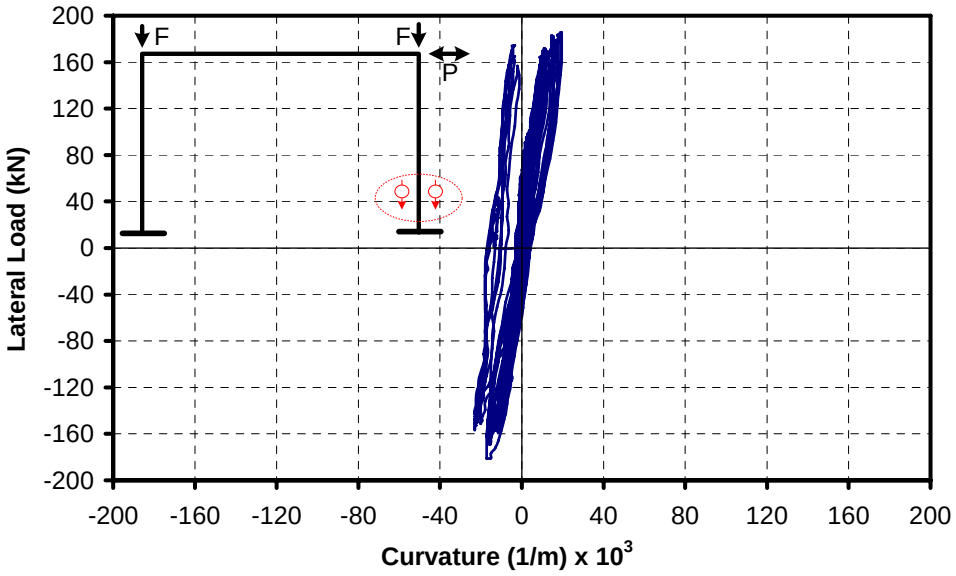

Figure 3.37. Load vs. Curvature just above the Base of Right Column for LS-FRP

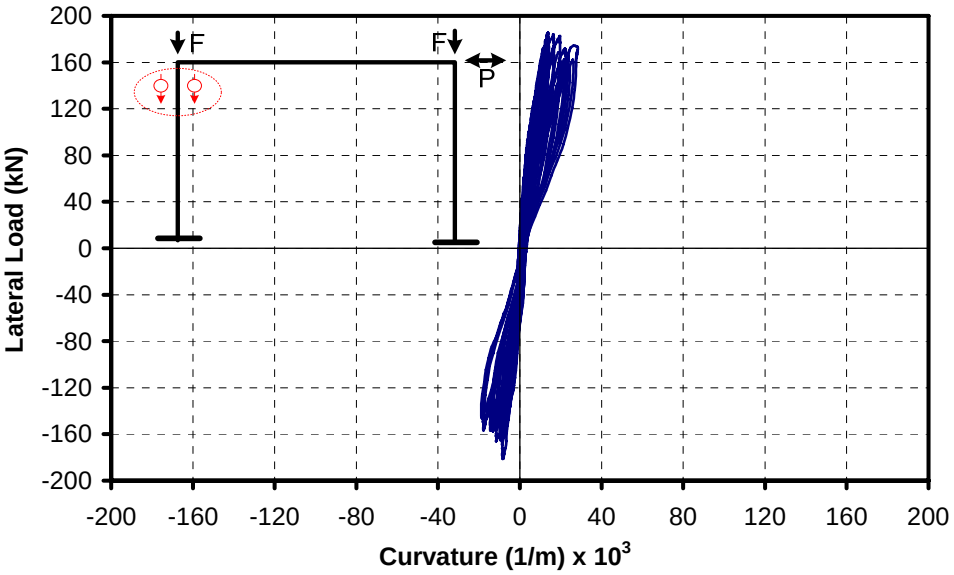

Figure 3.38. Load vs. Curvature at the Top of Left Column for LS-FRP

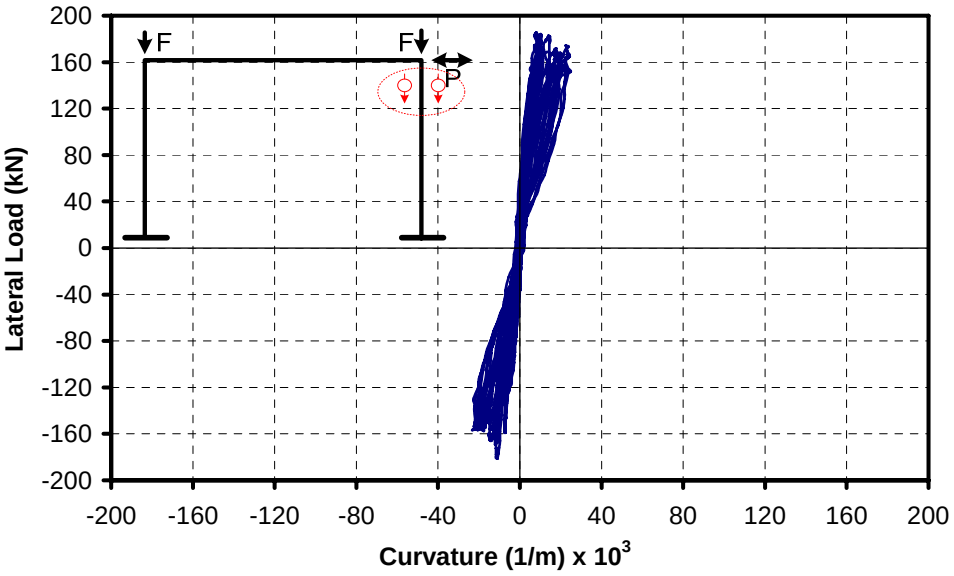

Figure 3.39. Load vs. Curvature at the Top of Right Column for LS-FRP

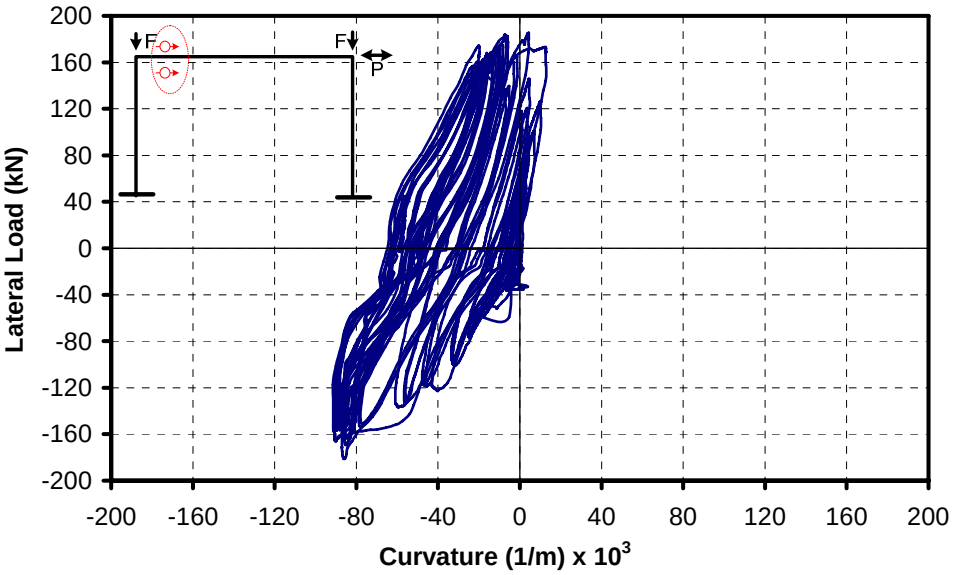

Figure 3.40. Load vs. Curvature at the Left end of the Beam for LS-FRP

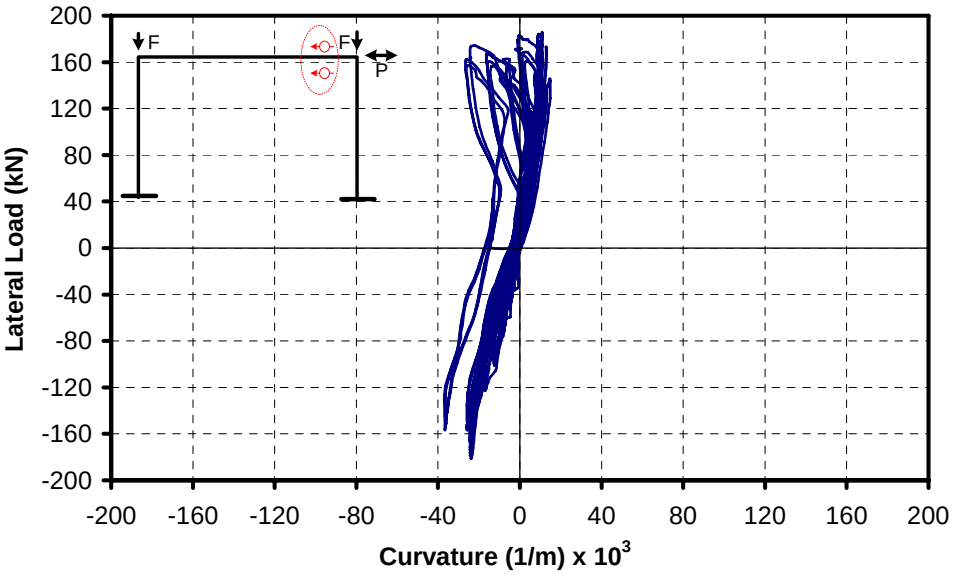

Figure 3.41. Load vs. Curvature at the Right end of the Beam for LS-FRP

3.2.2. Load versus Shear Deformations Relationships

For all three specimens, shear deformations were also measured at the beam column joint panel region using two diagonal LVDTs installed as shown in Figure 3.42. Using the readings from these LVDTs, the shear deformation of the joints can be calculated according to Eq (3.2)

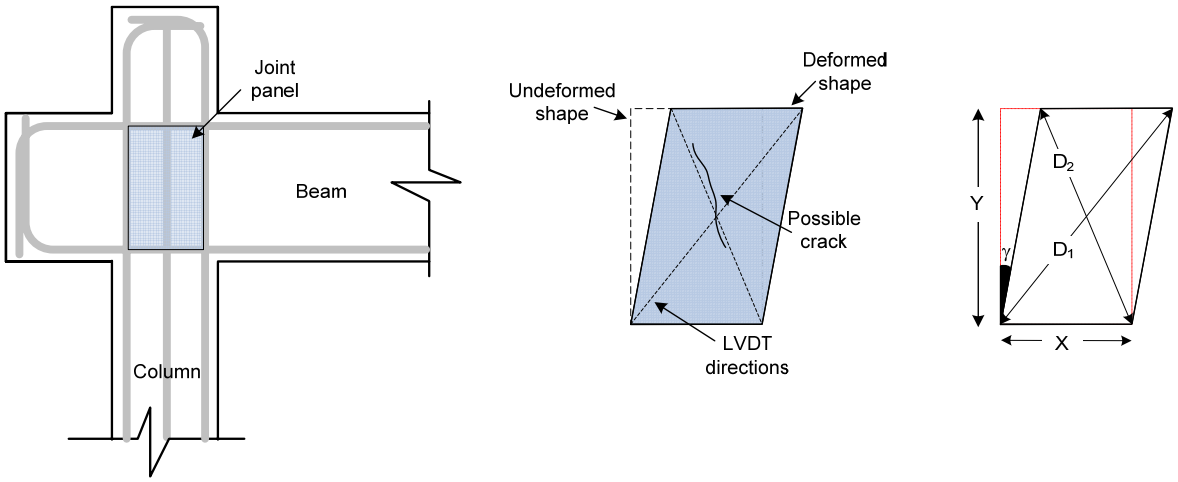

Figure 3.42. Shear Deformation Measurement

$$\gamma = \tan^{-1}\left(\frac{\sqrt{D1^2 - Y^2} - \sqrt{D2^2 - Y^2}}{2Y}\right) \tag{3.2}$$

where, γ is shear deformation (rad); *D1* and *D2* are gauge lengths of diagonally placed displacement sensors, and *X* and *Y* are the dimensions of undeformed joint panel. In this relationship, it is assumed that the dimensions of shear panel do not change due to small shear deformations.

By using the given equation, lateral load vs. shear deformation relationships of the right and left joint panels were obtained. These relationships are presented for the control, LS, and LS-FRP specimens in Figures 3.43 to 3.48.

3.2.2.1. Control Specimen

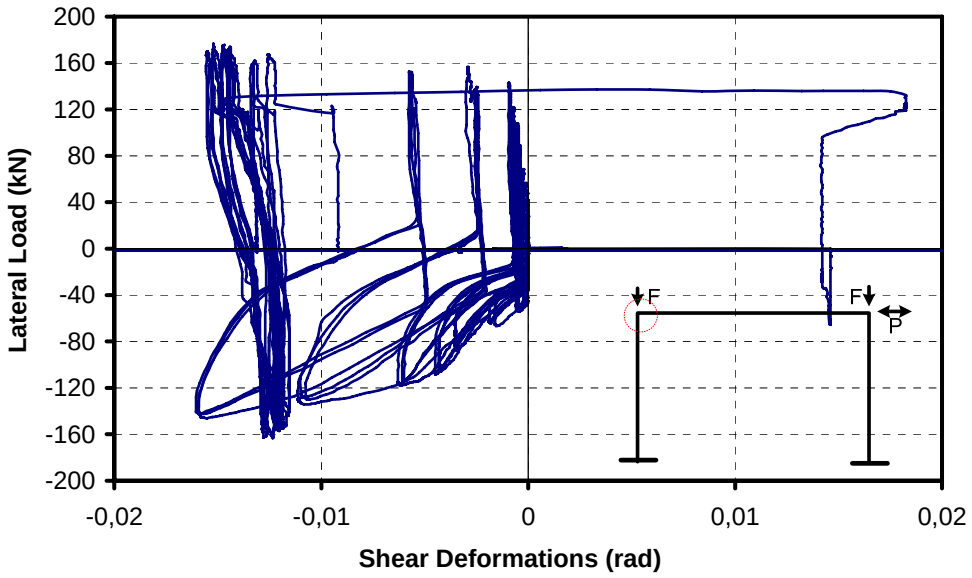

Figure 3.43. Load vs. Shear Deformations at the Left Joint Panel for Control Specimen

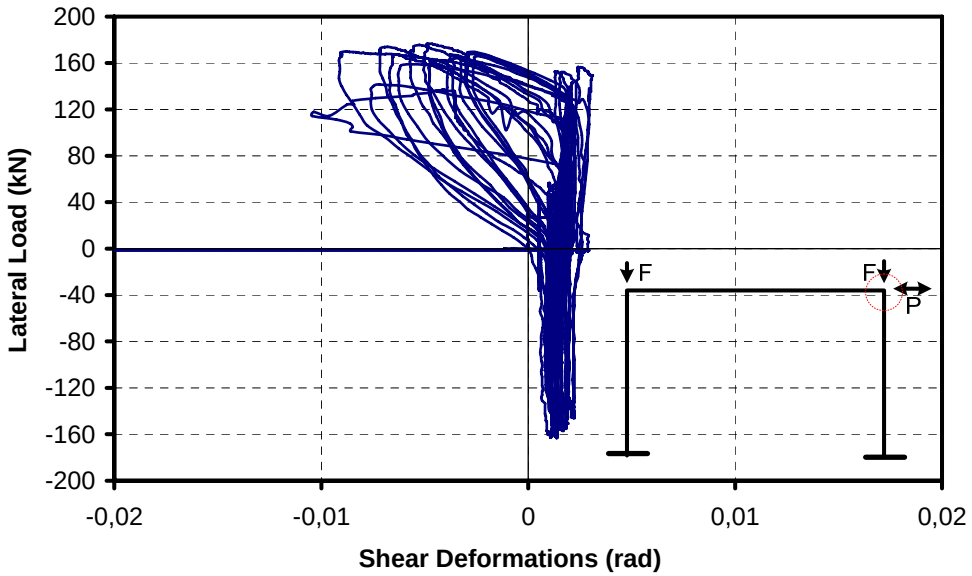

Figure 3.44. Load vs. Shear Deformations at the Right Joint Panel for Control Specimen

3.2.2.2. LS Specimen

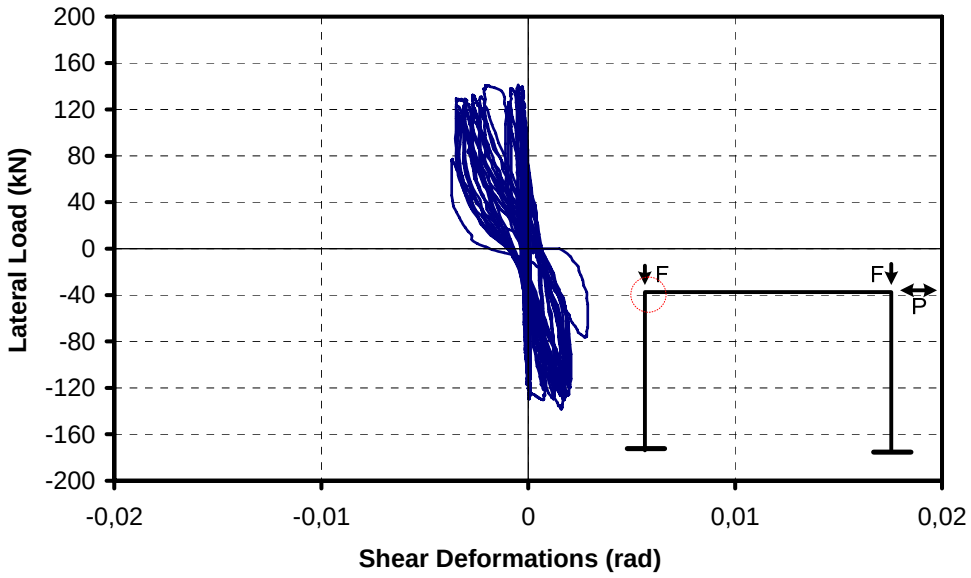

Figure 3.45. Load vs. Shear Deformations at the Left Joint Panel for LS Specimen

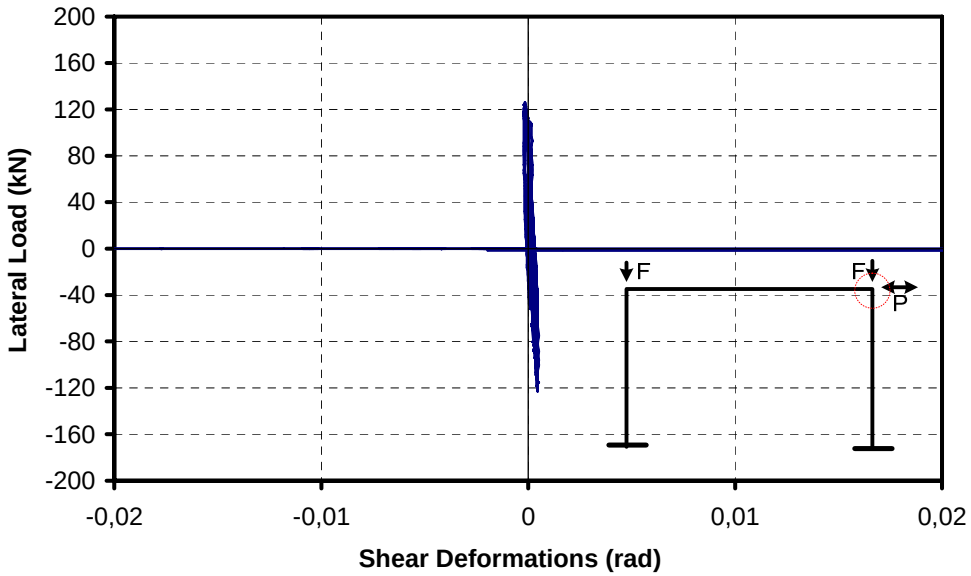

Figure 3.46. Load vs. Shear Deformations at the Right Joint Panel for LS Specimen

3.2.2.3. LS-FRP Specimen

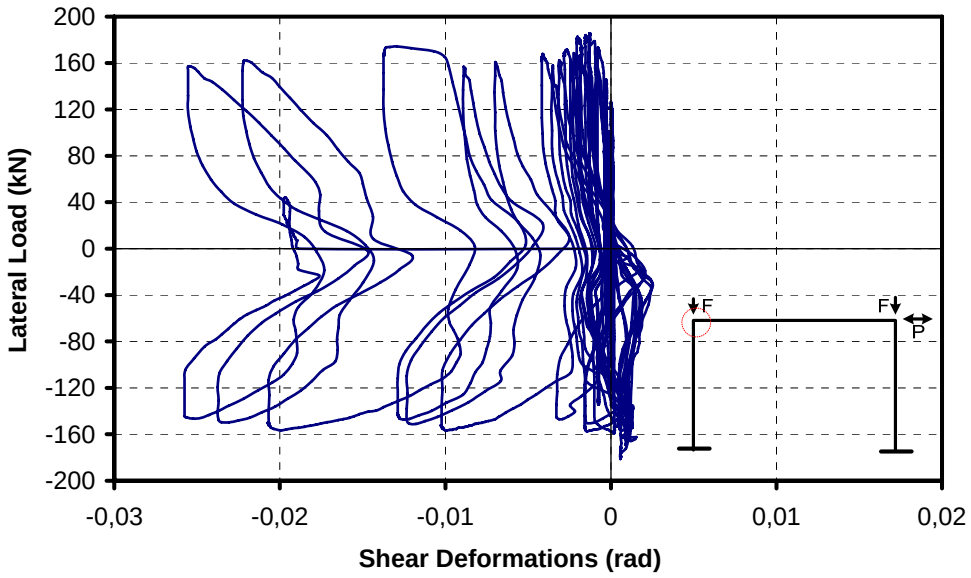

Figure 3.47. Load vs. Shear Deformations at the Left Joint Panel for LS-FRP Specimen

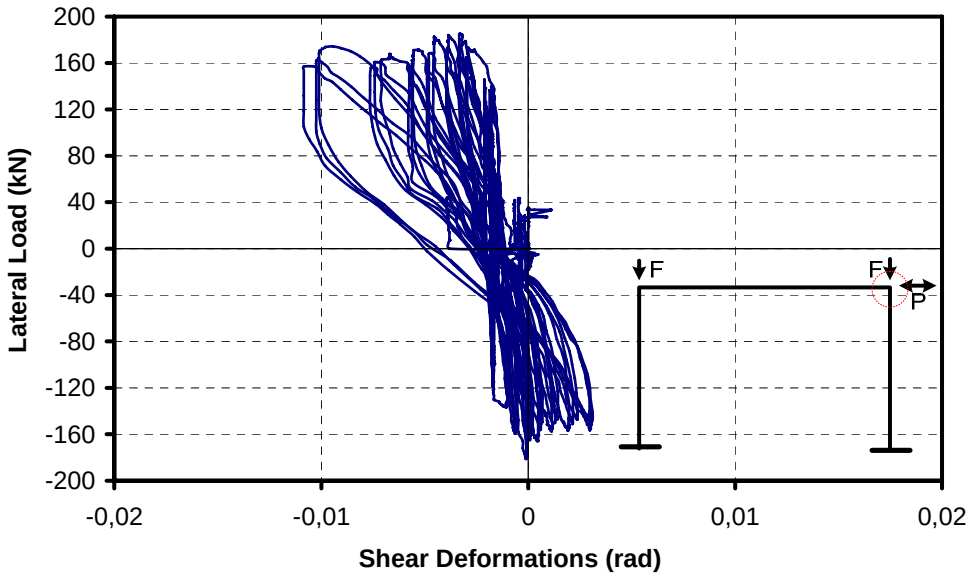

Figure 3.48. Load vs. Shear Deformations at the Right Joint Panel for LS-FRP Spec.

4. DISCUSSION OF TEST RESULTS

This chapter presents interpretation and comparison of the experimental results obtained from frame specimen tests. Lateral load behavior of frame specimens is evaluated in terms of lateral load vs. top displacement response, lateral load capacity, stiffness, energy dissipation characteristics, and local deformation behavior.

4.1. Lateral Load Capacity and Lateral Load vs. Story Drift Response

The envelopes of the hysteretic lateral load vs. story drift responses for the control, LS, and LS-FRP specimens are compared in Figure 4.1. The control specimen, which was designed to satisfy detailing provisions of the Turkish Earthquake Code (TEC-2007) behaved in a ductile manner, with no significant degradation in the lateral load capacity until a drift level of 5.00 % both in the push and pull directions of loading. Due to the inadequate lap splice, the capacity of the specimen LS reduced to 140 kN, which is approximately 20 % lower than that of the control specimen. However, using the strengthening methodology proposed, the lateral load capacity of the lap splice deficient frame reached, and even exceeded, that of control specimen, In addition, no significant degradation was observed in the lateral load capacity of the strengthened specimen at 5.00 % drift, which was the maximum drift level that can be applied by the experimental setup, indicating that ductility capacity of the strengthened specimen is not less compared to that of the control specimen.

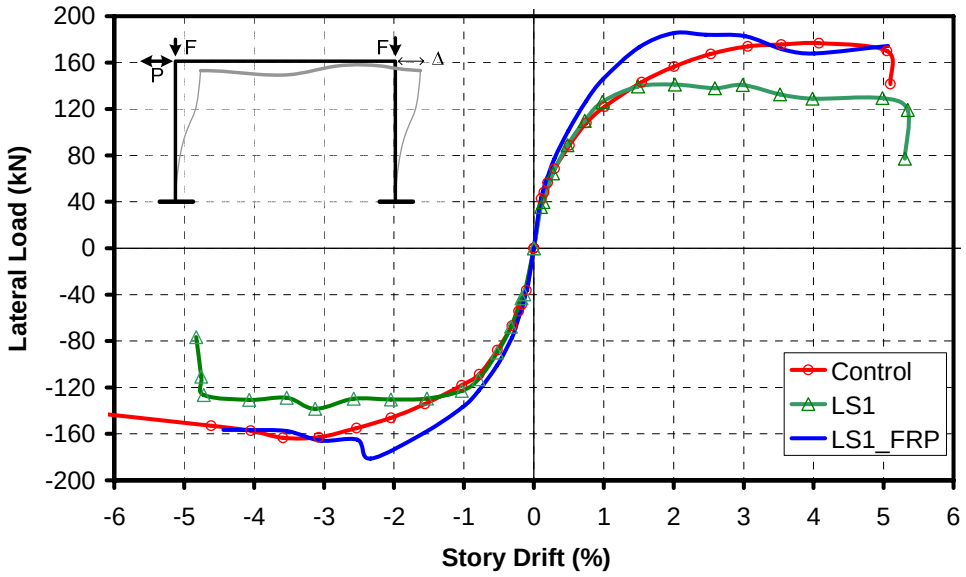

Figure 4.1. Comparison of Backbone Curves (envelopes)

4.2. Stiffness Degradation

The secant stiffness of peak points of the measured lateral load vs. top displacement response was also used for investigating the behavior of the specimens, in terms of stiffness degradation under cyclic lateral loads. The secant stiffness, *K*, is defined as the slope of the line that passes from the origin to a displacement reversal point of interest on the lateral load vs. story drift loops. Figure 4.2 illustrates the definition of the secant stiffness.

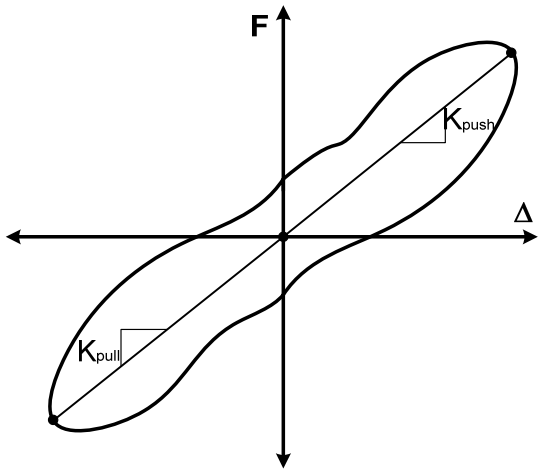

Figure 4.2. Calculation of Stiffness of Hysteresis Loops

Measured story drift vs. stiffness relationships for the test specimens are presented in Figure 4.3. As observed from the Figure 4.3, as well as Figure 4.1, the initial stiffness of the strengthened specimen (LS-FRP) is higher than that of both the control specimen and Specimen LS. The rate of stiffness degradation was, however, faster in the strengthened specimen compared with the control.

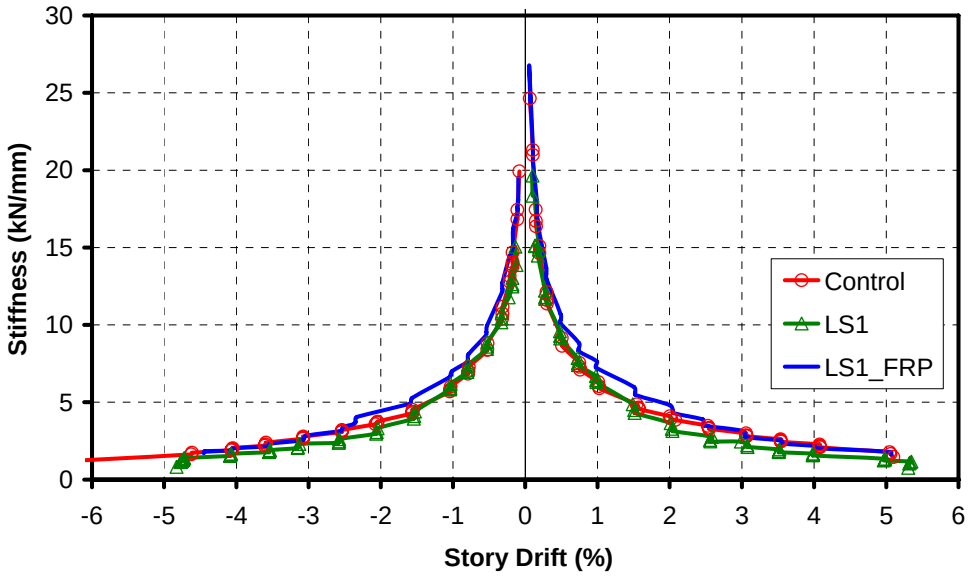

Figure 4.3. Comparison of Stiffness Degradation

4.3. Energy Dissipation and Ductility

To characterize the response of the frame specimens, one way to define the cumulative dissipated energy is the cumulative area under hysteresis loops of the lateral load vs. top displacement response. Figure 4.4 illustrates the calculation of dissipated energy for one hysteresis loop.

Accordingly, the cumulative dissipated energy vs. story drift relationships for the specimens is presented in Figure 4.5. As observed from the figure, the cumulative dissipated energy is highest in the control specimen. This is expected since the control specimen was detailed as a high-ductility-level frame and exhibited wide load vs. displacement loops, as evident in Figure 3.5. Specimen LS showed 40 % less cumulative energy dissipation compared with the control specimen, since the load displacement loops were not nearly as wide and followed a more origin oriented pattern (Figure 3.10). Even

though the shape of the load vs. displacement loops of specimen LS-FRP (Figure 3.14) were similar to those of specimen LS, due to its higher lateral load capacity, it dissipated only 25 % lower cumulative energy than the control specimen (Figure 4.5).

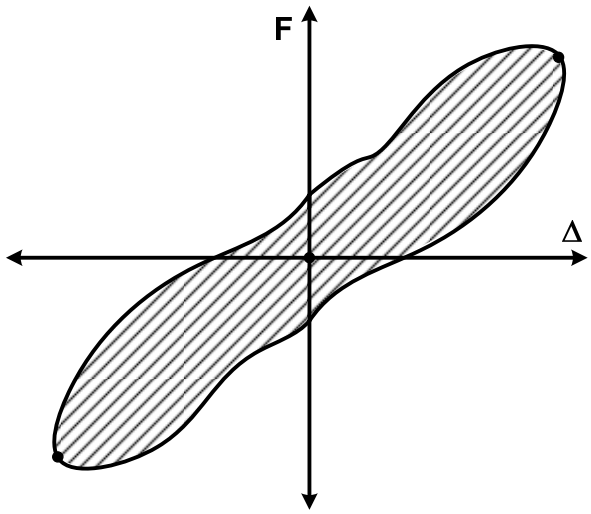

Figure 4.4. Calculations of Energy

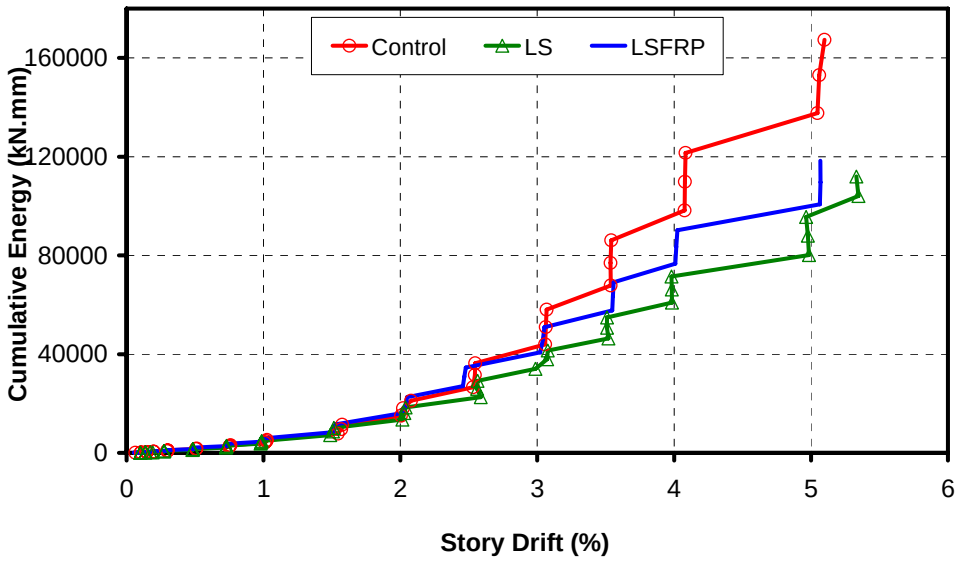

Figure 4.5. Comparison of Dissipated Cumulative Energy

4.4. Failure Modes, Local Deformations, and Distribution of Damage

4.4.1 Control Specimen

The test observations have revealed that for the control specimen, progressive damage was initiated in the form of flexural cracking at the beam ends, followed subsequently by flexural cracking at the bottom and top of the columns, flexural yielding (plastic hinge formation) at the beam ends, and flexural yielding (plastic hinge formation) at the base of the columns, ultimately resulting in the formation of a collapse mechanism. The lateral load of the specimen experienced significant degradation when one of the top bars of the beam fractured, at 5.00 % drift level, at which time testing was terminated. This behavior was desired and expected, since the specimen was designed and detailed to experience such form of progressive damage and ductile response.

Flexural yielding was not experienced at the top of the columns of the control specimen, since the beam-column joint was designed to satisfy the strong column – weak beam condition. For the columns, it was interesting to observe that flexural damage was concentrated at the very bottom (base), along the gauge length of the lowermost displacement sensors for measuring curvature. The curvature sensors placed just above the base did not measure significant curvature values (Figure 3.20 and 3.21). This observation was contrary to the expectation that nonlinear flexural deformations (inelastic curvatures) would be distributed along a larger distance (plastic hinge length) at the base of the columns. Similarly, the curvature readings taken from the displacement sensors placed at the beam ends were also very small in magnitude (Figure 3.24 and 3.25), although flexural yielding was obvious at the beam ends. The reason for this discrepancy is that nonlinear flexural deformations at the beam ends were also localized and concentrated at locations very close to the intersection of the beam and the joint region (a single wide flexural crack developed at these locations), which fell outside of the gauge length of the beam curvature sensors. It would have been more desirable to place the beam curvature sensors to include the beam-joint interface within their gauge length.

The shear deformation sensors installed in the beam column joint regions of the control specimen did not measure significant amount of shear deformation (Figure 3.43

and 3.44), which was consistent with visual observation of the joint damage during the test. Diagonal cracking was not significant in the joint regions, and the few diagonal cracks that have formed did not widen throughout the entire test.

4.4.2 Specimen LS

For the deficient lap splice specimen that was not strengthened (Specimen LS), progressive damage was initiated in the form of flexural cracking at the beam ends, followed subsequently by flexural and longitudinal (bond-slip) cracking at the bottom of the columns, and progressive flexural yielding (plastic hinge formation) at the beam ends together with increasing bond slip deformations at the base of the columns. Bond slip deformations across the lap splice region were visually observed in the form widening of the longitudinal splitting cracks and of significant widening of a single horizontal crack at the column-footing interface. This behavior was also expected, since the specimen incorporated an inadequate lap splice length (approximately one-third of that required by the code). It was interesting to observe that although the lap splice length was very inadequate, the effect of the presence of the lap splice reduced the lateral load capacity of the specimen to only 80 % of that of the control specimen, and the overall response was still ductile, although the shape of the lateral load vs. displacement loops of the specimen were narrower.

This finding is important in pointing out that bond-slip failure in columns with inadequate lap splices may not influence the lateral load behavior of a frame system, as much as it would influence the behavior of a single column, due to internal redistribution of the bending moments in the frame when bond-slip failure is initiated. Due to such redistribution, the failure mode of specimen LS was a combination of bond-slip deformations in the lap splice region, together with flexural hinging in the beam. The reduction of the capacity might have been much more severe and the response much more non-ductile, if single columns were tested instead of frames.

Similar to the control specimen, flexural yielding was not experienced at the top of the columns of the specimen LS, since the beam-column joint was designed to satisfy the strong column – weak beam condition. The curvature sensors placed just above the base

did not measure significant curvature values (Figure 3.28 and 3.29). The curvature readings taken from the displacement sensors placed at the beam ends were also very small in magnitude (Figure 3.32 and 3.33), since nonlinear flexural deformations at the beam ends were again localized and concentrated at locations very close to the intersection of the beam and the joint region. Shear deformations in the beam column joint regions of the specimen were again, small in magnitude (Figure 3.45 and 3.46).

4.4.3 Specimen LS-FRP

For the deficient lap splice specimen strengthened with the CFRP-strengthening methodology proposed (Specimen LS-FRP), progressive damage was initiated in the form of flexural cracking at the beam ends, followed subsequently progressive flexural yielding (plastic hinge formation) at the beam ends together with progressive flexural deformations at the base of the columns (in the strengthened lap splice region), ultimately resulting in rupture of the CFRP sheets. Damage at the base of the columns was not visually observed due to obstruction of the view by the CFRP material; however, curvature readings taken from the displacement sensors at column base indicated large flexural deformations (Figure 3.34 and 3.35). The lateral load capacity of the strengthened specimen reached, and even exceeded the capacity of the control specimen, whereas deformation capacity of the strengthened specimen was not lower than that of the control specimen, and the initial stiffness was considerably higher. The shape of the load vs. displacement loops for the specimen were, however, not as wide as those of the control specimen.

The behavior of specimen LS-FRP demonstrated, for the most part, that the CFRP-strengthening technique proposed in this study was very effective. The significant increase in the lateral load capacity, compared with that of the unstrengthened specimen, as well as the rupture of the CFRP, all indicate that the “L-shaped” CFRP sheets worked effectively in the longitudinal direction of the column, increasing its flexural capacity. Importantly, no debonding of the CFRP was observed, indicating that the “L-shaped” steel plates were very effective in anchorage of the “L-shaped” sheets at the critical location, which is the column-footing intersection. As well, the CFRP anchors efficiently prevented debonding of the CFRP sheets from the column surface. It can be stated that the CFRP strengthening technique proposed is very effective for increasing the flexural capacity of a column at a

critical region, such as an inadequate lap splice region. It is speculated that if more layers of “L-shaped” CFRP sheets were used in the longitudinal direction of the column, the lateral load capacity of the strengthened frame would have reached even higher values, although additional tests are required to qualify this statement.

Similar to the control specimen and the unstrengthened lap splice deficient specimen, flexural yielding was not experienced at the top of the columns of specimen LS-FRP. The curvature readings taken from the displacement sensors placed at the beam ends were also very small in magnitude (Figure 3.40 and 3.41), since nonlinear flexural deformations at the beam ends were again localized at locations very close to the intersection of the beam and the joint region. Shear deformations in the beam column joint regions of the specimen were also small (Figure 3.47 and 3.48).

5. SUMMARY, CONCLUSIONS, AND FUTURE WORK

This study investigated the effectiveness of a novel strengthening technique using Carbon Fiber Reinforced Polymers on reinforced concrete frames with inadequate lap splices on the columns. An experimental program was conducted at the Boğaziçi University Structural Engineering Laboratory to investigate the effects of lap splice deficiency on the behavior of one-bay one-story frames (portal frames) subjected to reversed cyclic lateral loads, as well as to discuss the improvements on the response, provided by the CFRP strengthening technique proposed. Strength and ductility attributes, failure modes, and damage distributions were investigated in detail for the frame specimens tested. The following conclusions can be drawn on the basis of the results obtained in this study:

- RC portal frame specimens designed and detailed to satisfy the provisions of the latest Turkish Earthquake Code were found to exhibit a desirable and ductile response reversed cyclic lateral loads, with the intended progressive damage sequence of plastic hinge formation in the beams followed by the columns, with no premature shear, joint shear, or bond-slip failure, provided that the column longitudinal reinforcement is continuous. However, nonlinear flexural deformations may be concentrated at locations very close to the beam and column ends, as opposed to being distributed across a plastic hinge length.

- The lateral load capacity of such frames are susceptible to noticeable reduction due to the presence of deficient lap splices in the columns, although the reduction may not be as severe as it would be for a single column, due to internal redistribution of the bending moments in a frame when bond-slip failure is initiated. In this study, presence of inadequate lap splices with a length of 20 bar diameters reduced the lateral load capacity of the test frame by only 20 % compared to that of the frame with continuous column reinforcement. However, for the same specimen, the hysteretic energy dissipation capacity (defined in this case as the cumulative area under the load-displacement response) was influenced to a more undesirable extent, and was reduced by as

much as 40 % compared to the frame with continuous column reinforcement. The reason for this was that the load displacement loops of the lap splice deficient frame are significantly narrower and follow a more origin-oriented pattern.

- The CFRP-strengthening technique proposed in this study noticeably improved the behavior of the lap splice deficient frame. The lateral load capacity of the test frame strengthened with the proposed methodology reached the capacity of the control specimen, whereas the deformation capacity was maintained and the initial stiffness was noticeably increased. The cumulative energy dissipated by the strengthened frame was approximately 20 % more than that of the unstrengthened specimen; however, this was mainly due to increase in the lateral load capacity, since the shape of the load vs. displacement loops were not significantly different.

- It can be stated that the CFRP strengthening technique proposed in this study can be used efficiently for increasing the flexural capacity of a member at a critical region, such as an inadequate lap splice region. Importantly, no debonding of the CFRP was observed prior to rupture of the CFRP under longitudinal stresses, indicating that anchorage attributes of the proposed technique are adequate.

Based on findings of this study, the following investigations are recommended as future research topics in this area:

- Experimental investigations on the assessment of the behavior and influence of the proposed CFRP strengthening technique on lap splice deficient frame systems with multiple stories and multiple spans,

- Application of the proposed CFRP strengthening technique on interior, exterior, and corner joints of frames with other types of detailing deficiencies (e.g., strong beam–weak column condition, inadequate beam anchorage, inadequate transverse reinforcement in plastic hinge regions and beam column joints, etc.),

also considering the prospect of using the diagonal steel anchorage rods to improve joint shear response,

- Analytical modeling studies to simulate the contribution of the “L-shaped” CFRP sheets to the flexural capacity of a reinforced concrete member.

REFERENCES

1. Ersoy, U., "Seismic Rehabilitation", Repair and Strengthening of Existing Buildings", *Second Japan-Turkey Workshop on Earthquake Engineering*, Istanbul Technical University, Volume 1, February 1998.

2. Bett, B. J., R. E. Klinger, and J. O. Jirsa, "Lateral Load Response of Strengthened and Repaired Reinforced Concrete Columns", *ACI Structural Journal*, Vol. 85, No. 5, pp. 499-508, September-October 1998.

3. Ersoy, U., T. Tankut, and R. Suleiman, "Behavior of Jacketed Columns", *ACI Structural Journal*, V.90, No. 3, pp. 288-293, May-June 1993.

4. Aboutaha, R., M. D. Engelhardt., J. O. Jirsa, M. E. Kreger, "Retrofit of Concrete Columns with Inadequate Lap Splices by the Use of Rectangular Steel Jackets," *Earthquake Spectra*, Vol. 12, No. 4, pp. 693-714, November 1996

5. Watson, S., F. A. Zahn, and R. Park, "Confining Reinforcement for Concrete Columns", *Journal of Structural Engineering*, Vol. 120, No. 6, pp.1798-1824, 1994.

6. Ignatiev, N., "Some Problems of Strengthening of Existing Buildings with New Structural Components", *Repair and Strengthening of Existing Buildings, Second Japan- Turkey Workshop on Earthquake Engineering*, Istanbul Technical University, Volume 1, pp.11-21, February 1998.

7. Wu, Y. F., M. C. Griffith and D. J. Oehlers, "Improving the Strength and Ductility of Rectangular Reinforced Concrete Columns through Composite Partial Interaction: Tests", *Journal of Structural Engineering*, Vol. 129, No. 9, pp.1643-1661, 2003.

8. Yalcin, C., *Seismic Evaluation and Retrofit of Existing Reinforced Concrete Bridge Columns*, Ph.D. Thesis, University of Ottowa, 1997.

9. Saadatmanesh, H., M. R. Ehsani, and L. Jin, “Repair of Earthquake-Damaged RC Columns with FRP Wraps”, *ACI Structural Journal*, V.94, No. 2, pp. 206-215, March-April 1997.

10. Aboutaha, R. S., M. D. Engelhardt, J. O. Jirsa, and M. E. Kreger., “Experimental Investigation of Seismic Repair of Lap Splice Failures in Damaged Concrete Columns”, *ACI Structural Journal*, V.96, No. 2, pp. 297-306, March-April 1999.

11. Paulay, T, T. M. Zanza, A. Scarpas, “Lapped Splices in Bridge Piers and in Columns of Earthquake Resisting Reinforced Concrete Frames”, *Research Report 81-6, Dept. of Civil Engineering, Univ. of Canterbury*, Christchurch, New Zealand, Aug. 1981.

12. Ersoy, U., “Seismic Rehabilitation”, *Repair and Strengthening of Existing Buildings, Second Japan- Turkey Workshop on Earthquake Engineering*, Istanbul Technical University, Volume 1, February 1998.

13. Valluvan, R., E. K. Kreger, and J. O. Jirsa, “Strengthening of Column Splices for Seismic Retrofit of Non-ductile Reinforced Concrete Frames”, *ACI Structural Journal*, V.90, No. 4, pp. 432-440, July-August 1993.

14. Lynn, A. C., J. P. Moehle, S. A. Mahin, and W.T. Holmes, “Seismic Evaluation of Existing Reinforced Concrete Building Columns”, *Earthquake Spectra*, Vol. 12, No. 4, pp. 715-739, Nov. 1996.

15. Chai, Y., M. Priestley and F. Seible, "Seismic Retrofit of Circular Bridge Columns for Enhanced Flexural Performance," *ACI Structural Journal*, Vol. 88, No.5, pp. 572-584, September-October 1991.

16. Coffman, H. L., M. L. Marsh, C. B. Brown, "Seismic Durability of Retrofitted Reinforced-Concrete Columns", *Journal of Structural Engineering*, Vol. 119, No. 5, pp.1643-1661, 1993.

17. Panahshahi, N., N. W. White and P. Gergely, “Reinforced Concrete Compression Lap Splices under Inelastic Cyclic Loading,” *ACI Structural Journal*, V. 89, No. 18, March-April 1992, pp. 164-175, 1992.

18. Sheikh, S. A., and G. Yau, “Seismic Behavior of Concrete Columns Confined with Steel and Fiber-Reinforced Polymers”, *ACI Structural Journal*, Vol.99, No. 1, pp. 72-80, January-February 1994.

19. Bayrak O., and S. A. Sheikh, “High-Strength Concrete Columns under Simulated Earthquake Loading”, *ACI Structural Journal*, Vol.94, No. 6, pp. 708-722, November-December 1997.

20. Bakis,C. E., L. C. Bank, V. L. Brown, E. Cosenza, J. F. Davalos, J. J. Lesko, A. Machida, S. H. Rizkalla and T. C. Triantafillou, “Fiber-Reinforced Polymer Composites for Construction—State-of-the-Art Review”, *Journal of Composites for Construction, ASCE*, Vol. 6, No. 2, pp. 73-87, 2002.

21. Eindea, L. V. D., L. Zhaob and F. Seible, "Use of FRP Composites in Civil Structural Applications", *Construction and Building Materials, Elsevier Ltd.*, Vol. 17, pp. 389-403, 2003.

22. Campione, G., “Influence of FRP Wrapping Techniques on the Compressive Behavior of Concrete Prisms”, *Cement & Concrete Composites, Elsevier Ltd.*, Vol. 28, pp. 497-505, 2006.

23. Antoniades, K. K, T. N. Salonikios and A. J. Kappos, “Evaluation of Hysteretic Response and Strength of Repaired R/C Walls Strengthened with FRPs”, *Engineering Structures, Elsevier Ltd*., Vol. 29, pp. 2158-2171, 2007

24. Yalcin, C., O. Kaya and M. Sinangil, “Seismic Retrofitting of R/C Columns having Plain Rebars Using CFRP Sheets for Improved Strength and Ductility”, *Construction and Building Materials, Elsevier Ltd.*, Vol. 22, pp. 295-307, 2008.

25. Kaya, O., Seismic Retrofitting of Existing R/C Columns For Improved Ductility, M.S. Thesis, Dept. of Civil Engineering, Boğaziçi University, 2003.

26. Sinagil, M., Seismic Retrofitting of RC Columns with Lap-splicing Problem for Improved Ductility, M.S. Thesis, Dept. of Civil Engineering, Boğaziçi University, 2004.

27. Val, D. V., "Reliability of Fiber-Reinforced Polymer-Confined Reinforced Concrete Columns", *Journal of Structural Engineering, ASCE*, Vol. 129, No. 8, pp. 1122-1130, August 2003.

28. Chaallal, O., and M. Shahawy, "Performance of Fiber-Reinforced Polymer-Wrapped Reinforced Concrete Column under Combined Axial-Flexural Loading", *ACI Structural Journal*, V.97, No. 4, pp. 659-668, July-August 2000.

29. Engindeniz, M., F. K. Lawrence and A. Zureick, ''Repair and Strengthening of Reinforced Concrete Beam-Column Joints: State of the Art,'' *ACI Structural Journal*, (2005), 102(2), 1–14.

30. Ghobarah, A. and T. El-Amoury, "Shear Strengthening of RCT-Joint Using CFRP Composites", *Journal of Composites for Construction, ASCE*, Vol. 9, No. 5, pp. 408-416, 2005.

31. Sheikh, S. A., and G. Yau, "Seismic Behavior of Concrete Columns Confined with Steel and Fiber-Reinforced Polymers", *ACI Structural Journal*, Vol. 99, No. 1, pp. 72-80, January-February 2002.

32. Saadatmanesh, H., M. R. Ehsani, and M. W. Li, "Strength and Ductility of Concrete Columns Externally Reinforced with Fiber Composite Straps", *ACI Structural Journal*, Vol. 91, No. 4, pp. 434-447, July-August 1994.

33. Harajli, M. H., and A. A. Rteil, "Effect of Confinement Using Fiber-Reinforced Polymer or Fiber-Reinforced Concrete on Seismic Performance of Gravity Load-Designed Columns", *ACI Structural Journal*, Vol. 101, No. 1, pp. 47-56, January-February 2004.

34. Iacobucci, R. D., S. A. Sheikh, and O. Bayrak, "Retrofit of Square Concrete Columns with Carbon Fiber-Reinforced Polymer for Seismic Resistance", *ACI Structural Journal*, Vol. 100, No. 6, pp. 785-794, November-December 2003.

35. Mirmiran, A., and M. Shahawy, "Behavior of Concrete Confined by Fiber Composites", *Journal of Structural Engineering, ASCE*, Vol. 123, No. 5, pp. 583-590, May 1997.

36. Berthet, J.F., E. Ferrier and P. Hamelin, "Compressive behavior of concrete externally confined by composite jackets. Part A: experimental study", *Construction and Building Materials, Elsevier Ltd.*, Vol. 19, pp. 223-232, 2005.

37. TEC 2007, *Specification for Buildings to be Built in Seismic Zones*, 2007.

38. TS-500, *Requirements for Design and Construction of Reinforced Concrete Structures*, Turkish Standard Institute, February 2000.

39. Response-2000: Reinforced Concrete Sectional Analysis Software, University of Toronto

40. Rochette, P. Labossiere, P., "Axial testing of Rectangular Column Models confined with composites," *Journal of Composites for Construction*, Vol.4 No.3, 129-136, 2000.

41. ACI T1.1-01, "Acceptance Criteria for Moment Frames Based on Structural Testing," *American Concrete Institute*, 2001.